Investigating the Lipid Coverage of the Dried Blood Spot Metabolome using Liquid Chromatography – Mass Spectrometry for Global Metabolomics

Hege Sofie Haugan

Thesis for the Master's
Degree in Chemistry
60 credits

Department of Chemistry
Faculty of Mathematics and Natural Sciences

UNIVERSITY OF OSLO

May 2020

Investigating the Lipid Coverage of the Dried Blood Spot Metabolome using Liquid Chromatography – Mass Spectrometry for Global Metabolomics

Hege Sofie Haugan

Thesis for the Master's Degree in Chemistry

60 credits

Department of Chemistry

Faculty of Mathematics and Natural Sciences

University of Oslo

May 2020

2020

Investigating the Lipid Coverage of the Dried Blood Spot Metabolome using Liquid Chromatography – Mass Spectrometry for Global Metabolomics

Hege Sofie Haugan

http://www.duo.uio.no/

Trykk: Reprosentralen, Universitetet i Oslo

Abstract

Using global metabolomics for the diagnosis of inborn errors of metabolism can provide greater insight into the diseased metabolic pathway, but it is important to understand the limitations of the analytical technique in terms of which metabolites are covered by it. In this project, the lipid coverage of a global metabolomics method using liquid chromatography-electrospray ionization-mass spectrometry and dried blood spots was investigated. The lipid coverage and possible expansion of the coverage was investigated by extraction of commercially available lipid standards, metabolite standards, and dried blood spots, using a selection of solvents in different ratios with water: methanol, acetonitrile, 1-propanol, iso-propanol, 1-butanol, or methyl-tert-butyl-ether. The methods ability to detect physiological change in the metabolome and lipidome was also investigated. Quality control samples were implemented to assess the precision of the acquired data. Increasing the amount of organic solvent used in the extraction solution was found to increase lipid coverage, but it was not greatly affected by type of organic solvent used. The method detected changes in the metabolic profile of seven healthy volunteers participating in a high intensity exercise. Several metabolites and lipids were identified and affected by the exercise. Pooled quality controls were implemented in the global metabolomics workflow and showed that the data acquired had high precision. A series of diluted pooled quality controls showed that there was a linear relationship between signal intensity and metabolite concentration, with R^2>0.98. This method will be a useful for researching differences in metabolic profiles, but also as a supplementary diagnostic tool for inborn errors of metabolism.

Preface

The work done in this thesis was done at the National Unit of Screening and Congenital Pediatric Metabolic Disorders at Oslo university hospital, Rikshospitalet from January 2019 to May 2020. My supervisors have been Katja B. P. Elgstøen, and Hanne B. Skogvold at Rikshospitalet, and Steven R. H. Wilson at the Department of Chemistry, University of Oslo.

I would like to thank Katja for the motivation and encouragement she has provided throughout this work. Being a part of her research group has really been inspiring, and I will always remember this time with fondness.

Steven deserves a thank you for assigning me to this work. He has been a wonderful supervisor, a great help and motivator, and I appreciate all the constructive feedback he has provided.

Hanne has been a fantastic supervisor and has always been willing to help and guide me. I especially appreciate the help she provided editing this manuscript.
Anja Østeby and Elise Sandås deserves a special thank you for all the guidance, insight and help they provided throughout my thesis. Having you three to take care of me and being so helpful with everything has meant a lot to me.

Helge Rootwelt deserves a huge thank you for helping me understand the medical aspects of my work, and for his enthusiasm and humor.

I would also like to thank my fellow students Katrine Pettersen and Monica Kaur Toor. I really appreciated getting to know you, and you made this time fun and social. Thank you to everyone at IKB for the conversations and lunches.

The Bioanalytics group at the Department of Chemistry also deserves a thank you for being so inclusive and friendly.

I would like to thank Norsk Kjemisk Selskap – Faggruppe for Analytisk Kjemi for providing me with financial support which gave me the opportunity to attend “Det 24. Norske Symposium i Kromatografi” in Sandefjord. I presented my work in a poster, shown in **Appendix**, section 6.5.

Finally, I would like to thank my friends and family for the love and support they have shown me during this time. Without them, this would not have been possible, and I look forward to spending more time with them.

Oslo, Norway, May 2020
Hege Sofie Haugan

Table of Content

1 Abbreviations

Abbreviation	Term
ACN	Acetonitrile
ADP	Adenosine 5´-diphosphate
AMP	Adenosine 5´-monophosphate
APCI	Atmospheric pressure chemical ionization
API	Atmospheric pressure ionization
APPI	Atmospheric pressure photoionization
ATP	Adenosine 5´-triphosphate
CE	Cholesterol ester
CE (18:1)	Cholest-5-en-3b-yl (9Z-octadecenoate)
CE (18:1 (d7))	Cholest-5-en-3b-yl (9Z-octadecenoate (d7))
Cer	Ceramide
Cer (d18:1/15:0)	N-(pentadecanoyl)-sphing-4-enine
Cer (d18:1 (d7)/15:0)	N-(pentadecanoyl)-sphing-4-enine (d7)
D1	Day one
D2	Day two
D3	Day three
DBS	Dried blood spot
DDA	Data dependent acquisition
DG	Diacylglycerol
DG (15:0/18:1)	1-pentadecanoyl-2-(9Z-octadecenoyl)-sn-glycerol
DG (15:0/18:1 (d7))	1-pentadecanoyl-2-(9Z-octadecenoyl (d7))-sn-glycerol
dGMP	Deoxy-guanosine 5'-monophosphate
DNA	Deoxyribonucleic acid
EIC	Extracted ion chromatogram
ESI	Electrospray ionization
ESI+	Positive ionization mode
ESI-	Negative ionization mode
FA	Formic acid
FT	Fourier transformation
FT-ICR	Fourier transformation-ion cyclotron resonance

FWHM	Full width half maximum
GC	Gas chromatography
GMP	Guanosine 5’-monophosphate
HCD	Higher collision-induced dissociation
HESI	Heated electrospray ion source
HILIC	Hydrophilic interaction chromatography
HPLC	High performance liquid chromatography
IEM	Inborn errors of metabolism
IMP	Inosine-5’-monophosphate
LC	Liquid chromatography
LC-ESI-MS	Liquid chromatography-electrospray ionization-mass spectrometry
LC-MS	Liquid chromatography-mass spectrometry
LOD	Limit of detection
LPC (18:1)	1-(9Z-octadecenoyl)-2-glycero-3-phosphocholine
LPC (18:1 (d7))	1-(9Z-octadecenoyl (d7))-2-glycero-3-phosphocholine
LPE (18:1)	1-(9Z-octadecenoyl)-2-glycero-3-phosphoethanolamine
LPE (18:1 (d7)))	1-(9Z-octadecenoyl (d7))-2-glycero-3-phosphoethanolamine
m/z	Mass-to-charge ratio
MeOH	Methanol
MG	Monoacylglycerol
MG (18:1)	1-(9Z-octadecenoyl)-glycerol
MG (18:1 (d7))	1-(9Z-octadecenoyl (d7))-glycerol
MS	Mass spectrometry
MTBE	Methyl tert-butyl ether
NAD^+	Nicotinamide adenine dinucleotide
NBS	Newborn screening
ND	Not detectable
NH_4Ac	Ammonium acetate
NMR	Nuclear magnetic resonance
NP	Normal phase
PA	Peak area
PC	Phosphatidylcholine
PC	Principal component

PC (15:0/18:1)	1-pentadecanoyl-2-(9Z-octadecanoyl)-glycero-3-phosphocholine
PC (15:0/18:1 (d7))	1-pentadecanoyl-2-(9Z-octadecanoyl (d7))-glycero-3-phosphocholine
PCA	Principle component analysis
PE	Phosphatidylethanolamine
PE (15:0/18:1)	1-pentadecanoyl-2-(9Z-octadecenoyl)-glycero-3-phosphoethanolamine
PE (15:0/18:1(d7))	1-pentadecanoyl-2-(9Z-octadecenoyl (d7))-glycero-3-phosphoethanolamine
PG	Phosphatidylglycerol
PG (15:0/18:1)	1-pentadecanoyl-2-(9Z-octadecenoyl)-glycero-3-phospho-(1'-sn-glycerol)
PG (15:0/18:1 (d7))	1-pentadecanoyl-2-(9Z-octadecenoyl (d7))-glycero-3-phospho-(1'-sn-glycerol)
PI	Phosphatidylinositol
PI (15:0/18:1)	1-pentadecanoyl-2-(9Z-octadecenoyl)-glycero-3-phospho-(1'-myo-inositol)
PI (15:0/18:1 (d7))	1-pentadecanoyl-2-(9Z-octadecenoyl (d7))-glycero-3-phospho-(1'-myo-inositol)
PQC	Pooled quality control
PS	Phosphatidylserine
PS (15:0/18:1)	1-pentadecanoyl-2-(9Z-octadecenoyl)-glycero-3-phosphoserine
PS (15:0/18:1 (d7))	1-pentadecanoyl-2-(9Z-octadecenoyl (d7))-glycero-3-phosphoserine
QIT	Quadrupole ion trap
QqQ	Triple quadrupole
RF	Radio frequency
RNA	Ribonucleic acid
RP	Reversed phase
RP-LC	Reversed phase-liquid chromatography
RSD	Relative standard deviation
Rt	Retention time
SEC	Size exclusion chromatography
SM	Sphingomyelin
SM (d18:1/18:1)	N-(9Z-octadecenoyl)-sphing-4-enine-1-phosphocholine

SM (d18:1/18:1 (d9))	N-(9Z-octadecenoyl (d9))-sphing-4-enine-1-phosphocholine
sn	Stereospecific numbering
SRM	Selected reaction monitoring
TG	Triacylglycerol
TG (15:0/18:1/15:0)	1-pentadecanoyl-2(9Z-octadecenoyl)-3-pentadecanoyl-sn-glycerol
TG (15:0/18:1/15:0 (d7))	1-pentadecanoyl-2(9Z-octadecenoyl)-3-pentadecanoyl (d7)-sn-glycerol
TIC	Total ion chromatogram
TOF	Time-of-flight
UDP	Uridine diphosphate
UHPLC	Ultra-high-performance liquid chromatography

2 Introduction

2.1 Inborn Errors of Metabolism

Metabolism is a series of complex biochemical reactions occurring in cells and living organisms that provide the biological system with energy and the building blocks needed for survival. Metabolism include the synthesis of endogenous compounds and the degradation of both endogenous and exogenous compounds. These biochemical reactions are linked together by metabolic pathways. The general pattern of these pathways is similar, one compound the substrate, is enzymatically transformed into another compound, the product. The enzymes that catalyze these reactions are proteins, whose structure and composition is transcribed from its gene in the ribonucleic acids (RNA), which in turn derive from deoxyribonucleic acid (DNA) [1].

Inborn errors of metabolism (IEMs) are a group of diseases caused by DNA mutations, resulting in a defective gene product, usually as a dysfunctional enzyme. **Figure 1** shows a simplified illustration of how an IEM can affect a biochemical pathway. An enzymatic defect can result in disease by several means, for instance by the accumulation of a substrate, the lack of a product, or because the substrate or intermediary products undergo alternative metabolic pathways affecting and changing other biochemical processes [1, 2].

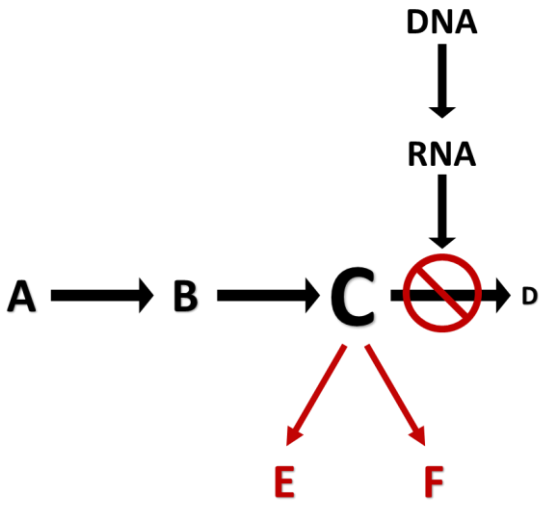

Figure 1: Error in a metabolic pathway caused by a genetic defect. A, B, C, D, E, and F represent metabolites in a metabolic pathway. The arrows represent enzymes. A mutation in DNA leads to the formation of a dysfunctional enzyme. The metabolic block at enzyme converting metabolite C to D could lead to the buildup of metabolite C, a deficiency in metabolite D, and possibly diversion of some of the increased amounts of metabolite C via alternative pathways, forming metabolites E and F. Figure adapted from [1].

Each IEM is rare, but there are more than a 1000 known IEMs [3], and the exact frequency of occurrence is hard to estimate [4]. Early diagnosis and treatment are important for improving the outcome for the affected individual. If an IEM is left untreated the consequences vary from a mild reduction in quality of life to severe disabilities or death [2].

2.1.1 Diagnostic Practice for Inborn Errors of Metabolism

The diagnosis of IEMs usually depends on a combination of clinical symptoms and signs, imaging techniques, different biochemical and enzymatic analyses and genetic tests, as different IEMs may be very difficult to distinguish from each other and other diseases. Since several IEMs even are asymptomatic before a metabolic crisis that can have devastating consequences appears, some of the IEMs are included in the newborn screening program to identify affected newborns and start treatment before symptoms arise.

Newborn screening is performed to detect possible abnormal levels of metabolic biomarkers and is an important tool for primary disease prevention and early treatment. The aim is to detect diseases in the latent asymptomatic stage of the disease and to facilitate intervention and improve outcomes. In Norway, the screening includes 25 congenital disorders, of which 21 are IEM, 2 are endocrinological conditions, one group consists of severe combined immunodeficiency and other severe T cell deficiencies, and finally cystic fibrosis [5].

If there are specific symptoms of an IEM, or the screening test returns positive for an IEM, multiple diagnostic analyses are performed, often by analysis of several biofluids. The multitude of approaches for diagnosing IEMs is time consuming and resource demanding.

With an untargeted, unbiased and hypothesis free approach for screening of multiple metabolites in one sample, the diagnostic practice of IEM can be made more time efficient and provide greater understanding of the mechanism of the disease [6, 7]. **Figure 2** illustrates the difference between a targeted and global approach to diagnosis of IEMs.

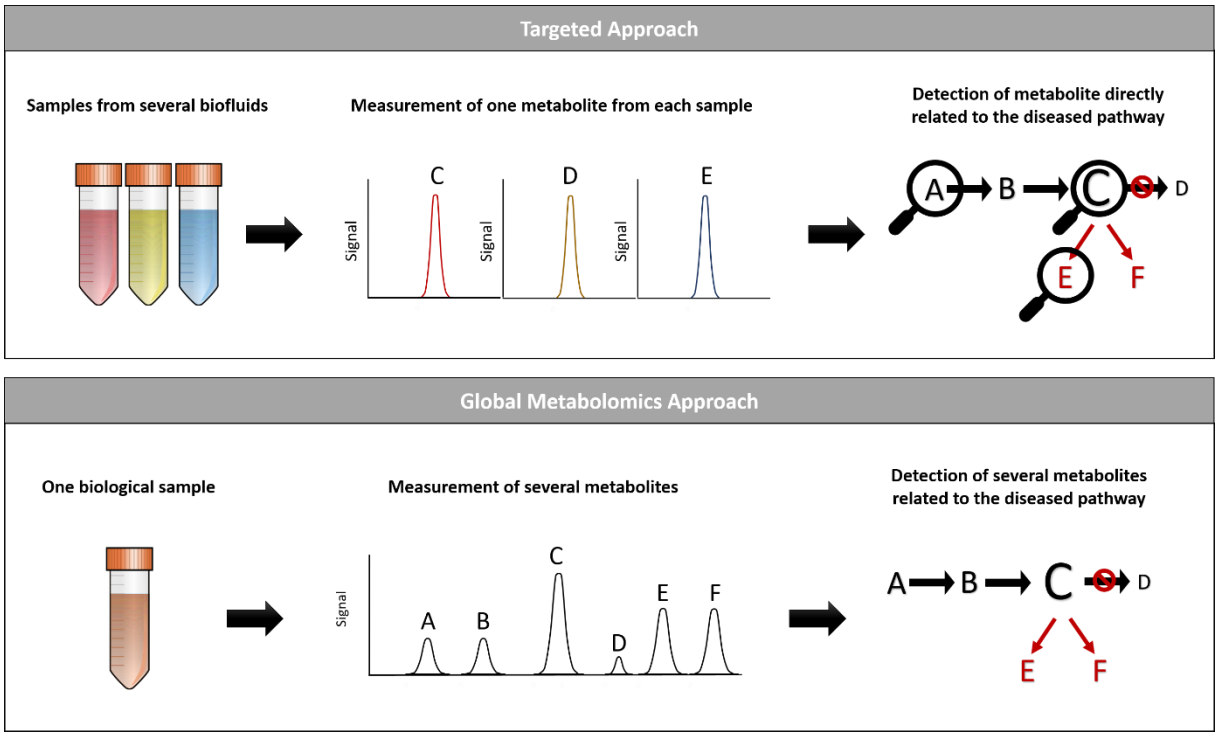

Figure 2: Comparing the traditional targeted approach for diagnosing inborn errors of metabolism (IEMs), to the global metabolomics approach. In the targeted approach for diagnosis of IEMs, several samples from different biofluids are analyzed using different targeted techniques that detect specific metabolites related to the diseased pathway. Using a global metabolomics approach, one sample can be analyzed for several metabolites, and provide a broader view IEMs effect on the diseased pathway, and other associated pathways. Figure adapted from [6].

IEMs can potentially affect any metabolic pathway, making any metabolite a potential biomarker of disease [8].

2.2 Metabolomics

Metabolites are low molecular weight (< 1500 Da) compounds that are substrates, intermediates, and products of enzymatic reactions. Metabolites are the building blocks of proteins (amino acids), transcripts, genes (nucleotides), and the cell walls (lipids) [9]. Global metabolomics is the study of the metabolites in present in a biological sample, and the metabolome refers to all metabolites present in a biological system or sample [9, 10].

The metabolome is composed of metabolites originating from a number of processes. Endogenous metabolites are synthesized and consumed within the biological system, and exogenous metabolites, for example drugs or nutrients, which are ingested by the biological system [9]. Endogenous metabolites are divided into different biochemical groups based on their structure, functional groups, and biological role. **Figure 3** shows how these biochemical

groups are distributed along a logP-scale. The logP value of a compound indicates its degree of hydrophobicity and is defined as the partitioning of a compound X in a mixture of two immiscible solutions, usually octanol and water [11], as shown in **Equation 1**.

$$logP = \frac{[X]_{Octanol}}{[X]_{Water}} \qquad \textit{Eq. 1}$$

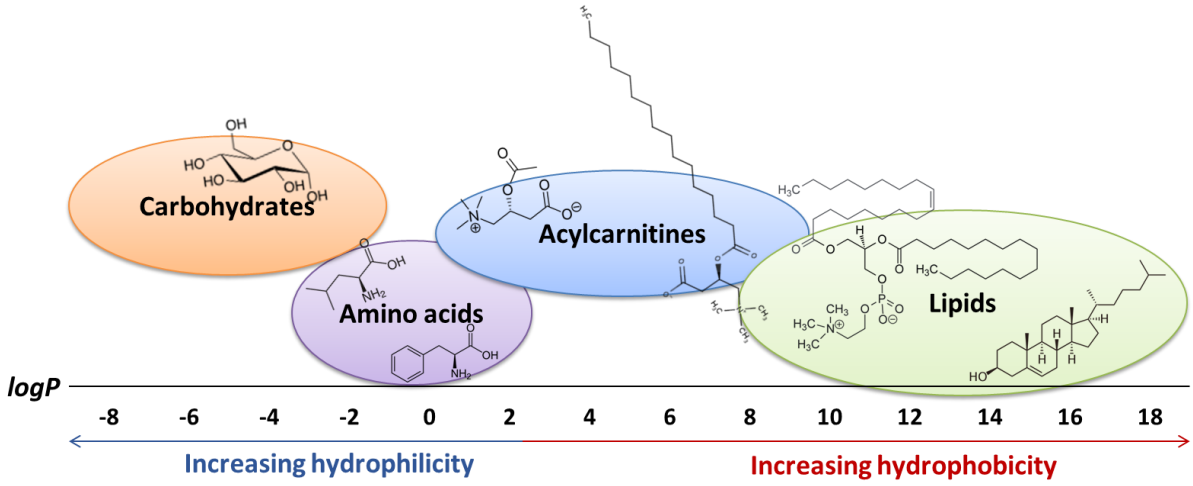

Figure 3: Example of metabolites constituting the metabolome. The metabolome consists of a variety of metabolites, ranging from hydrophilic to hydrophobic. The metabolome can also consist of compounds that do not belong in any of these groups.

This figure show that the can metabolome consists of a variety of compound with a wide range of physiochemical properties, especially in regard to hydrophobicity. A metabolite whose logP value is lower than two, is usually regarded as being hydrophilic, and metabolites with logP values greater than two are considered hydrophobic. Hydrophobicity usually increases with increasing size, saturation, and lack of polar functional groups [9].

2.2.1 The Lipidome

Lipids are a subgroup within the metabolome, because of their hydrophobicity and structural diversity. In the same way that metabolites make up the metabolome, the entire set of lipids in a biological sample can be regarded as the lipidome. Lipidomics is the analysis of lipids, and their interacting moieties [12]. Lipids are fuel for energy metabolism in the form triacylglycerols, signaling molecules in the form of steroids or phosphatic acid, and structural components of cell membranes in the form of phospholipids and sphingolipids [13].

The term lipid has been loosely defined as an organic compound that is insoluble in water, but soluble in organic solvent [14]. A more resent classification of lipids take into account the origin of the compounds, and define them as hydrophobic or amphipathic molecules that

originate entirely or in part by carbanion-based condensations of thioesters and/or by carbocation-based condensations of isoprene units [15]. Based on these two classifications, lipids are further divided into eight classes, and some of these classes are further divided into subclasses. **Figure 4** shows a classification of lipids proposed by Fahy et al. [15], with examples, and is the basis of the classification of lipids in this work.

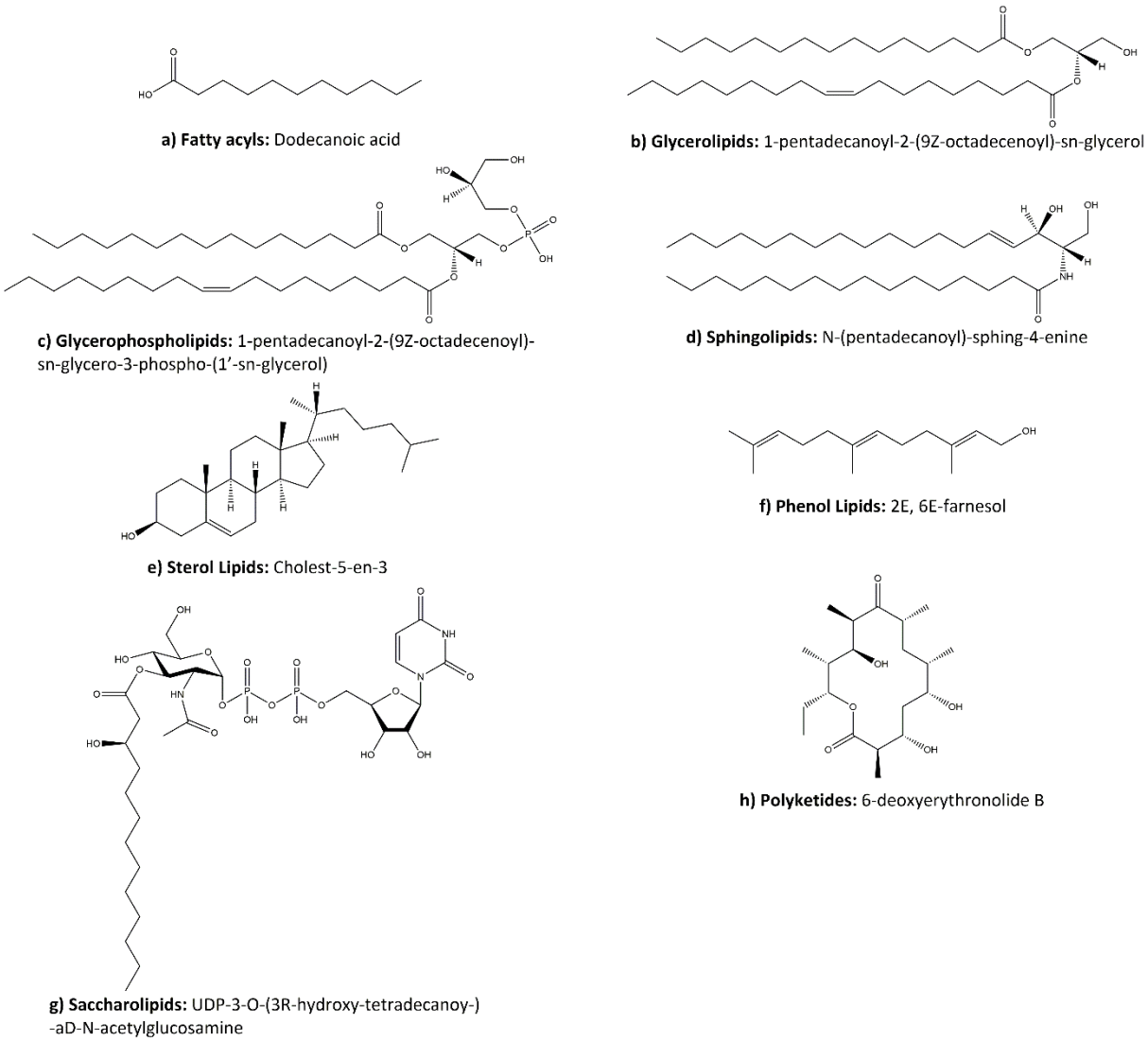

Figure 4: Examples of lipids from each of the eight lipid classes. a) Fatty acyl: dodecanoic acid, b) Glycerolipids: 1-pentadecanoyl-2-(9Z-octadecenoyl)-sn-glycerol, c) Glycerophospholipids: 1-pentadecanoyl-2-(9Z-octadecenoyl)-sn-glycero-3-phospho-(1'-sn-glycerol), d) Sphingolipids: N-(pentadecanoyl)-sphing-4-enine, e) sterol lipid cholest-5-en-3β-ol, f) phenol lipid 2E, 6E-farnesol, g) Saccharolipid: Uridine diphosphate (UDP)-3-O-(3R-hydroxy-tetradecanoy-)-αD-N-acetylglucosamine, h) Polyketide: 6-deoxyerythronolide B. Adapted from [15].

Fatty acyls are a diverse group of lipids, synthesized by chain elongation of an acetyl-CoA primer with malonyl-CoA. Structures with a glycerol group are divided into two distinct classes, glycerolipids which include acyl- alkyl- and alkenyl-glycerols, and glycerophospholipids, which contain a phosphate group esterified to one of the glycerol

hydroxy groups. Glycerophosphates are further divided into subclasses based on the different groups linked to the phosphate esters, and these are named headgroups. **Figure 5** shows a selection of different subclasses of glycerophospholipids, with their different headgroups, subclass names and abbreviations.

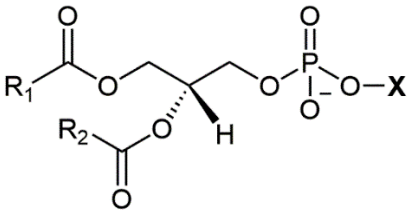

Headgroup (X)	Subclass name	Abbreviation
—H	Phosphatidic acid	
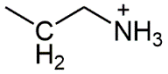	Phosphatidylethanolamine	PE
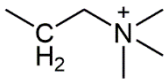	Phosphatidylcholine	PC
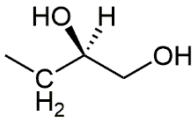	Phosphatidylglycerol	PG
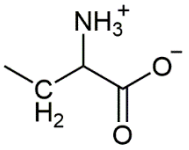	Phosphatidylserine	PS
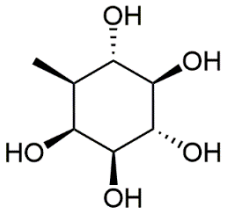	Phosphatidylinositol	PI

Figure 5: Headgroups, subclass names and abbreviations of a selection of the different glycerophospholipids. X represent the different headgroups of glycerophospholipids, and R_1 and R_2 represent acyl groups [15].

Sterol lipids and phenol lipids share a common synthetic pathway but differ in structure and function. Sphingolipids contain a long chained nitrogenous base in their core structure.

Saccharolipids have a direct link between the fatty acid and the sugar back bone. Polyketides are a diverse class containing different metabolites from animal, plant and microbial sources [15, 16].

The nomenclature of lipids can be complicated, and usually a lipid has a systematic name and a common name or abbreviated name. Using abbreviations makes it easier to define the position of acyl-, alkyl-, or alkenyl-chains in glycerolipids, sphingolipids and glycerophospholipids. Stereospecific numbering (*sn*) is also used to describe the position of acyl or alkyl chains in glycerolipids and glycerophospholipids [16]. **Figure 6** shows the Fischer projection of a glycerol derivative, and how the glycerol moiety in glycerolipids and glycerophospholipids is numbered. The *sn*-1 position refers to the first carbon atom of the glycerol moiety, *sn*-2 the second, and *sn*-3 the third [17].

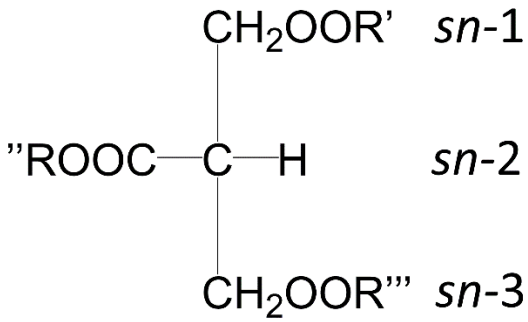

Figure 6: Stereospecific numbering (*sn*) of the glycerol moiety in glycerolipids and glycerophospholipids. The carbon atoms of glycerols are numbered stereospecifically in order to differentiate between different configurations [17].

The common name "lyso" is used for denoting that a glycerolipids or glycerophospholipids is lacking an acyl, alkyl, or alkenyl-group at the glycerol moiety. Abbreviated names are often written in the "headgroup or group abbreviation (*sn*-1/*sn*-2)" format (e.g. PC (16:0/18:1)) [16], where the length and saturation of the acyl, alkyl, or alkenyl -group is indicated within the parentheses. Double bond geometry is indicated using E/Z-notations if it is known [15, 16].

Several IEMs have been found to be associated with abnormal lipid metabolism [6], and the identification of lipid biomarkers is required for diagnosis and monitoring of these diseases, and global metabolomics could be a useful tool for this [8].

2.3 Analytical Techniques for Global Metabolomics

In global metabolomics, the goal is to identify as many metabolites as possible, and to understand the biological implications of the findings. This requires both qualitative and quantitative information about the metabolome. As the metabolome consists of many metabolites, the global metabolomics approach puts a high demand on the analytical technique used. Nuclear magnetic resonance (NMR) spectroscopy and mass spectrometry (MS) are the techniques most frequently used in metabolomics [9]. With NMR, metabolites are detected by their characteristic absorption spectra that are recorded when a magnetic nucleus (^{1}H and ^{13}C) absorb radio frequency energy in a magnetic field. NMR is a quantitative, reproducible, and non-destructive method where intact bio-fluids and tissues can be analyzed [9, 18]. With MS, charged metabolites are separated and detected according to their mass-to-charge (*m/z*) ratio. Fragmentation provides structural information, and is useful in identifying different metabolites [9]. NMR has lower sensitivity compared to MS, made apparent from the big difference in limit of detection (LOD), as illustrated in **Figure 7**. LOD is defined as the lowest amount of analyte necessary to obtain a signal that can be distinguished from the background signal [19]. For NMR the LOD is between micro- to milli-molar, and for MS the LOD is known to go down to pico-molar [20]. The concentration of different metabolites may vary, and for some compounds it can be as low as at femto-molar levels, therefore the LOD of the analytical technique needs to be low. Because of this, MS is usually preferred when developing a metabolomics method [9].

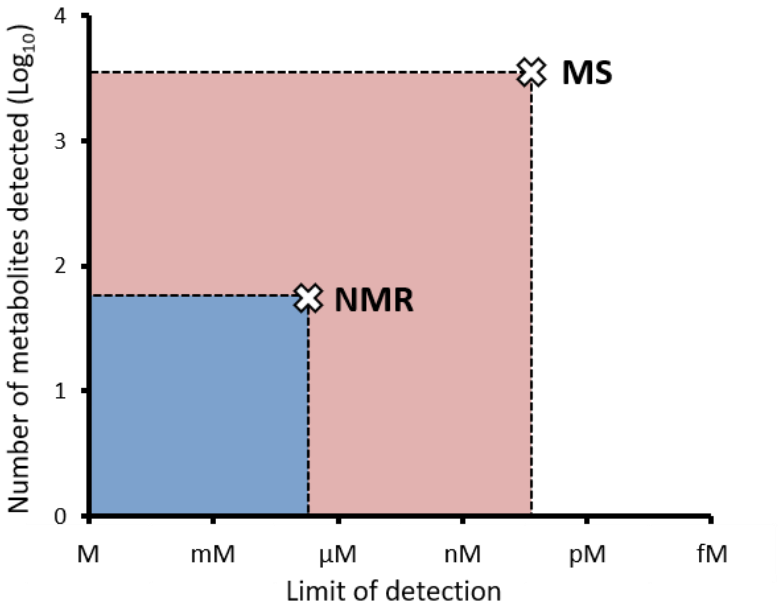

Figure 7: Relative sensitivity of nuclear magnetic resonance (NMR) and mass spectrometry (MS) metabolomics platform. NMR can measure metabolites in the millimolar to micromolar (mM-µM) concentrations, and MS can detect metabolites at nanomolar and picomolar (nM-pM) concentrations. The figure was adapted from [20].

Before metabolites can enter the MS, they must be in the form of gas phase ions which occurs in the ion source. Several types of ion sources are available, and the choice depends on the analyte and the sample matrix. Atmospheric pressure ionization (API) sources have been developed specifically for ionization of liquid samples at atmospheric pressure. Electrospray ionization (ESI), atmospheric pressure chemical ionization (APCI), or atmospheric pressure photoionization (APPI) are some of the different types of API sources [10]. When choosing an ion source, the size and polarity of the analytes should be considered. **Figure 8** shows the appropriate size and polarity range for the different API sources.

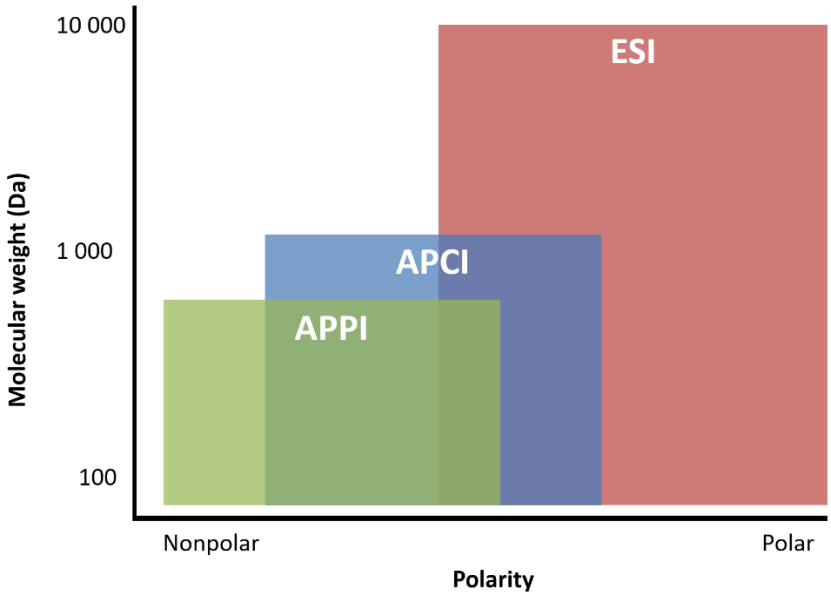

Figure 8: Choosing the right ion source depends on the polarity and molecular weight of the compound. Atmospheric pressure photoionization (APPI) and atmospheric pressure chemical ionization (APCI) are most suited for non-polar and lower molecular weight compounds, compared to electrospray ionization (ESI). ESI is a good ion source for analyzing medium-polar and polar compounds of low to high molecular weight. The figure was adapted from [21].

APPI and APCI are able to ionize compounds who are non-polar and of low molecular weight (<1000 Da). ESI is able to ionize a wider range of compounds both in terms of polarity and molecular weight. Metabolites are between 50-1500 Da and range from polar to non-polar, making ESI a suitable ion source for global metabolomics [21, 22].

Chromatography is often coupled to MS in global metabolomics studies [9]. Chromatography enables separation of metabolites in time, based on their interaction between a stationary phase and mobile phase. Based on whether the mobile phase is a gas or a liquid, there is two types of chromatography, gas chromatography (GC) and liquid chromatography (LC) [10]. Separating the metabolites prior to MS detection reduces the complexity of the sample, which increases MS sensitivity and resolution [21]. GC provides the fastest and highest efficiency of analysis per time unit. However, compounds analyzed by GC must be volatile and thermally stable, limiting the compounds appropriate for GC analysis. As many metabolites are non-volatile, samples must be derivatized prior to analysis, if GC is to be used [23, 24]. LC analysis provides the possibility of separating both non-polar and polar metabolites without the need for derivatization [21]. Several separation principles are available, making LC separation very versatile [21]. The liquid chromatography-electrospray ionization-mass spectrometry (LC-ESI-MS) method used in this project will be further described.

2.3.1 Mass Spectrometry

With MS, gas phase ions are separated and detected according to their *m/z* value, using magnetic or electric fields, or a combination of the two. **Figure 9** shows the basic schematic setup of a mass spectrometer, which consist of a sample inlet, ionization source, mass analyzer, detector, a vacuum system and a computer system [19].

The sample inlet introduces the sample to the mass spectrometer, via the ion source. The ion source transfers gas phase ions into the mass analyzer, where the ions are separated based on their *m/z* value, using magnetic or electric fields. Some mass analyzers that use Fourier transformation (FT) have combined mass analyzers and detectors. The detector measure incoming ions, as well as amplifying and storing the signal generated in the detector. Vacuum is required inside the mass spectrometer to avoid particle collisions and subsequent loss of ions, which is provided by a vacuum pumping system. The pressure is different in the different compartments, obtained by differential pumping. A computer is used for instrument control and data handling [19].

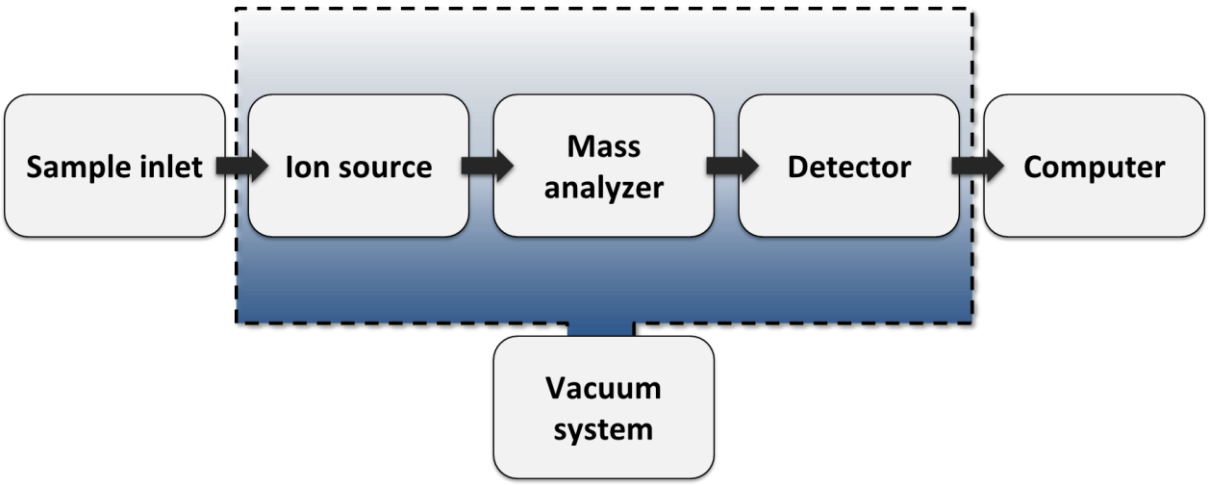

Figure 9: Schematic representation of the main constituents of a mass spectrometer. The sample inlet (gas chromatography, liquid chromatography, or by direct injection) introduces the sample to the ion source. The ion source transfer gas phase ions into the mass analyzer., where ions are separated according to their *m/z* ratio. The detector generates a signal in response to incoming ions for each *m/z* value. The vacuum system ensures high vacuum, reducing the collisions between ions and gas molecules. The figure was adapted from [19].

The performance of a mass spectrometer is described by its mass resolution and mass accuracy. Mass resolution quantifies the mass spectrometers ability to separate ions of different *m/z*, and is given by **Equation 2**,

$$R = \frac{m}{w_{0.5}} \qquad \textit{Eq. 2}$$

where *m* is the *m/z* value of the ion of interest, and w_{05} is the peak width at full width half maximum (FWHM) [25].

Mass accuracy is defined as the difference between measured accurate mass (*accurate mass*) and calculated mass (*exact mass*). It is often presented as the relative mass accuracy, given in parts per million (ppm), where the absolute mass accuracy (*accurate mass – exact mass*) is divided by the mass (*accurate mass*) of the ion it is determined for, as shown in **Equation 3** [25].

$$Relative\ Mass\ Accuracy\ (ppm) = \frac{exact\ mass - accurate\ mass}{accurate\ mass} \cdot 10^6 \qquad \textbf{\textit{Eq. 3}}$$

High mass resolution enables separation of ions with similar *m/z* values, and high mass accuracy (low ppm) enables more accurate detection of an ions *m/z* value [25].

Several mass spectrometers are available, each with their advantages and disadvantages. Quadrupole, time-of-flight (TOF), Fourier transformation-ion cyclotron resonance (FT-ICR) and orbitrap are the most common mass spectrometers. **Table 1** compares these with regard to resolving power, mass accuracy, and upper mass limit. Hybrid mass spectrometers also exist, combining two or more mass analyzers.

Table 1: Comparing the resolving power, mass accuracy, and upper mass limit of different mass spectrometers. Mass resolution is given for full width half maximum (FWHM), mass accuracy is given in parts per million (ppm) and the upper mass limit is given in Dalton. Table adapted from [26, 27].

Mass spectrometer	Mass resolution (FWHM)	Mass accuracy (ppm)	Upper mass limit (Da)
Triple quadrupole (QqQ)	Unit resolution	50	4 000
Time-of-flight (TOF)	20 000	3	350 000
Orbitrap	100 000	2	4 000
Fourier transform ion cyclotron resonance (FT-ICR)	1 000 000	1	4 000

Triple quadrupole (QqQ) instruments are the workhorses of targeted analysis, with high sensitivity and selectivity. The resolving power of these instruments are low, making them

unsuitable for detection of several unknown metabolites at the same time. TOF instruments are capable of high resolution, but the linear range and mass accuracy is still lower than that of orbitrap and FT-ICR instruments. FT-ICR can provide the highest resolution and mass accuracy, but because of the high cost of these instruments they are not widely available. Orbitrap instruments provide high resolution, mass accuracy and sensitivity, is much used for global metabolomics [26].

Q Exactive Orbitrap

High resolving power and high mass accuracy are characteristics of the Q Exactive Orbitrap, making it an appropriate choice of MS for global metabolomics [28]. **Figure 10** shows a schematic view of the main constituents in the Q Exactive Orbitrap.

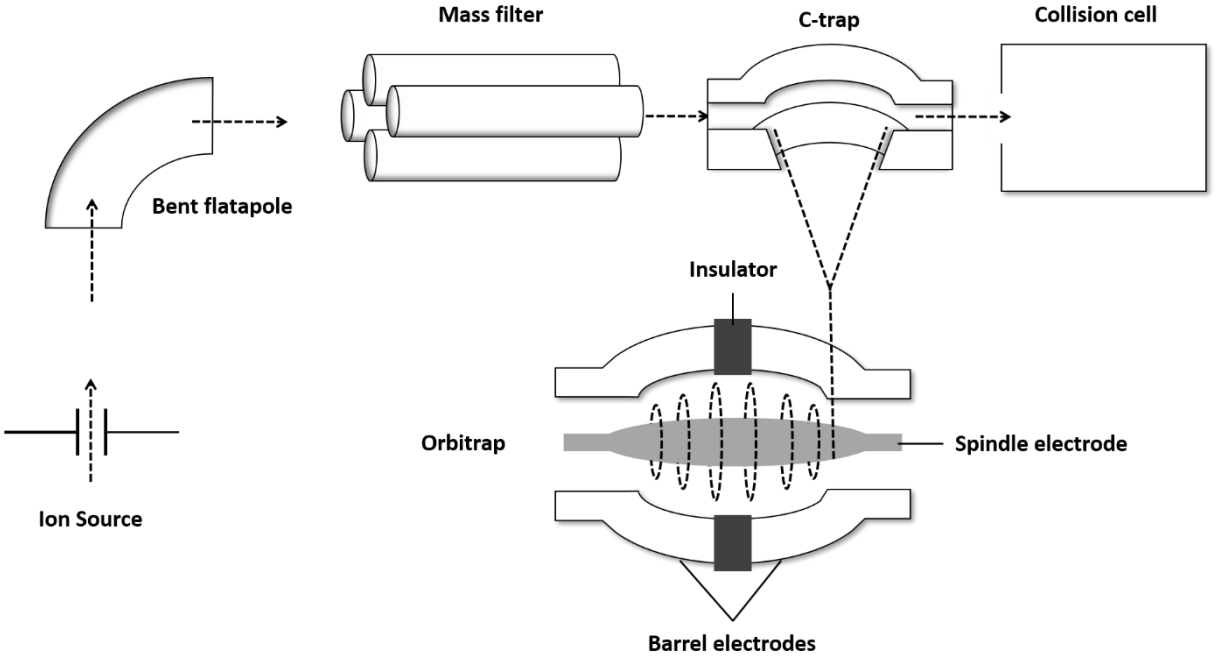

Figure 10: The main constituents of the Q Exactive Orbitrap mass spectrometer. Ions enter from the ion source. The bent flatapole transmits ions in a 90° curvature to the mass filter quadrupole, C-trap, collision cell, orbitrap mass analyzer. Figure adapted from [29].

Metabolites enter from the ion source, and a bent flatapole with a 90°-degree angle removes neutral gas jets and solvent droplets. Neutral components are not affected by the electric field and collide with the walls of the bent flatapole. A quadrupole functioning as a mass filter transmit ions with the appropriate *m/z* value [28]. The C-trap accumulates, stores, and thermalizes ions transmitted by the mass filter before injection into the orbitrap. The C-trap ensures injection of ions with the same speed and angle, avoiding collisions with the spindle

or barrel electrodes of the orbitrap. When enough ions are collected, the ions are injected as a packet into the Orbitrap using high voltage electric pulses [28, 30]. The Orbitrap mass analyzer consist of an inner spindle shaped electrode, and two outer barrel electrodes, separated by an insulator. The spindle electrode is held at a high voltage, and the two barrel-electrodes are held close to ground potential. The electric field cause the ions to oscillate along the spindle electrode in a complex spiral pattern. The frequency of oscillation is inversely proportional to the square root of the *m/z* value of a given ion [31]. The oscillation frequency induces an image current on the barrel electrodes, which is amplified and measured. With FT, the current is decomposed into its component frequencies and *m/z* values [30, 31].

Fragmentation of metabolites can be done in the higher-energy collisional dissociation (HCD) cell. For the Q Exactive Orbitrap, a specified number of ions with the highest intensity of that scan are sent to the HCD cell for fragmentation, in what is referred to as data-dependent acquisition (DDA). After fragmentation, the ions return to the C-trap before injection to the orbitrap [28].

2.3.2 Electrospray Ionization

ESI is a widely used ion source for liquid chromatography-mass spectrometry (LC-MS) [32]. With ESI, ions in solution are transformed into gas phase ions [32]. The sample solution enters a spray capillary applied with a high voltage. A voltage between 3-6 kV is applied, and can be either positive or negative [33]. In the positive ionization mode, a negative voltage is applied, and for the negative ionization mode a positive voltage is applied. The high voltage results in cone formation at the end of the capillary, referred to as a “Taylor cone”. A fine jet of ions is sprayed from the cone, and a coaxial nebulizing gas (N_2) flow along the capillary assists in directing the droplets. The jet breaks in to small, highly charged droplets. The solvent evaporates from the droplet, increasing the charge density. When the electrostatic repulsions become greater than the conservative surface tension of the droplet, it disintegrates into smaller subunits. This droplet shrinkage and disintegration occurs in several steps, resulting in gas phase ions [33]. **Figure 11** shows the formation of positive ions.

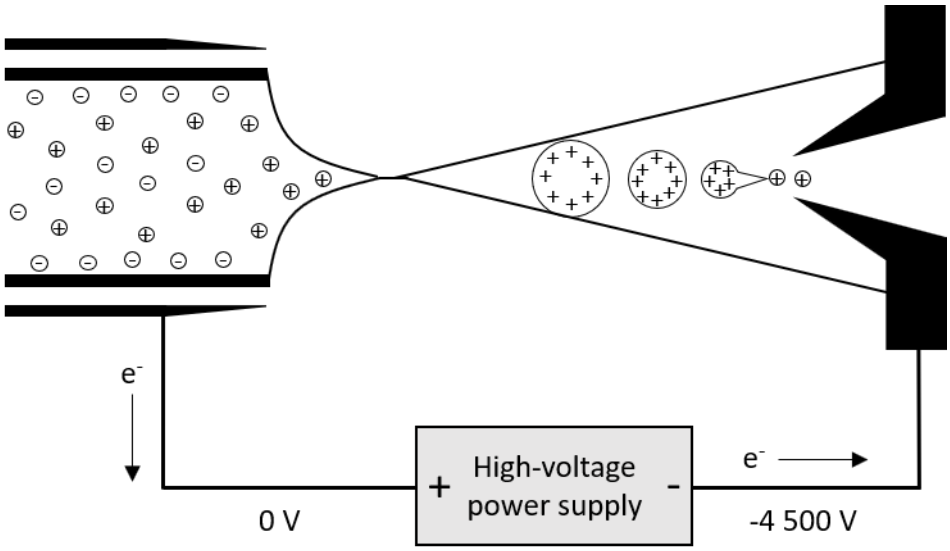

Figure 11: Electrospray ionization, in positive mode. The liquid enters a capillary with a co-axial flow of nebulizing gas. A "Taylor cone" is formed at the end of the capillary because of the strong electric field applied, and a fine spray of charged particles emit from the "Taylor cone". The charged droplets shrink because of solvent evaporation, and eventually smaller droplets are formed as the charges repel each other. This process repeats itself, until gas phase ions are formed and enter the MS inlet. Figure adapted from [34].

Ions are detected as molecular ions or as adducts. Molecular ions are found as $[M+nH]^{n+}$ or $[M-nH]^{n-}$ for positive and negative ionization modes, respectively, were M is the monoisotopic mass of the compound, H is the mass of a proton, and n is the number of protons accepted or donated. Adducts are formed by cationization or anionization with cations or anions present in the solution. In positive ionization, the $[M+Na]^{+}$ and $[M+K]^{+}$ adducts are readily observed as sodium and potassium salts are present on glassware, or as impurities in solvents [32].

Ion suppression and ion enhancement can be a problem when using ESI. Ion suppression or enhancement is the decrease or increase in detector response and occurs because metabolites compete with other compounds in the sample to become ionized. Ion suppression or enhancement can be reduced by using clean glassware, avoiding plastics, and reducing the flow rate of sample introduction. Chromatographic separation prior to ESI is also very useful for reducing ion suppression or enhancement, as less ions enter the ion source simultaneously [33].

2.3.3 High Performance Liquid Chromatography

High performance liquid chromatography (HPLC) can be used to separate metabolites prior to MS detection, which increases the MS resolution [21, 35, 36]. With HPLC, metabolites are separated in time, because of interactions with a mobile and a stationary phase [37]. A typical HPLC set up is shown in **Figure 12**.

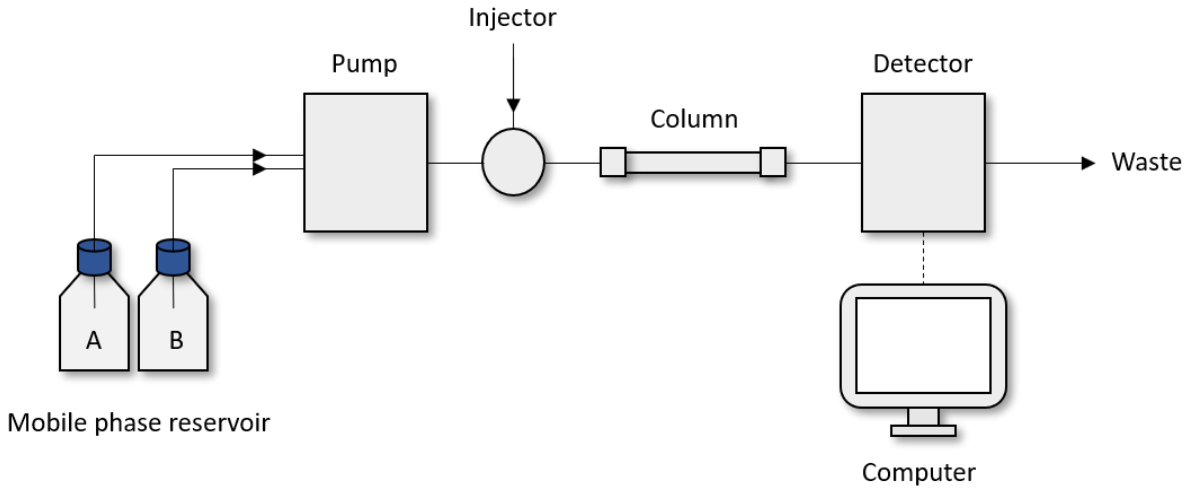

Figure 12: Schematic representation of a high-performance liquid chromatography (HPLC) set up. The pump makes mobile phase A and B flow through the analytical column. The sample is injected, and its components are separated on the analytical column, before detection. A computer is used for viewing the results and controlling the instrument.

The separation of metabolites occurs on the column. Different column types are available, with different dimensions and content. Most common are particle packed columns, but monolith filled and open tubular columns are also available [37]. In this project, packed columns were used. The particles in packed columns are spherical, porous beads with a uniform size. Particle size directly affects the chromatographic efficiency. Lowering the particle size increases chromatographic efficiency, but it also increases the pressure in the column. Conventional packed HPLC columns have an inner diameter in the range of 2-5 mm, and a length of 3-25 cm. Capillary and nanoflow columns have inner diameter ranges of 0.1-0.5 mm and 0.01-0.10 mm, respectively [37].

Several stationary phases are available for LC, and the type of stationary phase used governs the separation principle. Some of the separation principles available are normal phase (NP), reversed phase (RP), hydrophilic interaction (HILIC), and size exclusion (SEC). In metabolomics, RP materials are the most common [38]. For reversed phase-liquid chromatography (RP-LC), the stationary phase is hydrophobic, thus separating compounds according to hydrophobicity. In this project, a diphenyl stationary phase was used.

The mobile phase (often called eluent) is the liquid delivered by the pumping system at a given flow, and elutes the metabolites out of the column [37]. The time the metabolite uses to reach the end of the column and the detector, is called the retention time. The mobile phase composition can be isocratic, meaning constant throughout the separation, or delivered as a gradient, meaning that there is a change in the mobile phase composition throughout the analysis. Gradient elution is essential when separating complex samples, as is the case in metabolomics. It ensures elution of metabolites within a reasonable timeframe, as well as providing narrow peaks, compared to isocratic elution. In this project, gradient elution was used. The mobile phase is polar in RP-LC, often as water in combination with relatively polar organic solvents, e.g. acetonitrile (ACN) or methanol (MeOH). A mobile phase with high water content has lower eluent strength compared to a mobile phase with high organic solvent content.

HPLC-ESI-Q-Exactive Orbitrap MS was used as the analytical platform for global metabolomics in this project.

2.4 Dried Blood Spots

The choice of biofluid and ways of sampling them is an important part of the experimental setup of a global metabolomics approach. Dried blood spot (DBS) sampling has been used in newborn screening because of its many advantages compared to traditional venipuncture sampling [39]. Specially made lancets are used for puncturing the skin, and capillary blood from a finger (or foot) is collected on filter cards. DBS sampling is less invasive because of the low amount of blood that is drawn, and the DBS samples take up less space than a traditional blood sample. The card can also be stored and transported at ambient temperatures [39]. Another advantage is that sampling can be performed by anyone with a little introduction to the procedure. These benefits make DBS an attractive sampling technique for studies with many participants, and it has been implemented for metabolomics [40, 41] and a lipidomics studies [38, 42].

The amount of blood in the spot varies, depending on person and card type. The type of card used in this project is shown in **Figure 13**, and the spot had a diameter of 1.2 cm, holding approximately 50 µL of whole blood. The whole spot, or only a part of the spot can be used for analysis. A punched-out disk with a diameter of 3.2 mm, contains about 2.5 to 5 µL blood

[38]. DBS cards are made of a non-cellulose or cellulose matrix with specific pore size and thickness. Commercial DBS cards are available, namely Whatman 903, FTA DMPK type A, B, C, and FTA Elute card (GE Healthcare) [43].

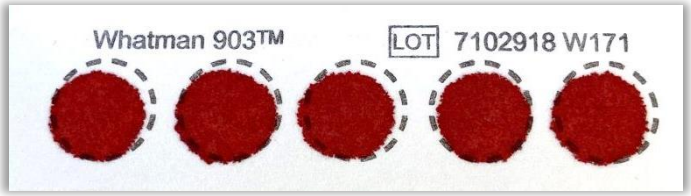

Figure 13: Blood spots on a filter card. One drop of blood is applied to each circle and dried, before storage or analysis.

Hematocrit is the portion of blood volume that is occupied by red blood cells, and levels vary from person to person. Blood viscosity is directly proportional to the hematocrit level, which can influences the spot size and distribution on the card, and directly affects quantification [44].

Drying of the blood spots before transport or storage is important. Generally, drying for 3-4 hours at room temperature away from direct sunlight is recommended. The effect of long term storage on is not clear for all metabolites [44]. Acylcarnitines for instance, are unstable if stored at room temperature on DBS due to hydrolysis, but stability increases to up to 330 days when stored at -18 °C or lower [45]. The stability of metabolites should therefore be considered when storing DBS [46].

2.4.1 Extraction of Dried Blood Spots

Sample preparation of DBS requires extraction of metabolites from the filter card to an appropriate solvent. In the targeted analysis of DBS for newborn screening, 80% acidic methanol is often used for extraction of amino acids and acylcarnitines [47]. For global metabolomics purposes, the sample preparation and extraction procedure of DBS should be able to extract a large variety of metabolites with a wide range of physicochemical properties [48]. Optimizing the extraction of DBS for global metabolomics can therefore be challenging.
It is important to know what type of interaction the solvent and metabolite can have. By using an extraction solvent that interacts strongly with the metabolite, the extraction of a metabolite can be improved [49].

The types of molecular interactions occurring in liquid extraction are hydrophobic interactions, dispersion interactions, dipole interactions or hydrogen bonding interactions. The

different molecular interactions are listen in order of increasing strength [49], and are illustrated in **Figure 14.**

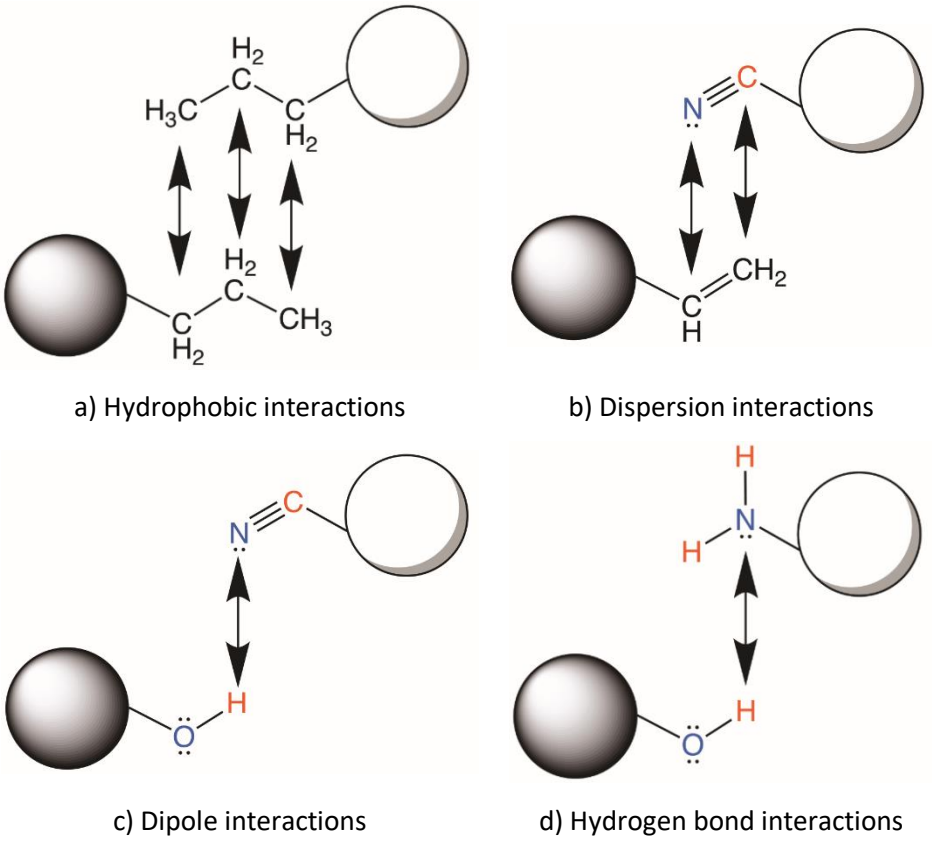

Figure 14: Molecular interactions that can occur during liquid extraction. a) Hydrophobic interactions are nonpolar interactions based on Van der Waals forces. b) Dispersion interactions occur between nonpolar electron-rich molecules and polar charged molecules. c) Dipole interactions occur between two molecules with a permanent dipole moment. d) Hydrogen bond interactions are a type of dipole interaction, between a hydrogen bond donor and acceptor. Blue atoms symbolize a negative dipole, and red atoms positive dipole. Figure adapted from [49].

Hydrophobic interactions occur between non-polar hydrocarbon moieties near each other. The electron distribution is distorted, causing small temporary dipole moments in the molecular structure. Dispersion interactions also known as induced dipole interactions, are weak attractive interactions between non-polar electron rich molecules and polar molecules. The polar molecule disrupts the electron density of the non-polar molecule, inducing a dipole moment in the electron rich non-polar molecule. Dipole interactions are attractive electrostatic forces between two molecules with permanent dipole moments. The positive end of one molecule is attracted to the negative end of the other. Hydrogen interactions are another type of dipole interactions, where the interaction occurs between a hydrogen that is a part of a polar bond (hydrogen donor) and an electronegative atom with a lone-pair of electrons (hydrogen acceptor) [49]. The solubility of a compound in a given solvent will be determined

by the number of individual contributions from the different interactions mentioned above, and if the analyte contain more than one functional group, predicting the solubility is further complicated [50]. When developing a procedure for extraction of DBS for global metabolomics, a compromise must be made to get the best metabolite coverage as possible, while knowing the limits of the procedure [51, 52].

2.4.2 Snyder's Solvent Selectivity Triangle

Selection of an appropriate solvent for extraction of metabolites can be guided by using the Snyder's solvent selectivity triangle, shown in **Figure 15.** This model is an alternative way of considering solubility, using the concept of polarity. Polarity in this model is defined as a compounds relative ability to engage in in strong interactions with other polar molecules. The polarity represents the ability of a molecule to enter interactions of all kinds, and the relative polarity is the sum of all possible interactions [50, 53]. Using this assumption, solvents are grouped in eight different groups, according to their properties for making selective interactions as proton donors (X_d), proton acceptors (X_e), and permanent dipoles (X_n) [54, 55].

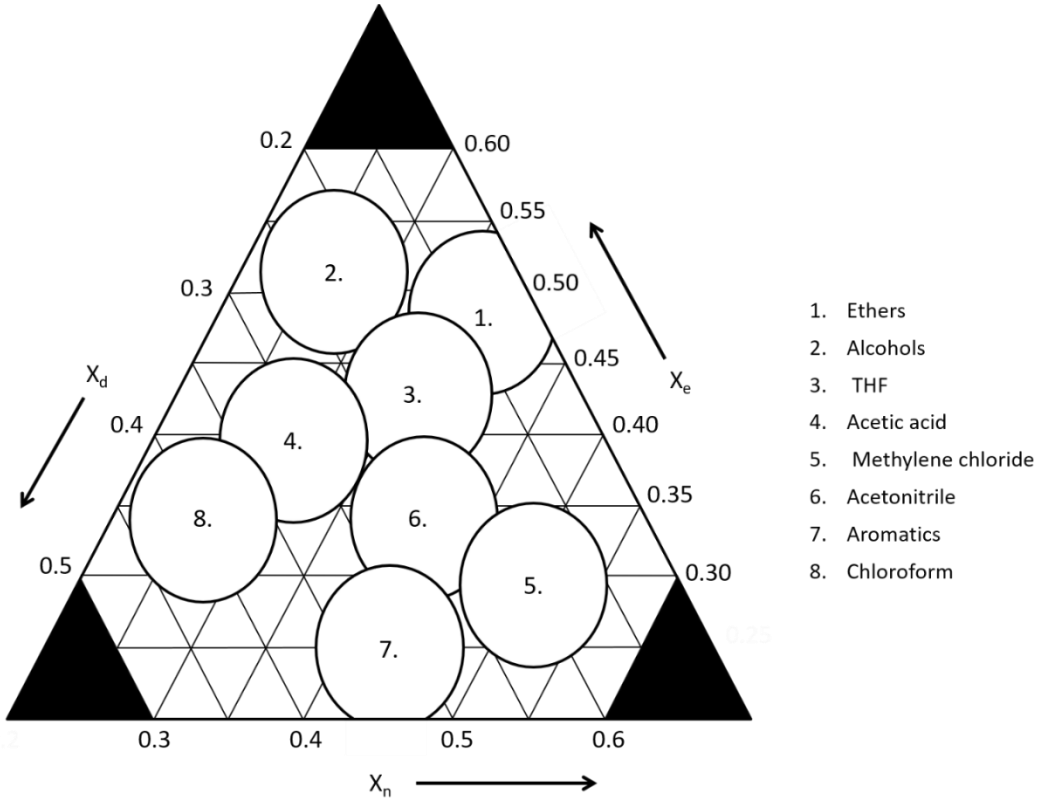

Figure 15: Snyder's Solvent Selectivity Triangle. Common organic solvents are classified according to proton donor (X_d), proton acceptor (X_e) and dipole-interacting properties (X_n). Adapted with permission from [55].

The values for X_d, X_e, and X_n are ratios calculated based on each solvents gas liquid partitioning coefficient *K''* and a polarity value *P'*, and the sum of the values X_d, X_e, and X_n is one [50, 55]. The values do not take into account the ability of forming dispersive interactions [50, 53]. Differences in solubility for solvents of similar polarity are collectively referred to as solvent selectivity and indicates the solvents ability to dissolve different solutes of similar polarity. Solvents that interact with primarily one of these interactions are have a high value for X_d, X_e, or X_n, and is placed in the corner of the triangle. Solvents that can interact with several interactions are grouped in the middle of the triangle. The biggest difference in interaction and extraction should be seen between solvents of different groups [50, 54].

Solvents from group one, two and six were chosen for the extraction of spotted standards and DBS in this thesis. To represent group one, methyl tert-butyl ether (MTBE) was chosen. To represent group two, several solvents were chosen, MeOH, iso-propanol, 1-propanol, and 1-butanol. Group six was represented by ACN. The different groups were chosen to find if extraction of DBS was affected by the different selectivity of the solvents.

2.5 Global Metabolomics Workflow

The metabolomics workflow follows a generic workflow, which includes study design, data acquisition by the analysis of samples, data processing, identification, and interpretation of the results. **Figure 16** shows the typical steps of a global metabolomics workflow. The objective is to acquire information about a wide range of metabolites present in multiple metabolic pathways, and that the data can provide insight into metabolic changes related to the biological question being asked [9]. This approach is hypothesis generating, and the hypothesis generated can be further tested in a more targeted approach to be confirmed or denied [9].

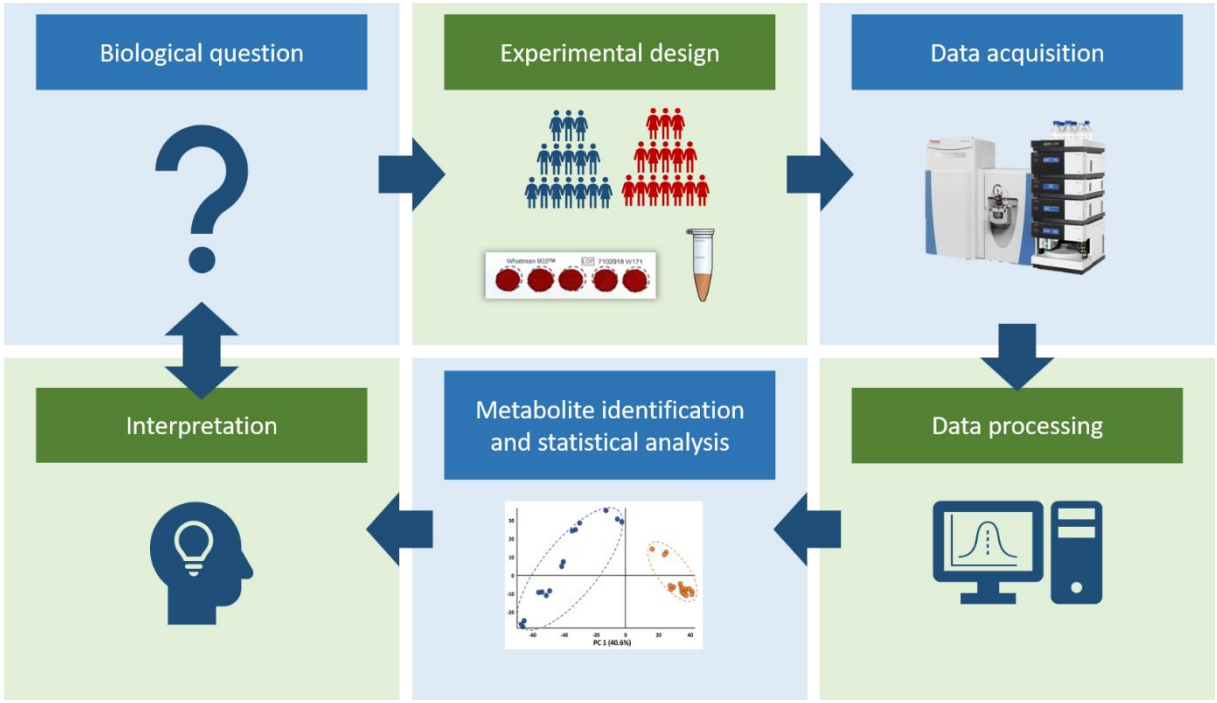

Figure 16: Typical metabolomics workflow. The experimental design includes collection and treatment of samples. Data is acquired by the analytical instruments and is followed by data alignment. Metabolites are identified (annotated) and statistical analysis can be done. Interpretation of the results is time-consuming and may generate a hypothesis related to the biological question. Figure adapted from [56, 57].

Sample type and instruments used for data acquisition that are appropriate for use in global metabolomics has already been discussed. In global metabolomics, hundreds to thousands of metabolites are detected, and the chemical identity of these metabolites are not known prior to data acquisition. Internal standards can be used for a selection of metabolites, but it impossible to use them in a comprehensive manner. Because of this, it is not possible to generate metabolite specific calibration curves for all metabolites, making the global metabolomics approach semi-quantitative [58].

Identification of metabolites is a challenge and can be divided into different levels of confidence [59], as showed in **Figure 17**.

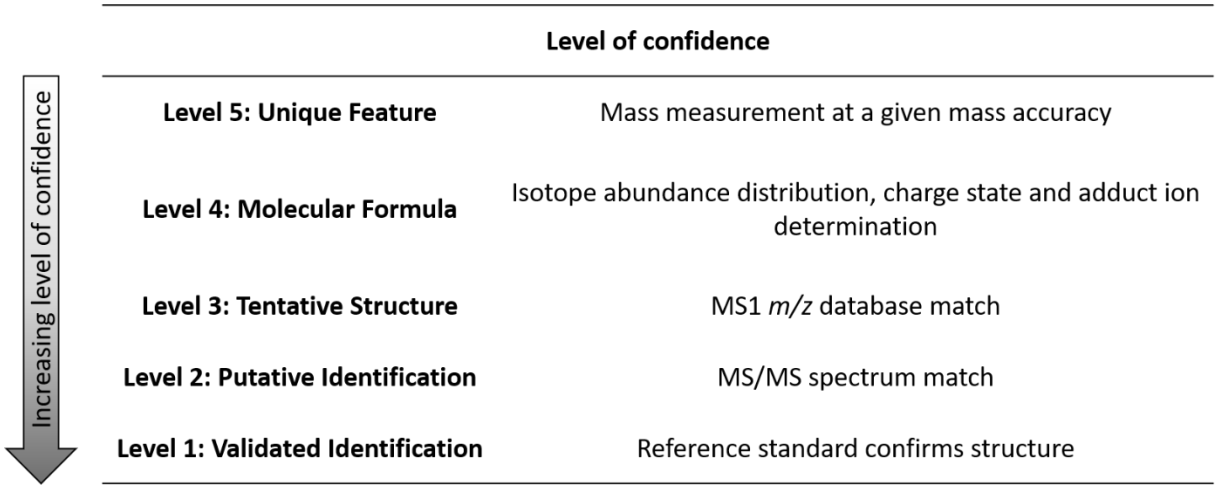

Figure 17: The different levels of confidence for metabolite identification using mass spectrometry. The lowest level of confidence is obtained by mass measurements at a given mass accuracy. The level of confidence is increased if isotopic patterns are known and can help identify a molecular formula. A tentative structure can be obtained by database searching. Matching the fragmentation patterns with that found in databases increases the level of confidence. A validated identification is obtained by analyzing a reference standard of the given metabolite at identical analytical conditions. Figure adapted from [59].

The lowest levels of confidence in metabolite identification is the measurement of a *m/z* at a given mass accuracy. This can be used for database searches for the molecular formula, but it will potentially result in many potential candidates. The level of confidence can be increased with additional information, like retention time, isotopic pattern, identifying adducts, and fragmentation. The highest level of confidence is obtained by analysis of a reference standard under identical analytical conditions [59].

2.5.1 Quality Control in Global Metabolomics

A challenge for global metabolomics is the desire to maximize the number and diversity of metabolites measured, while maintaining high precision, repeatability and reproducibility [9]. To assess the quality of the collected data, some type of quality control sample should be implemented. The quality control should represent a qualitative and quantitative composition of the subject samples being analyzed, which can be obtained by using a pooled quality control (PQC) [60]. The PQC is made by taking an aliquot of each sample, and mixing to a homogenous pooled sample, the PQC. Aliquots from the PQC are taken out, and treated the same way as the rest of the samples [58], as shown in **Figure 18**.

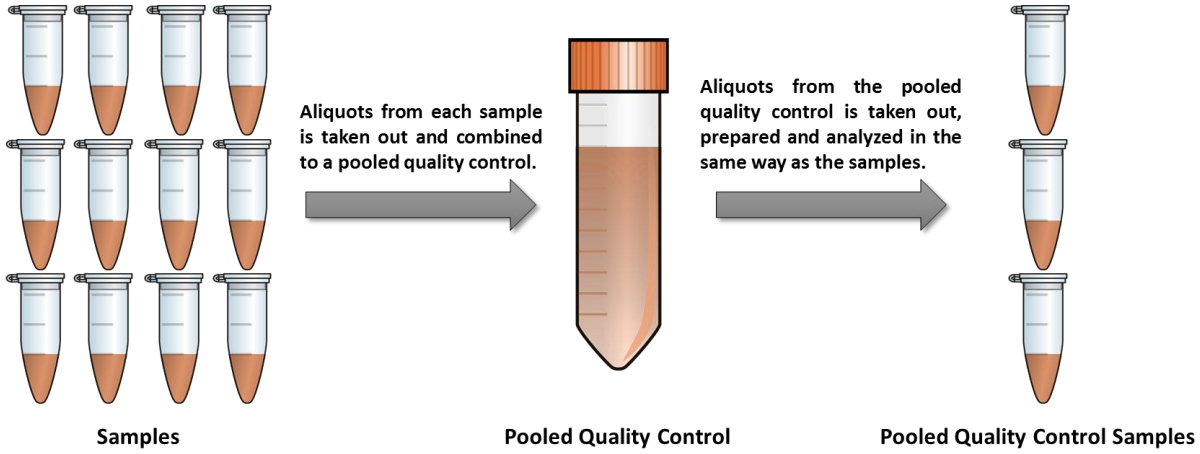

Figure 18: Preparation of pooled quality control samples (PQC). To make a PQC, a small aliquot of each sample is taken out, and combined. Aliquots of the PQC are then taken out and treated the same as the rest of the samples. Figure adapted with permission from [58].

The PQC will mimic the sample matrix and metabolite composition of the samples analyzed quantitatively and qualitatively [60]. Using PQCs makes evaluating the precision of each metabolite detected possible. It should be noted that this can only be done if the metabolite is present in the PQC. The PQC can also be used for conditioning the analytical platform prior to analysis, and for correcting for systematic measurement bias [58].

2.6 Aim of Study

The aim of this study was to:

a) Determine the lipid coverage of the DBS LC-ESI-Q Exactive MS global metabolomics method, and to find if altering the solvent used for extraction of DBS affected lipid coverage.

b) Investigate the methods ability to detect physiological changes in the metabolome and lipidome, while implementing PQCs.

The lipid coverage of the method was investigated using a set of standards representing the metabolome and lipidome. The standards were applied to blank filter cards, as well as spiked to DBS, and extracted by a set of extraction solutions. The extraction solutions were made using organic solvents, which were selected based on their position in the Snyder's solvent selectivity diagram. The organic solvents were: MeOH, ACN, iso-propanol, 1-propanol, 1-butanol, and MTBE. The solvents were also chosen based their logP value and water solubility. The extraction solutions were made in high, medium, and low volume/volume ratios with 0.1% formic acid. The hypothesis was that solvents from different groups in the Snyder solvent selectivity diagram will have different selectivity, which could affect lipid coverage. It was also thought that solvents with higher logP values would provide better lipid coverage than that of solvents with lower logP.

To assess the methods ability to detect changes in the metabolome and lipidome, DBS were taken from healthy volunteers participating in a high intensity workout. The hypothesis was that exercise has an immediate impact on metabolism, which can be detected using the global metabolomics approach. The PQCs would provide information about data precision.

3 Experimental

3.1 Small Equipment

The analytical balance weight used was AG 245 from Mettler-Toledo (Columbus, OH, USA). The pipettes used were Fisherbrand Elite adjustable-volume single-channel pipettes, obtained from Fisher Scientific (Waltham, MA, USA). The syringe used for direct injection into the MS was obtained from SGE Analytical Sciences (Victoria, Australia), and had a volume of 1 mL.

3.2 Chemicals

3.2.1 Solvents

The solvents used are listed in **Table 2**, together with its abbreviation, purity, the manufacturer, and place of origin. All water used was type 1 water, (resistivity of 18.2 MΩ•cm at 25 °C) taken from a Millipore Milli-Q purification system with a Q-guard cartridge, a Quantum cartridge, and a filter membrane with 0.22 μm pores purchased from Merck. Type 1 water is referred to as water from here on.

Table 2: List of solvents used, with abbreviation, purity, manufacturer, and place of origin.

Name	Abbreviation	Grade	Manufacturer	Place of origin
Methanol	MeOH	LC-MS	Rathburn Chemical Lrd	Walkerburn, Scotland
Acetonitrile	ACN	LC-MS	Merck KGaA	Darmstadt, Germany
1-propanol		LC-MS	Merck KGaA	Darmstadt, Germany
Iso-propanol		LC-MS	Merck KGaA	Darmstadt, Germany
1-butanol		LC	Merck KGaA	Darmstadt, Germany
Methyl tert-butyl ether	MTBE	HPLC, ≥99.8%	Sigma-Aldrich	St. Louis, MO, USA
Formic acid	FA	98-100%	Merck KGaA	Darmstadt, Germany

3.2.2 Reagents

Ammonium acetate (NH_4Ac) with MS purity was obtained from Sigma-Aldrich (Steinheim, Germany). Adenosine 5′-monophosphate (AMP) disodium salt and guanosine 5'-monophosphate (GMP) disodium salt with ≥99.0% (HPLC) purity was obtained from Merck Life Science AS (Darmstadt, Germany). LightSPLASH™ LIPIDOMIX® quantitative mass spec primary standard and EquiSPLASH™ LIPIDOMIX® quantitative isotopically labeled internal standards of lipids were both obtained from Avanti® Polar Lipids inc, (Alabaster, AL, USA). The contents of the LightSPLASH™ LIPIDOMIX® and EquiSPLASH™ LIPIDOMIX® are listed with systematic name and abbreviation in **Table 3** and **4**, respectively. Both mixtures had a volume of 1 mL, and the concentration of each compound was 100 µg/mL solved in MeOH. The compounds in the mixture will be referred to as their abbreviations from here on.

Table 3: Compounds in the LightSPLASH™ LIPIDOMIX®, with systematic name and abbreviation.

Systematic name	Abbreviation
1-pentadecanoyl-2-(9Z-octadecanoyl)-glycero-3-phosphocholine	PC (15:0/18:1)
1-(9Z-octadecenoyl)-2-glycero-3-phosphocholine	LPC (18:1)
1-pentadecanoyl-2-(9Z-octadecenoyl)-glycero-3-phosphoethanolamine	PE (15:0/18:1)
1-(9Z-octadecenoyl)-2-glycero-3-phosphoethanolamine	LPE (18:1)
1-pentadecanoyl-2-(9Z-octadecenoyl)-glycero-3-phospho-(1'-sn-glycerol)	PG (15:0/18:1)
1-pentadecanoyl-2-(9Z-octadecenoyl)-glycero-3-phospho-(1'-myo-inositol)	PI (15:0/18:1)
1-pentadecanoyl-2-(9Z-octadecenoyl)-glycero-3-phosphoserine	PS (15:0/18:1)
1-pentadecanoyl-2-(9Z-octadecenoyl)-3-pentadecanoyl-sn-glyserol	TG (15:0/18:1/15:0)
1-pentadecanoyl-2-(9Z-octadecenoyl)-sn-glycerol	DG (15:0/18:1)
1-(9Z-octadecenoyl)-glycerol	MG (18:1)
Cholest-5-en-3β-yl (9Z-octadecenoate)	CE (18:1)
N-(9Z-octadecenoyl)-sphing-4-enine-1-phosphocholine	SM (d18:1/18:1)
N-(pentadecanoyl)-sphing-4-enine	Cer (d18:1/15:0)

Table 4: Compounds in the EquiSPLASH™ LIPIDOMIX® quantitative isotopically labeled internal standard, with systematic name and abbreviation.

Systematic name	Abbreviation
1-pentadecanoyl-2-(9Z-octadecanoyl (d7))-glycero-3-phosphocholine	PC (15:0/18:1 (d7))
1-(9Z-octadecenoyl (d7))-2-glycero-3-phosphocholine	LPC (18:1 (d7))
1-pentadecanoyl-2-(9Z-octadecenoyl (d7))-glycero-3-phosphoethanolamine	PE (15:0/18:1 (d7))
1-(9Z-octadecenoyl (d7))-2-glycero-3-phosphoethanolamine	LPE (18:1 (d7))
1-pentadecanoyl-2-(9Z-octadecenoyl (d7))-glycero-3-phospho-(1'-sn-glycerol)	PG (15:0/18:1 (d7))
1-pentadecanoyl-2-(9Z-octadecenoyl (d7))-glycero-3-phospho-(1'-myo-inositol)	PI (15:0/18:1 (d7))
1-pentadecanoyl-2-(9Z-octadecenoyl (d7))-glycero-3-phosphoserine	PS (15:0/18:1 (d7))
1-pentadecanoyl-2-(9Z-octadecenoyl)-3-pentadecanoyl (d7)-sn-glyserol	TG (15:0/18:1 (d7)/15:0)
1-pentadecanoyl-2-(9Z-octadecenoyl (d7))-sn-glycerol	DG (15:0/18:1 (d7))
1-(9Z-octadecenoyl (d7))-glycerol	MG (18:1 (d7))
Cholest-5-en-3b-yl (9Z-octadecenoate (d7))	CE (18:1 (d7))
N-(9Z-octadecenoyl (d9))-sphing-4-enine-1-phosphocholine	SM (d18:1/18:1 (d9))
N-(pentadecanoyl)-sphing-4-enine (d7)	Cer (d18:1 (d7)/15:0)

3.3 Solutions

3.3.1 Stock Solution

A stock solution of 101 mM NH_4Ac was made by weighing out 3.8944 g NH_4Ac, and solving in 500 mL of water, giving a concentration of 101 mM. A stock solution of 5.5 mM AMP was made by weighing out 21.6 mg the AMP disodium salt and solving in 10 mL of water. Similarly, a stock solution of 5.2 mM GMP was made by weighing 21.2 mg of the GMP disodium salt and solving in 10 mL water. All stock solutions were kept refrigerated at 4 °C prior to use.

3.3.2 Extraction Solutions

Extraction solutions containing high (80%), medium (50%) and low (20%) volume/volume percentages of organic solvent with 0.1% FA were prepared, and their name and contents shown in **Table 5**. The solutions were stored at 4°C before use.

Table 5: Extraction solutions and their volume/ volume percentage content (v/v%) of organic solvent and 0.1% FA.

Name of extraction solution	Content, (v/v%)
Water	0.1% FA
80% MeOH	40 mL MeOH / 10 mL 0.1% FA
50% MeOH	25 mL MeOH / 25 mL 0.1% FA
20% MeOH	10 mL MeOH / 40 mL 0.1% FA
80% ACN	40 mL ACN / 10 mL 0.1% FA
50% ACN	25 mL ACN / 25 mL 0.1% FA
20% ACN	10 mL ACN / 40 mL 0.1% FA
80% iso-propanol	40 mL iso-propanol / 10 mL 0.1% FA
50% iso-propanol	25 mL iso-propanol / 25 mL 0.1% FA
20% iso-propanol	10 mL iso-propanol / 40 mL 0.1% FA
80% 1-propanol	40 mL 1-propanol / 10 mL 0.1% FA
50% 1-propanol	25 mL 1-propanol / 25 mL 0.1% FA
80% 1-propanol	10 mL 1-propanol / 40 mL 0.1% FA
40% 1-butanol + 40% MeOH	20 mL 1-butanol + 20 mL% MeOH / 10 mL 0.1% FA
25% 1-butanol + 25% MeOH	12.5 mL 1-butanol + 12.5 mL MeOH / 25 mL 0.1% FA
40% MTBE+ 40% MeOH	20 mL MTBE+ 20 mL MeOH / 10 mL 0.1% FA

3.3.3 Mobile Phases

The mobile phases used in this project are shown in **Table 6**. All mobile phases were kept at room temperature, approximately 30 °C. New mobile phases were prepared for each experiment. The original mobile phase was used, unless specifically stated.

Table 6: Mobile phases used in this project.

	Mobile phase A	Mobile phase B
Original mobile phases	Water + 0.1% FA	MeOH + 0.1% FA
Alternative mobile phases	Water + 10.1 mM NH_4Ac	MeOH + 10.1 mM NH_4Ac

3.3.4 Calibration Solution

Pierce LTQ Velos ESI Positive Ion Calibration solution and Pierce ESI Negative Ion Calibration solution were obtained from Thermo Fisher Scientific (Waltham, MA, USA) (stored at -18 °C).

3.3.5 Internal Standard Solutions

The EquiSPLASH™ LIPIDOMIX® quantitative isotopically labeled internal standard and LightSPLASH™ LIPIDOMIX® quantitative mass spec primary standard was diluted with 10 mL MeOH, and stored at -20 °C, giving the concentrations shown in **Table 7**, and are referred to as the isotopically labeled lipidome standard, and the lipidome standard from this point.

Table 7: Contents of the isotopically labeled lipidome standard and the lipidome standard, with name of compounds and concentration.

Isotopically labeled lipidome standard		Lipidome standard	
Compound	**Concentration (µM)**	**Compound**	**Concentration (µM)**
PC (15:0/18:1 (d7))	13.3	PC (15:0/18:1)	13.4
LPC (18:1 (d7))	18.9	LPC (18:1)	19.2
PE (15:0/18:1 (d7))	14.1	PE (15:0/18:1)	14.2
LPE (18:1 (d7))	20.5	LPE (18:1)	20.9
PG (15:0/18:1 (d7))	13.1	PG (15:0/18:1)	13.2
PI (15:0/18:1 (d7))	11.8	PI (15:0/18:1)	11.9
PS (15:0/18:1 (d7))	12.9	PS (15:0/18:1)	13.0
TG (15:0/18:1 (d7)/15:0)	12.3	TG (15:0/18:1 /15:0)	12.4
DG (15:0/18:1 (d7))	17.0	DG (15:0/18:1)	17.2
MG (18:1 (d7))	27.5	MG (18:1)	28.0
CE (18:1 (d7))	15.2	CE (18:1)	15.4
SM (d18:1/18:1 (d9))	13.5	SM (d18:1/18:1)	13.7
Cer (d18:1 (d7)/15:0)	18.8	Cer (d18:1/15:0)	19.1

A standard mixture named the metabolome standard was obtained, and its content are shown in **Table 8**. The mixture was stored refrigerated at 4 °C.

Table 8: Content of the metabolome standard with compound name and concentration.

Compound	Concentration (µM)
D3 Acylcarnitine C2	10.0
D3 Acylcarnitine C12	10.0
D3 Acylcarnitine C16	10.0
^{13}C Creatine	10.3
^{13}C2 Guanidinoacetic acid	10.0
D4 Succinic acid	10.2

3.4 Sample Preparation of Lipidome and Metabolome Standards Spotted to Filter Cards

Filter cards of the type Whatman 903 Protein Saver cards were obtained from GE Healthcare Bio-Sciences Corp. (Chicago, IL, USA). To the marked circle of the cards, 50 µL of the isotopically labeled lipidome standard and 50 µL of the metabolome standard was applied to for each of the five marked circles and was set to dry for four hours. One punch was taken from the center of the spot, with a manual puncher, obtained from McGill (Jacksonville, FL, USA). The punched-out disk was 3.2 mm in diameter, and three punches of clean paper were punched out in between spot punches to prevent contamination. The disk was collected in individual micro tubes (1.5 mL) from Sarstedt AG & Co (Nümbrecht, Germany). The disks were extracted in replicates of five with 100 µL of the extraction solutions listed in **Table 5**. After adding the extraction solution, the micro tube was mixed for 45 min, at 45 °C and 700 rpm with a Thermomixer Comfort from Eppendorf (Hamburg, Germany). After this, the liquid part of the sample was transferred in to individual HPLC vials with insert glass and caps, all from La-Pha-Pack (Langerwehe, Germany). The sample was then placed in the autosampler rack at 4 °C before analysis.

3.5 Sample Preparation of Spiked Dried Blood Spots

Approximately 4 mL venous blood from one healthy volunteer was collected in a Vacuette® Tube 4 mL K2E K3EDTA, obtained from Greiner Bio-One (Kremsmünster, Austria). To the blood, 40 µL of the lipidome standard and 40 µL of the metabolome standard was added and combined. To the Whatman 903 Protein Saver cards, 50 µL of the spiked whole blood was placed in the middle of the marked circles of the card, for each of the five marked circles. The card was set to dry for four hours. One punch was taken from the center of the blood spot, with the manual puncher. The punched-out disk was 3.2 mm in diameter, containing approximately 3 µL whole blood. The disks were collected in individual micro tubes. Three punches of clean paper were punched out in between spot punches to prevent contamination. In replicates of three, 100 µL of the high and medium percent organic solvent extraction solutions listed in **Table 5** were added to the micro tubes, and mixed for 45 min, at 45 °C and 700 rpm using the Thermomixer Comfort. Following this, the liquid part of the sample was transferred to an HPLC vial with insert glass and caps. The sample was then placed in the autosampler rack at 4 °C before analysis.

3.6 Sample Preparation of Dried Blood Spots

To Whatman 903 Protein Saver Cards, one drop of capillary blood was placed in the middle of the marked circle on the card, one for each circle. The card was set to dry for four hours. One punch was taken from the center of the blood spot, with the manual puncher. The disks were placed in individual micro tubes. To each of the micro tubes, 100 µL of 80% MeOH with 0.1% FA was added. The micro tubes were mixed for 45 min, at 45 °C and 700 rpm with the with the Thermomixer Comfort. For making PQCs, 20 µL from each sample was taken out and collected in a separate micro tube and whirl mixed to combine. The remaining 80 µL of each sample was transferred to separate HPLC vials with insert glass and caps. From the PQC, aliquots of 80 µL were taken out and transferred to separate HPLC-vials with insert glass and caps. Diluted PQCs were made by taking 16, 32, 48, and 64 µL of the PQC to separate micro tubes (1.5 mL), and adding 64, 48, 32, and 16 µL of MeOH, respectively to the separate micro tube. The contents were whirl mixing and transferred to individual HPLC vial with insert glass and caps.

From the PQC, 290 µL was taken out to a micro tube, and spiked with 5 µL of the 5.5 mM AMP stock solution and 5 µL of the 5.2 GMP stock solution. The sample was mixed to

combine and transferred to an HPLC vial with insert glass and caps. All samples were placed in the autosampler rack kept at 4 °C before analysis.

3.7 Liquid Chromatography-Mass Spectrometry Instrumentation and Settings

The liquid chromatography used was a Dionex Ultimate 3000 ultrahigh performance liquid chromatography (UHPLC) system coupled to a Q Exactive Orbitrap mass spectrometer, both from Thermo Scientific. The instrumental settings were set based on findings made by Sandås [61], Skogvold [62], and Arnesen [63]. The settings for the liquid chromatograph are shown in **Table 9** and **10,** and **Figure 23**. The analytical column used was a Pursuit XRs Diphenyl column (250 x 2.0 mm, particle size 3µm) from Agilent Technologies (Santa Clara, CA, USA).

Table 9: Initial settings for the liquid chromatograph used in this project.

Parameter	Setting
Mobile phase A	See **Table 6**
Mobile phase B	See **Table 6**
Gradient	See **Figure 19** and **Table 10**
Injection volume	2 µL
Column temperature	30 °C
Flow rate	300 mL/min
Analysis time	32.5 min
Re-equilibration time	10 min

Table 10: The mobile phase gradient used in all experiments.

Time (min)	Mobile phase B (%)
0	2
6	10
8.5	75
25	100
32.5	100

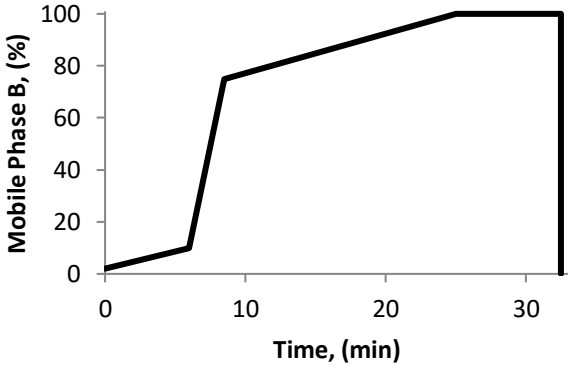

Figure 19: The mobile phase gradient used in all experiments.

The settings for the mass spectrometer and the electrospray ion source are found in **Table 11** and **12**, respectively.

Table 11: Settings for the mass spectrometer used in this project.

Parameter	Setting
Scan type	Full MS Data dependent acquisition (DDA), Top 5
Scan range (*m/z*)	80-1200
Polarity	Positive and negative
Resolution	Full MS: 70 000 DDA, Top 5: 17 500
Micro scans	1
Lock masses	Off
Automatic gain control target value	Full MS: 1e6 DDA Top 5: 5e5
Maximum injection time (ms)	Full MS: 250 DDA Top 5: 100
Stepped normalized collision energy	20, 50, 80
Analysis time (min)	32.5
Re-equilibration time (min)	10

Table 12: Settings for the electrospray used in this project.

Parameter	Setting
Sheat gas (N_2) flow rate (a.u.)	40
Auxiliary gas (N_2) flow rate (a.u.)	10
Sweep gas (N_2) flow rate (a.u.)	2
Capillary temperature (°C)	250
S-lens RF level	50
Auxiliary gas heater temperature (°C)	300
Electrospray voltage (kV)	|3.50|
Electrospray needle position	C

For the direct injection to mass spectrometer, the settings used are shown in **Table 13**. The flow rate of injection from the 1 mL syringe was 3.0 µL/min.

Table 13: Settings used for the direct injection to mass spectrometer.

Parameter	Setting
Scan type	Full MS
Scan range (*m/z*)	80-1200
Fragmentation	None
Polarity	Negative
Resolution	70 000
Micro scans	1
Lock masses	Off
Automatic gain control target value	3e6
Maximum injection time (ms)	200
Analysis time (min)	10

3.8 Computer Software

Xcalibur (version 4.2) was used for data acquisition and processing. Thermo Scientific SII for Xcalibur (version 4.2) was used for controlling the chromatographic instrument. Tune (version 2.11) was used for calibration of the mass spectrometry instrument and controlling the mass spectrometric parameters. Mass Calculator in Tune was used for calculating the exact masses of compounds. FreeStyle (version 1.6) was used for viewing chromatograms and mass spectra, for peak detection and peak integration. Compound Discoverer (version 3.1) was used for data processing, statistical analysis, and online database searches (mzCloud, ChemSpider, and Metabolica). All software mentioned above are from Thermo Scientific.

4 Results and Discussion

In this study the main objective was to investigate and describe the lipid coverage of a previously developed and evaluated DBS global metabolomics approach. This was done by selecting a variety of standards representing the polar and hydrophobic part of the metabolome, which were analyzed using the global metabolomics method. The analytical settings developed previously were preserved, and the extraction of DBS was changed to possibly improve the lipid coverage, and a selection of solvents were evaluated for standard and DBS extraction. To investigate the methods applicability for detecting changes in the lipidome and metabolome, DBS from seven healthy volunteers were analyzed before and after participating in a high intensity exercise session.

The minimum acceptance criteria for identification of compounds were set based on criteria commonly used in LC-MS global metabolomics [64, 65]. The MS identification criteria used were that mass accuracy had to be ±5 ppm for the exact mass of the molecular ion or a specific adduct. The detected peak had to have ten or more data points across the chromatographic peak, and a peak area higher than 10^4 a.u. The relative standard deviation (% RSD) for the peak area and retention time was calculated for compounds when possible. The accepted % RSD of peak area and retention time was <30% and <1%, respectively.

4.1 Retention and detection of lipids using the method

4.1.1 Compounds chosen to represent the lipidome

For this project two standard mixtures containing seven different glycerophospholipids, one triacylglycerol (TG), one diacylglycerol (DG), one monoacylglycerol (MG), one cholesterol ester (CE), one ceramide (Cer) and one sphingomyelin (SM), were selected to represent the lipidome. These lipids were chosen, as they represent a variety of different lipid groups with varied molecular weight and hydrophobicity. These lipids are expected, but not quantified in whole blood [66]. **Table 14** shows the names of the selected lipids, formula, structure, logP value, and the monoisotopic mass.

Table 14: Structure, formula, monoisotopic mass and logP of the compounds selected to represent the lipidome in this project. All values are from PubChem [67].

Compound name	Structure	Formula	Monoisotopic mass	LogP
PC (15:0/18:1)	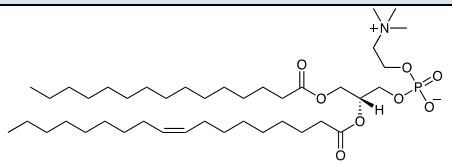	$C_{41}H_{80}NO_8P$	745.56216	13.1
LPC (18:1)	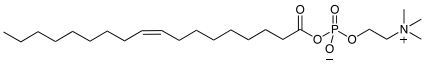	$C_{26}H_{52}NO_7P$	521.34814	5.7
PE (15:0/18:1)	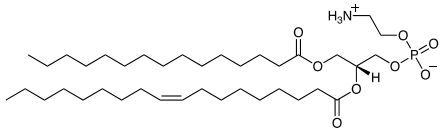	$C_{38}H_{74}NO_8P$	703.51520	9.9
LPE (18:1)	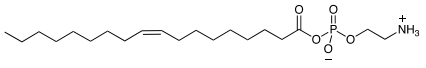	$C_{23}H_{46}NO_7P$	479.30119	2.5
PG (15:0/18:1)	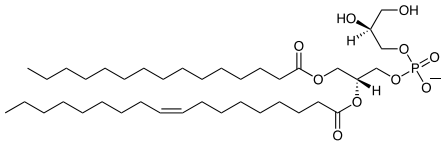	$C_{39}H_{75}O_{10}P$	734.50979	11.8
PI (15:0/18:1)	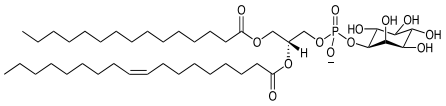	$C_{42}H_{79}O_{13}P$	822.52583	9.8
PS (15:0/18:1)	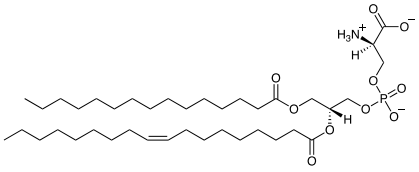	$C_{39}H_{74}NO_{10}P$	747.50504	9.5
TG (15:0/18:1/15:0)	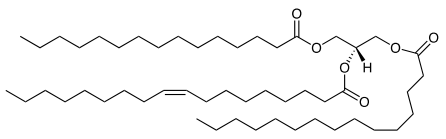	$C_{51}H_{96}O_6$	804.72069	21.0
DG (15:0/18:1)	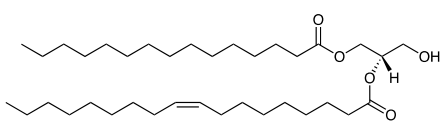	$C_{36}H_{68}O_5$	580.50668	13.7

Table 13 continues on the next page.

Compound name	Structure	Formula	Monoisotopic mass	LogP
MG (18:1)	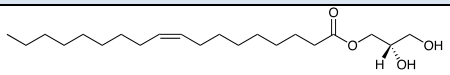	$C_{21}H_{40}O_4$	356.29266	6.5
CE (18:1)	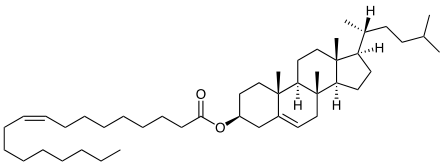	$C_{45}H_{78}O_2$	650.60018	16.6
SM (d18:1/18:1)	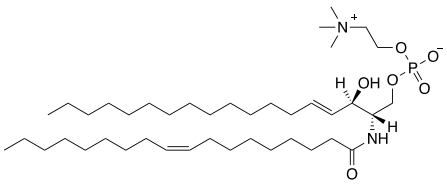	$C_{41}H_{81}N_2O_6P$	728.58323	12.4
Cer (d18:1/15:0)	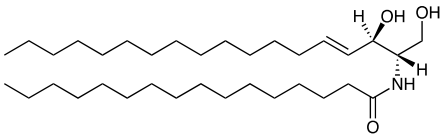	$C_{33}H_{65}NO_3$	523.49644	12.3

4.1.2 Compounds chosen to represent the metabolome

A standard consisting of isotopically labeled acylcarnitine C2, C12 and C16, creatine, guanidinoacetic acid and succinic acid was also used for representing the metabolome. These compounds were included to assess how changes affected the more hydrophilic metabolites in the metabolome. Acylcarnitines can be regarded as lipids but were included in the metabolome standard. **Table 15** shows the compounds name, formula, monoisotopic mass and logP values. The compounds were chosen to represent the metabolomes variation in molecular weight and hydrophobicity, and are compounds present in whole blood.

Table 15: Structure, formula, monoisotopic mass and logP of the compounds selected to represent the metabolome. All values are from PubChem [67].

Compound name	Structure	Formula	Monoisotopic mass	logP
Acylcarnitine C2	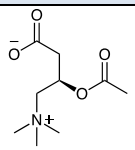	$C_9 H_{17}NO_4$	203.11576	-0.4
Acylcarnitine C12	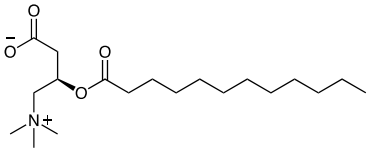	$C_{19}H_{37}NO_4$	343.27226	5.5
Acylcarnitine C16	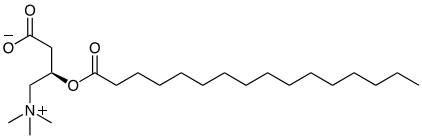	$C_{23}H_{45}NO_4$	399.33486	7.7
Creatine	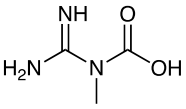	$C_4H_9N_3O_2$	131.06948	-1.2
Guanidinoacetic acid	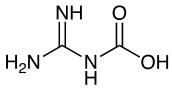	$C_3H_7N_3O_2$	117.05383	-1.6
Succinic acid	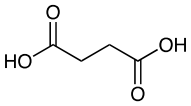	$C_4H_6O_4$	118.02661	-0.6

4.1.3 Not all lipids in the lipidome standard were detected using the method

The lipidome and metabolome standards were analyzed separately using the original method, to find the retention time of each compound. **Figure 20** shows the extracted ion chromatogram (EIC) of the detected lipids in positive and negative ionization mode, respectively. **Table 20** and **21** in **Appendix**, in section 6.2 shows the average and relative standard deviation (% RSD) for the peak area and retention time of these compounds.

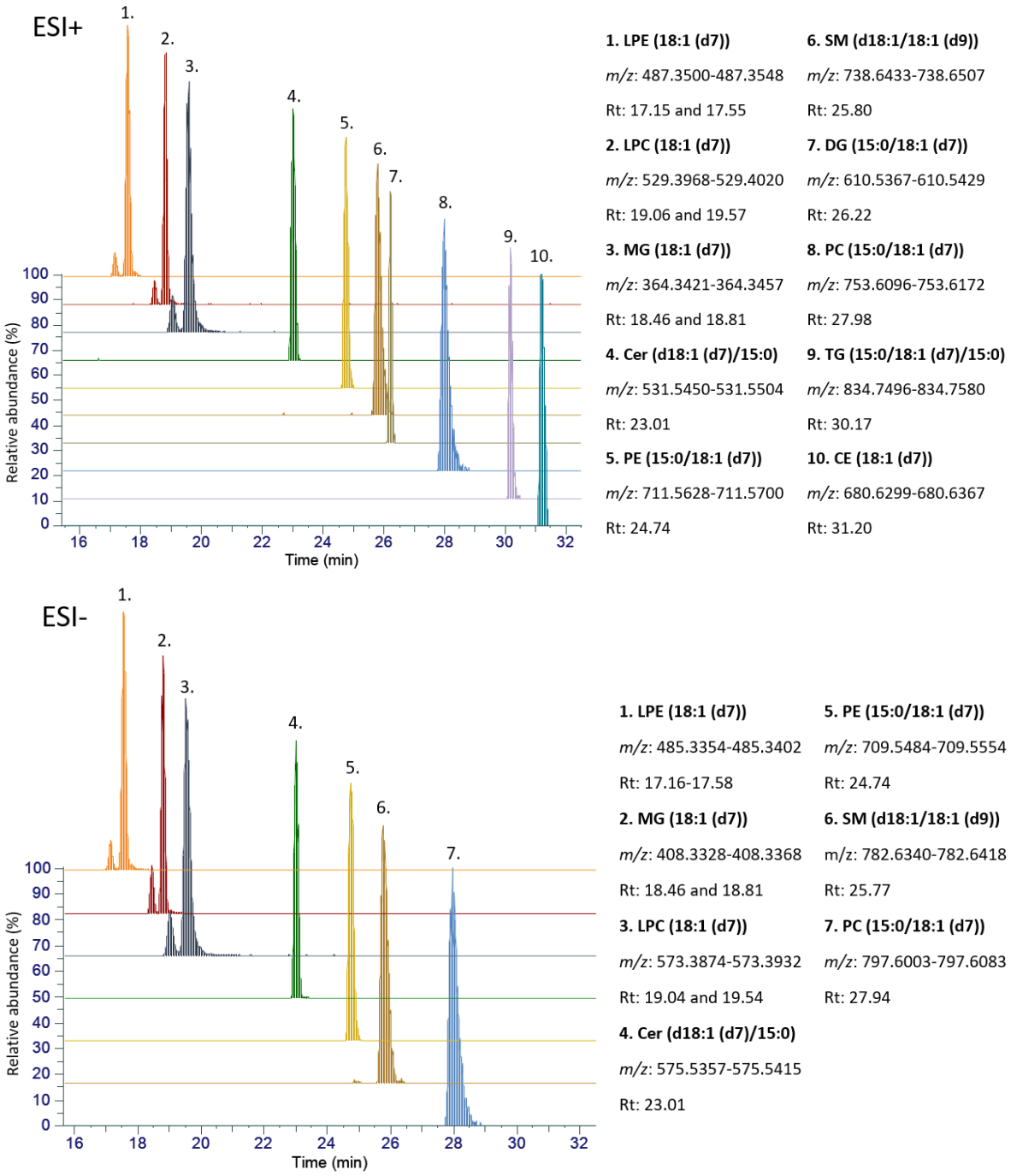

Figure 20: Extracted ion chromatogram (EIC) of the detected compounds in the isotopically labeled lipidome standard in positive (ESI+) and negative (ESI-) ionization. EIC of isotopically labeled lipids detected in positive (top) and negative (bottom) ionization, showing the Rt in minutes and the extracted *m/z*-range.

In positive ionization, 10 of the 13 lipids chosen to represent the lipidome were detected. In negative ionization mode, only 6 out of 13 lipids were detected. The lipids PG (15:0/18:1), PI (15:0/18:1) and PS (15:0/18:1) were not detected in either ionization mode. The lipids PG (15:0/18:1), PI (15:0/18:1) and PS (15:0/18:1) are reported being best detected in negative ionization [68].

The lipids LPC (18:1(d7)), LPE (18:1(d7)) and MG (18:1(d7)) all have acyl groups that can be located at the *sn*1 or *sn*2 position of the glycerol backbone. The standards contain both regioisomers which were separated chromatographically, as seen in **Figure 25**. The regioisomer with the acyl in the *sn*2 position elutes first, then the regioisomer with the acyl bound to the *sn*1 elutes second. Later when refereeing to the peak area of these compounds, it is as the combined peak area of the two peaks.
The lipid CE (18:1) was found to elute at 31.20 min, on the gradient lasing for 32.5 min and could be used as a reference for what to expect to elute in the chromatographic window.

The metabolome standard was also analyzed using the original method, and **Figure 21** shows the EIC of the compounds representing the metabolome, in positive ionization. **Table 22** in **Appendix**, section 6.2 shows the average and relative standard deviation (% RSD) for the peak areas and retention times of these compounds.

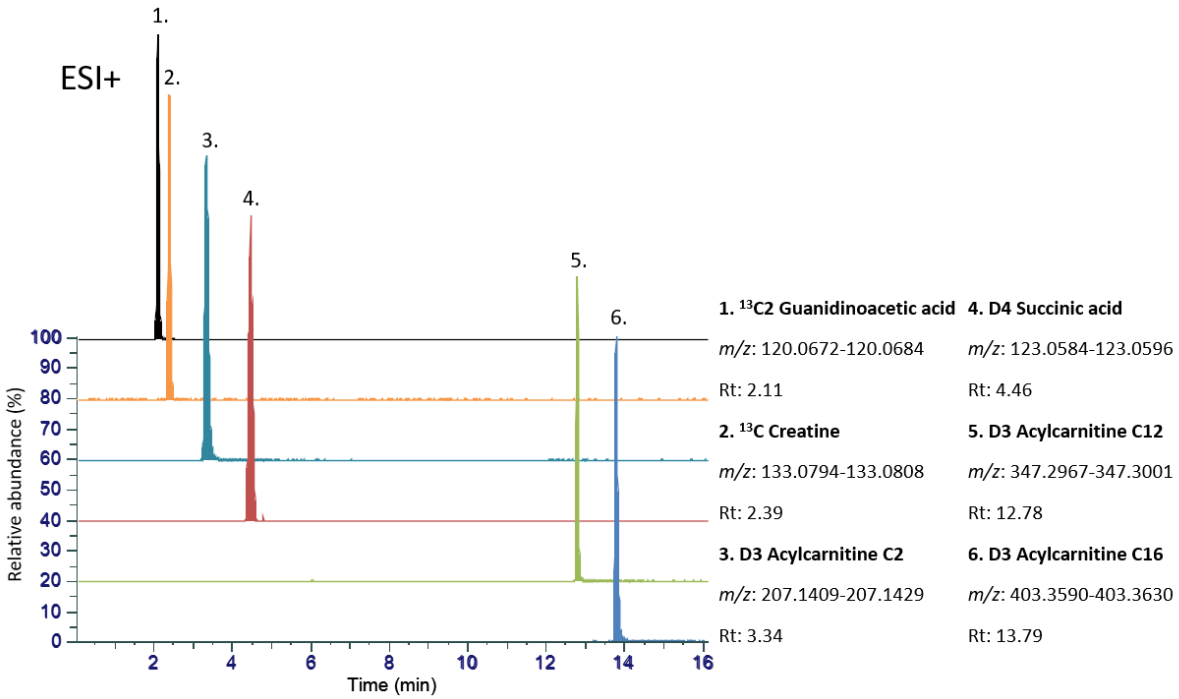

Figure 21: Extracted ion chromatogram (EIC) of the compounds representing the metabolome, in positive (ESI+). EIC of compounds detected in positive ionization with Rt in minutes and extracted *m/z*-range.

The compounds representing the metabolome were all detected in positive ionization. In the negative ionization mode, only D3 acylcarnitine C2, C12 and C16 were detected.

To summarize: For the lipidome standard, 10 of the 13 lipids were detected by the original method, and for the metabolome standards all compounds were detected.

4.1.4 Direct injection of lipidome standard to mass spectrometer

As three of the lipids in the lipidome standard were not detected using the original method, 250 µL of the isotopically labeled lipidome standard was directly injected into the mass spectrometer, to see if the lipids PG (15:0/18:1), PI (15:0/18:1) and PS (15:0/18:1) could be detected. **Figure 22** shows the mass spectrum acquired after direct injection of the standard, in the *m/z* range 740-830, in negative ionization.

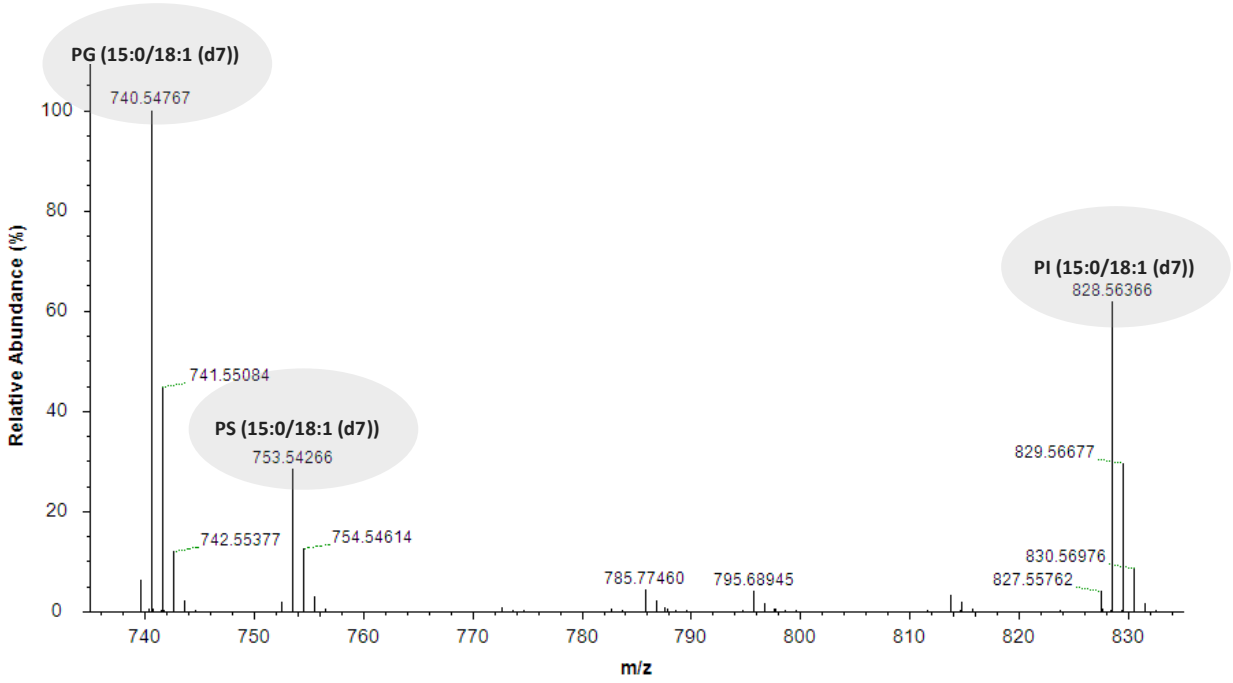

Figure 22: Mass spectra of compounds PG (15:0/18:1 (d7)), PI (15:0/18:1 (d7)), PS (15:0/18:1 (d7)). Direct injection of the isotopically labeled lipidome standard, showed the presence of the $[M-H]^-$ adducts of the lipids PG (15:0/18:1(d7)), PI (15:0/18:1(d7)), and PS (15:0/18:1(d7)), with the *m/z* value 740.54767, 828.56366, and 753.54266 respectively.

The detection of the lipids proved that they were in fact present in the standard, and that they could be detected by electrospray ionization. Further investigation was done to reveal why these lipids were not detected using the original method.

4.1.5 Lipids detected after removal of column

To ensure that the three lipids were not completely retained by the column, the column was removed and the isotopically labeled lipidome standard analyzed. **Figure 23** shows the EIC of the detected lipids in negative ionization.

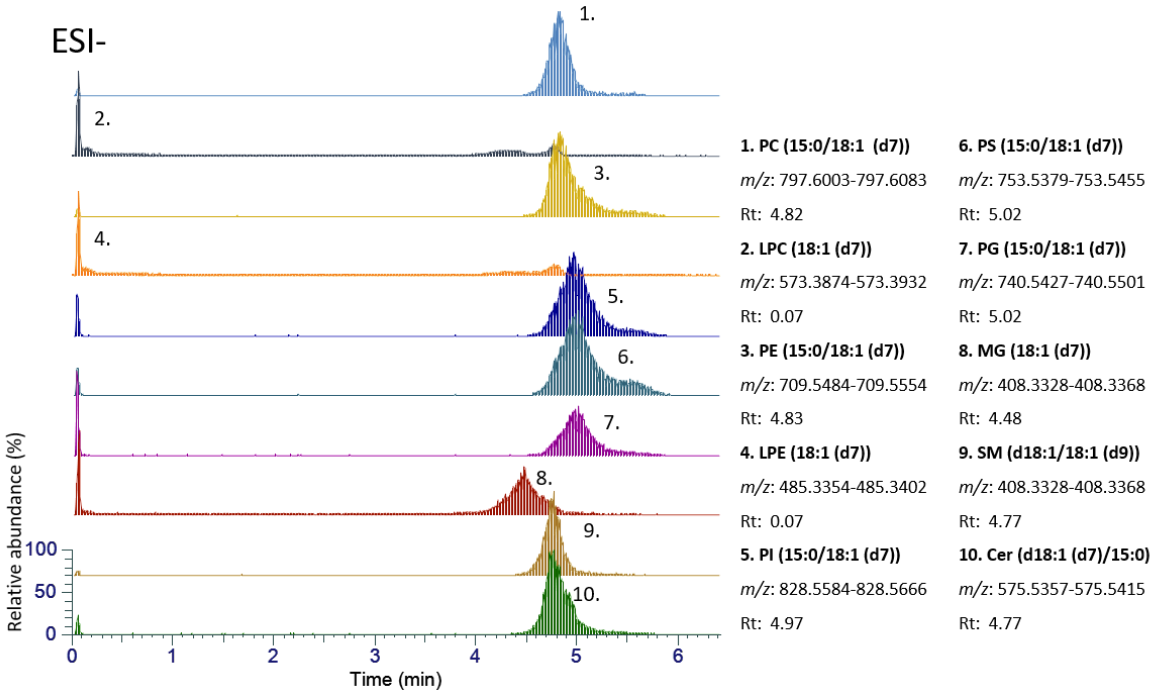

Figure 23: Extracted ion chromatogram (EIC) of the lipidome standards analyzed without column, in negative ionization. All lipids were detected except for TG (15:0/18:1 (d7)/15:0) and CE (18:1 (d7)).

All lipids in the standard except for TG (15:0/18:1 (d7)/15:0) and DG TG (15:0/18:1 (d7)) were detected. The three compounds PG (15:0/18:1), PI (15:0/18:1) and PS (15:0/18:1) have logP values of 11.9, 10.6 and 11.7 respectively, indicating that they are relatively hydrophobic. Despite this, they are not the most hydrophobic compounds in the lipidome standard, as TG (15:0/18:1/15:0) has a logP value of 21.0 and is elutes at 30.2 minutes when analyzing the standards with the original method, as seen in **Figure 20**. This could indicate that the compounds are not retained in the column, but rather not ionized at pH of the original mobile phase.

4.1.6 Changing the mobile phase pH enabled detection of lipids that were not detected using the original method

The mobile phase modifier was changed from FA to NH_4Ac, to obtain higher mobile phase pH. The original mobile phase containing FA, had a pH of approx. 2, and the alternative mobile phase had a pH of approx.7. **Figure 24** shows the EIC of the isotopically labeled lipidome standard analyzed with the alternative mobile phase, in positive and negative ionization mode, respectively.

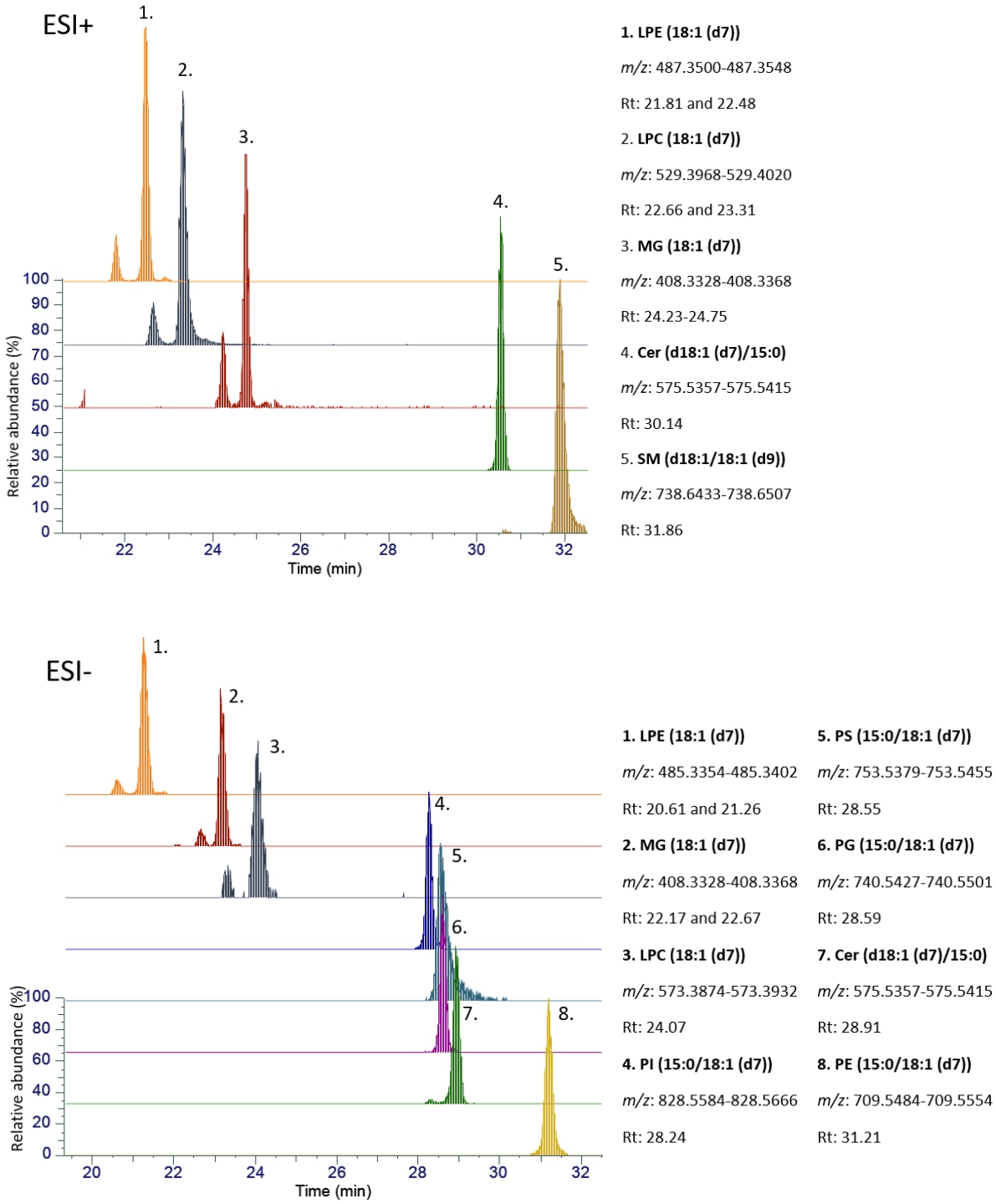

Figure 24: Extracted ion chromatogram (EIC) of the isotopically labeled lipidome standard analyzed using the alternative mobile phase, in positive (ESI+) and negative (ESI–) ionization. With the alternative mobile phase, using NH_4AC as the modifier, detection of the lipids PG (15:0/18:1 (d7)), PI (15:0/18:1 (d7)) and PS (15:0/18:1 (d7)) in negative ionization mode was possible.

For the first eluting peak of LPC (18:1 (d7)), only seven points of the chromatographic peak could be detected, so only the Rt of the second peak is shown.

By changing the mobile phase modifier, and subsequently the pH, the three lipids PG (15:0/18:1 (d7)), PI (15:0/18:1 (d7)) and PS (15:0/18:1 (d7)) were detected in negative ionization mode. When changing the modifier, the retention times of all the lipids increased, and the selectivity was altered. This is as expected in RP-LC, as selectivity is dependent on mobile phase pH [69]. In positive ionization, only five lipids were detected using the alternative mobile phase, namely LPE (18:1 (d7)), LPC (18:1 (d7)) MG (18:1 (d7)), Cer (d18:1 (d7)/15:0) and SM (d18:1/ 18:1 (d9)).

The three lipids, PG (15:0/18:1 (d7)), PI (15:0/18:1 (d7)) and PS (15:0/18:1 (d7)), are only ionizable at the phosphate group, which is most readily ionized in the negative mode. The other glycerophospholipids in the lipidome standards, PE and PC, can be detected with positive ionization because the headgroup of PE contains an amine, and PC has a headgroup that is a cation.

It is expected that the retention time of a compound is the same in positive and negative ionization mode, but it was not the case for these results. The reason for this was not clear, but it could be because of lack of conditioning of the column when changing from the original mobile phase to the alternative mobile phase. Although the identity of the lipids detected in this experiment was not uncertain, these results emphasizes the importance of sufficient equilibration times to ensure the same retention time in both ionization modes.

Arnesen compared the use of FA and NH_4Ac as modifiers when developing this method and found that using NH_4Ac as the organic additive in the mobile phase contaminated the ion cone. It was also found that using NH_4Ac gave worse chromatographic distribution of compounds, compared to when using FA [63]. This was also the case for the lipids PG (15:0/18:1 (d7)), PI (15:0/18:1 (d7)), PS (15:0/18:1 (d7)) and Cer (d18:1 (d7)/ 15:0), where the alternative mobile phase resulted in close elution of these lipids, which is not ideal. However, in metabolomics, as the analytes are so diverse and numerous, co-elution is to be expected. Also, using this alternative mobile phase resulted in fewer lipids being detected in the positive ionization mode compared to when using the original mobile phase. An alternative to obtain better lipid coverage could be to use two different sets of mobile phases, one for positive ionization and one for negative ionization. The drawback of this approach is that it is more time consuming to prepare two sets of mobile phases, and that the retention times of compounds found in both modes could then differ.

To summarize: The original method was able to detect 10 of 13 lipids in the lipidome standard, and all compounds in the metabolome standard. Changing the mobile phase modifier enabled detection of the missing lipids, PG (15:0/18:1), PI (15:0/18:1) and PS (15:0/18:1) in the negative ionization mode. Using the original method, the three lipids PG (15:0/18:1), PI (15:0/18:1) and PS (15:0/18:1) will not be detected.

4.2 Lipid coverage using different extraction solution

4.2.1 Extraction of spotted standards using different extraction solutions

The isotopically labeled lipidome and metabolome standards were spotted on to Whatman 903 Protein Saver cards and extracted using different extraction solutions (shown in **Table 5**) and analyzed in positive ionization. The lipids PG (15:0/18:1 (d7)), PI (15:0/18:1 (d7)) and PS (15:0/18:1 (d7)) were disregarded. **Table 16** shows the logP values of the solvents used in the extraction solutions. The average peak area with relative standard deviation for the extraction of both the isotopically labeled lipidome and metabolome standard using the different extraction solutions are shown in **Appendix**, Section 6.2 **Table 27-42**.

Table 16: logP values of the solvents used. Values are from PubChem [67]. The water solubility is given at 20 °C.

Solvent	logP value	Water solubility	Color in bar chart
Water	-0.5		
MeOH	-0.5	Miscible	
ACN	0	Miscible	
Iso-propanol	0.3	Miscible	
1-propanol	0.3	Miscible	
1-butanol	0.9	7.7 g/100 mL	
MTBE	0.9	4.2 g/ 100 mL	

Figure 25 shows the average peak area of the isotopically labeled lipidome standards extracted using the different extraction solutions. The extraction solutions only containing water and 20% organic solvent did not extract any of these standards and were thus not included in the figure.

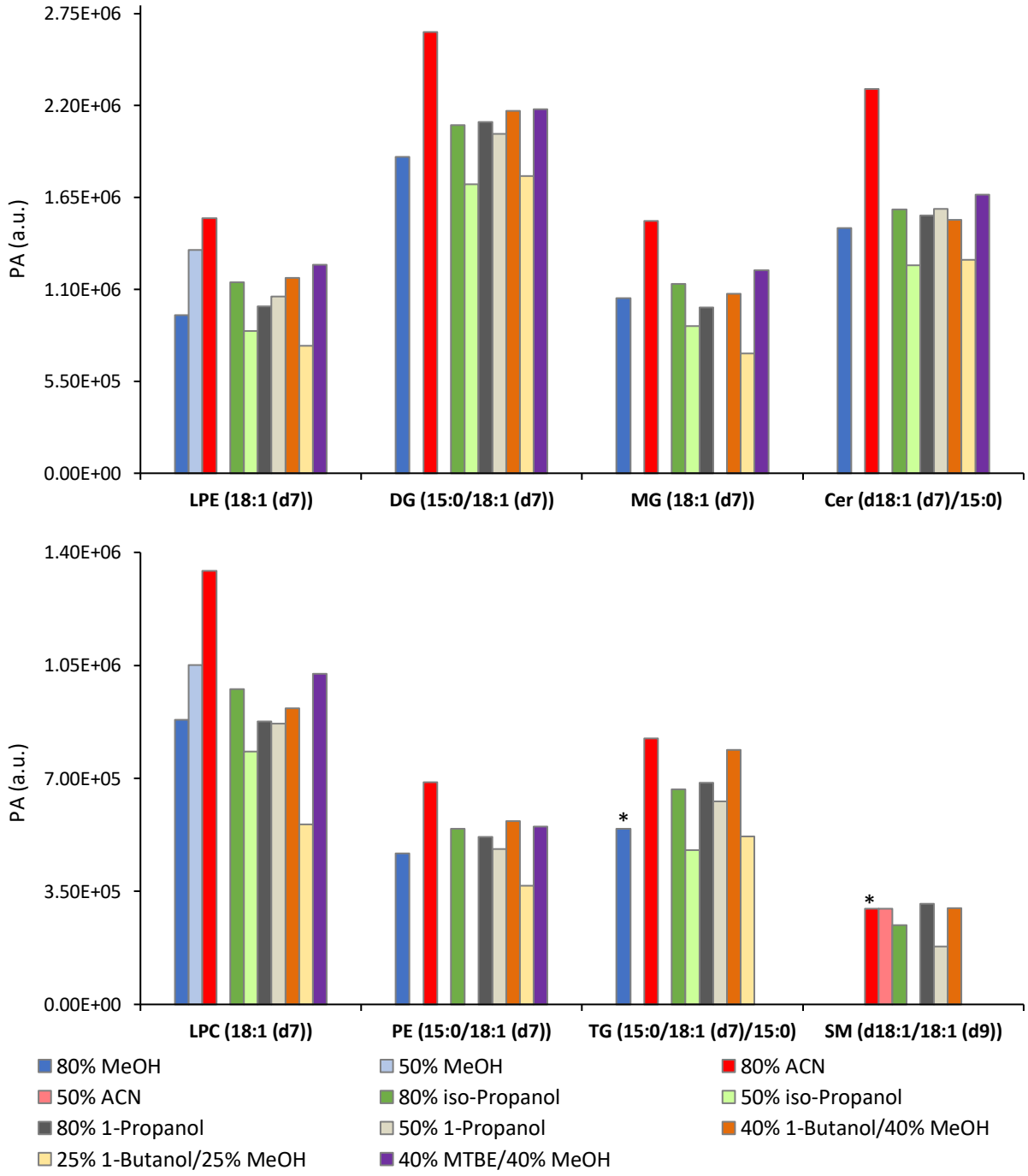

Figure 25: Peak area (PA) of the detected compounds in the isotopically labeled lipidome standard, extracted using the different extraction solutions. Isotopically labeled lipidome standard were applied to Whatman 903 Protein Saver cards and extracted by a selection of extraction solutions, all containing 0.1% FA. Each colored bar represents the peak area detected when extracted by different extraction solution. *Only detected in one replicate.

As alredy mentioned, none of the lipids were extracted using only water or 20% organic solvent. The lipids PC (15:0/18:1 (d7)) and CE (18:1 (d7)) were not extracted using any of the extraction solutions. For each of the different solvents, lipid coverage was increased using a higher amount of organic solvent. With 80% iso-propanol, 80% 1-propanol and 40% 1-butanol/40%MeOH, eight of ten lipids were extracted, providing the best lipid coverage. With 80% MeOH, 80% ACN, and 50% iso-propanol, seven of the ten lipids were extracted, and compared to the before mentioned extraction solutions, SM (d18:1/18:1 (d9)) was the lipid not extracted. Also with 50% propanol and 25% 1-butanol/ 25% MeOH, seven out of ten lipids were extracted, were LPC (18:1 (d7)) was not extracted.

Figure 26 shows the average peak area of the compounds in the metabolome standard extracted using the different extraction solution.

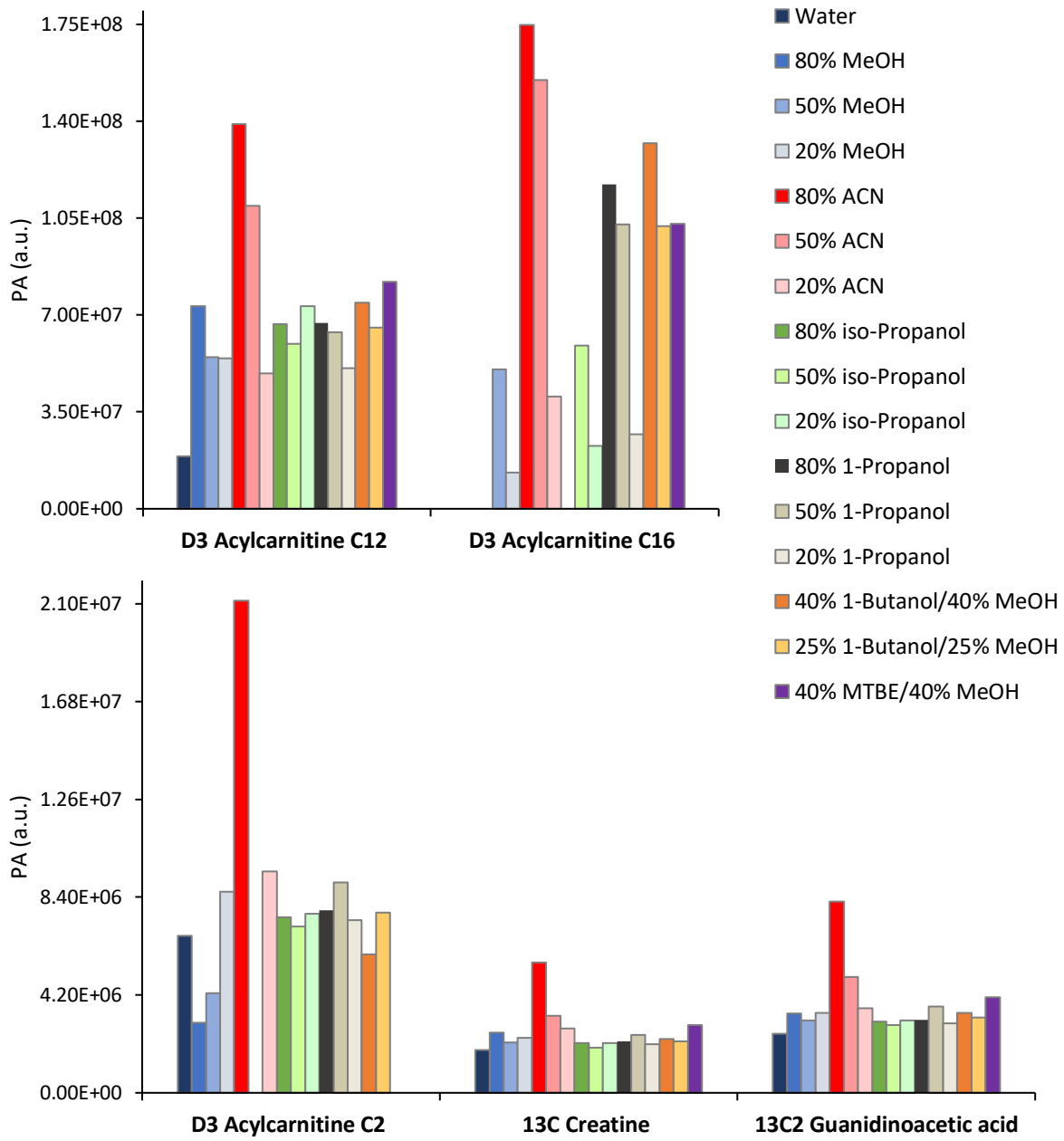

Figure 26: Peak area (PA) of the compounds in the isotopically labeled metabolome standard, extracted using the different extraction solutions. The isotopically labeled metabolites standards were applied to Whatman 903 Protein Saver cards and extracted using different extraction solutions, all containing 0.1% FA. Each color represents a different extraction solution, and bar represents the peak area of the given compound extracted by the given extraction solution.

D4 succinic acid was only detected when the mass accuracy was set to 50 ppm and was therefore disregarded. D3 acylcarnitine C16 was not extracted using water, 80% MeOH, and

80% iso-propanol, D3 acylcarnitine C2 was not extracted using 50% ACN. Other than this, all extraction solutions provided full coverage for the metabolome standard.

Using 80% ACN provided the highest peak area for all the extracted standards, except for SM (d18:1/18:1 (d9)), which could indicate that extraction was more efficient.

To summarize: For the lipid standard, coverage was most affected by amount of organic solvent in the extraction solution. Not all lipids were extracted, but the best lipid coverage was obtained by extraction of the spotted standard using 80% iso-propanol, 80% 1-propanol or 40% 1-butanol/40%MeOH. The metabolome coverage was the same for most extraction solutions, except when using water, 80% MeOH, 50% ACN or 80% iso-propanol who gave poorer coverage.

4.2.2 Extraction of spiked dried blood spots using different extraction solutions

DBS spiked with the lipidome and metabolome standards were extracted by the high and medium percentage organic solvent extraction solutions, shown in **Table 5**. These extraction solutions were chosen as they yielded better lipid coverage for extraction of the spotted isotopically labeled lipidome standard. The DBS was made with blood from one healthy volunteer, and the blood was spiked with the lipidome and metabolome standard prior to spotting. The samples were analyzed using the original method in positive and negative ionization, so the lipids PG (15:0/18:1), PI (15:0/18:1) and PS (15:0/18:1) were disregarded. D4 succinic acid in the metabolome standard was only detected with 50 ppm and was also disregarded. Only the results from positive ionization are shown, as the negative results yielded no additional information. The average peak area with relative standard deviation for the different extractions of both the lipidome and metabolome standards are shown in **Appendix**, Section 6.2 **Table 43-54**. **Figure 27** shows the average peak area of the detected lipids in the lipidome standards spiked to the DBS, extracted using the selected extraction solutions.

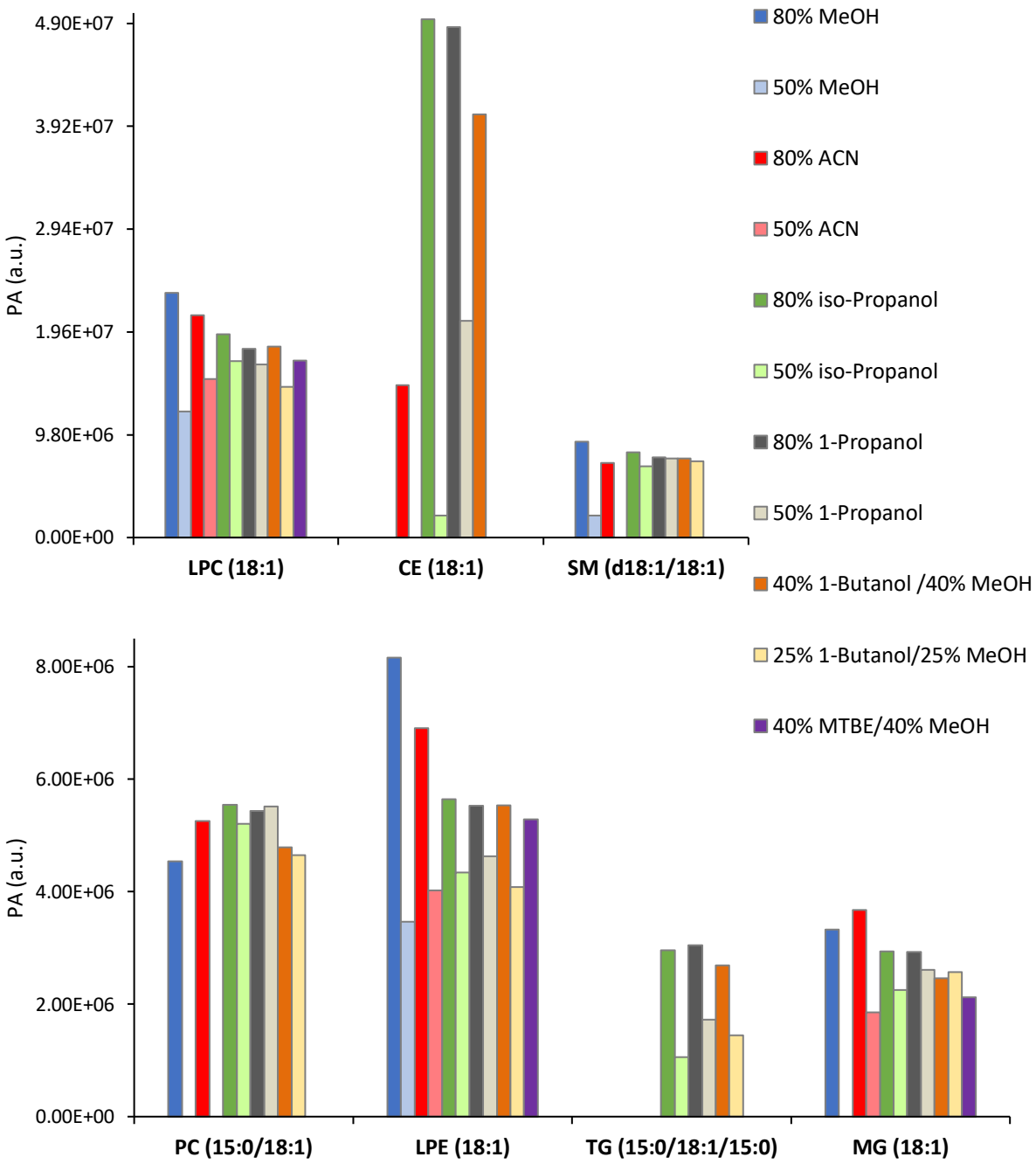

Figure 27: Peak area (PA) of the extracted compounds from the lipidome standard in the spiked dried blood spot (DBS), extracted using the different extraction solutions. The lipidome standrard was spiked to the DBS, and extracted using the selected extraction solutions, all containing 0.1% formic acid (FA). Each color represents a different extraction solution, and each bar represent the peak area of the given compound extracted by the different extraction solutions.

The lipids Cer (d18:1/15:0), DG (15:0/18:1) and PE (15:0/18:1) were not detected using any of the extraction solutions. The lipids CE (18:1) and PC (15:0/18:1) were detected in most extractions, which was not the case when the isotopically labeled lipidome standard was spotted and extracted from filter cards without blood.

The high percentage of organic solvent extraction solutions provided better lipid coverage and extraction efficiency, compared to the medium organic solvent extraction solutions, which was also found the isotopically labeled lipidome standard spotted and extracted from filter cards without blood. The extraction solutions that provided the best lipid coverage were 80% ACN, 80% iso-propanol, 80% 1-propanol and 40% 1-butanol/40% MeOH, extracting seven out of ten lipids in the standard. For 80% MeOH only five lipids were extracted, LPC (18:1), SM (d18:1/18:1), PC (15:0/18:1), LPE (18:1) and MG (18:1).

Figure 28 shows the average peak area of the detected compounds in the metabolome standard spiked to DBS, extracted using the selected extraction solution.

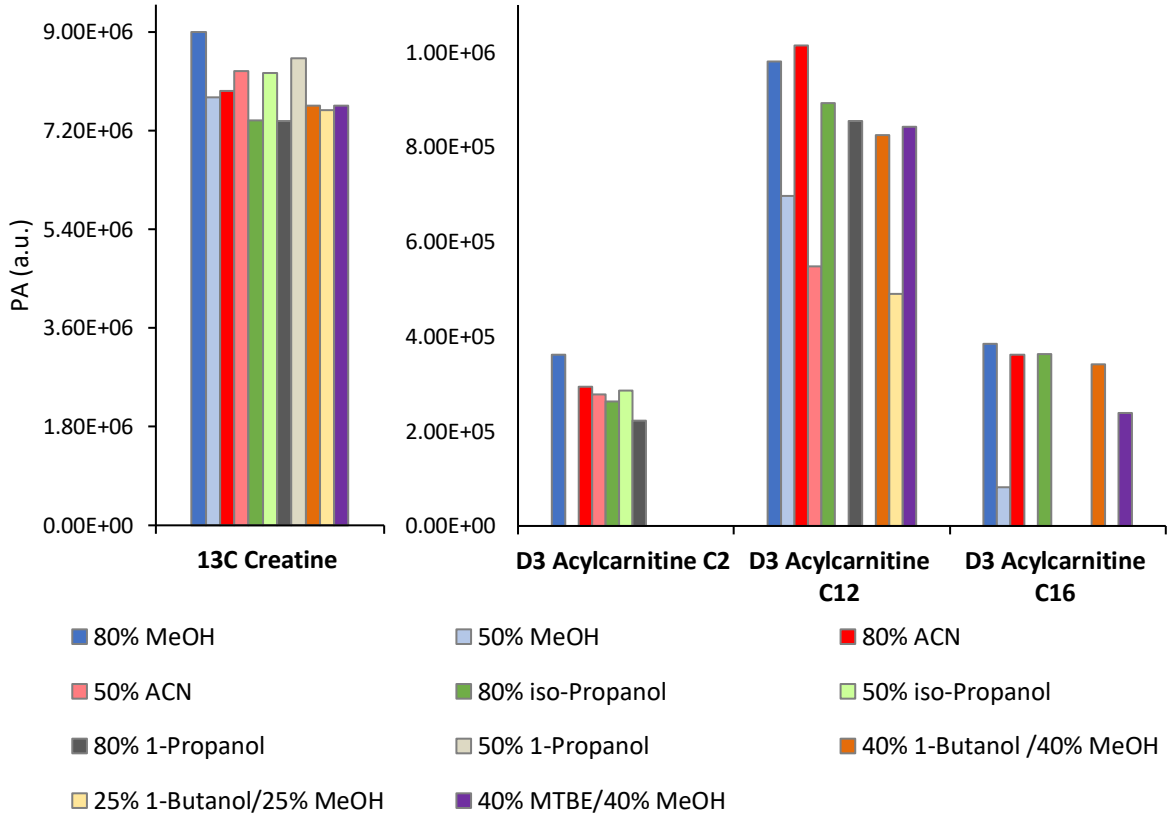

Figure 28: Peak area (PA) of the compounds from the metabolome standard spiked to a dried blood spot (DBS), and extracted using the different extraction solutions. The metabolome standrard was spiked to a DBS, and extracted using the selected extraction solutions, all containing 0.1% formic acid (FA). The different colors represent different extraction solutions, and each bar represent the peak area of the given compound extracted by the different extraction solutions.

$^{13}C_2$ guanidinoacetic acid was not detected using any of the extraction solutions. Metabolome coverage improved when using a higher percentage of organic solvent. The best extraction coverage was found using 80% MeOH, 80% ACN, and 80% iso-propanol.

The different organic solvents used for the different extraction solutions were chosen based on logP value, water solubility and position in the Snyder solvent selectivity triangle. Increasing the logP value of the extraction solvent was thought to increase the coverage and extraction efficiency of the lipid standards. The extraction solutions that gave the best lipid coverage for the two approaches were iso-propanol, 1-propanol, and 1-butanol/MeOH, which could indicate that increasing logP had a slight influence on coverage. However, the difference in coverage was only by a few lipids, when comparing the high percentage organic solvents. This could be because range of logP values were too small to make a significant difference in hydrophobicity of the solvents. Also, the addition of water could affect the actual hydrophobicity of the extraction solutions. The addition of some water to the extraction solution has been shown to increase extraction of many metabolites from DBS, as the water degrades the interactions between the cellulose of the filter card and the metabolites [70].

MTBE and 1-butanol were the solvents with the highest logP values, and because of limited water solubility they had to be mixed with MeOH to avoid formation of two-phases when mixed with water. This was also done to make them soluble in the LC gradient. This could have been avoided by including a solvent evaporation step during sample preparation. This is quite common, but work done by Sandås showed that evaporation with N_2 to dryness and re-solving of DBS extracts reduced the signal intensity of hydrophobic and low abundant metabolites [61]. Evaporation of solvent and re-solving in the LC start-gradient is done to avoid formation of a sample solvent plug in the column [71], but is likely not a problem in this method because of the low injection volume (2 µL). The process of evaporation and re-solving is also time consuming, so avoiding this step was a major reason for using only LC-gradient compatible solvents for the extraction solutions.

The solvents were also chosen with regards to their position in the Snyder solvent selectivity triangle. MeOH, iso-propanol, 1-propanol and 1-butanol all belong in group two and form mainly hydrogen donors interactions. ACN belongs group six, a group of solvents that possess a permanent dipole, causing strong interactions with other compounds with a dipole or induced dipoles. MTBE is an ether and can interact with compounds as a hydrogen acceptor. The alcohols and MTBE are closely positioned in the Snyder solvent selectivity triangle and should therefore have somewhat similar selectivity. Compared to the other organic solvents, ACN should show different selectivity [49, 50, 54].

The lipids all have a hydrophobic tail, double bonds, permanent dipoles, hydrogen donors and acceptor functional groups, except for the TG and CE who do not have a hydrogen donor functional group. These two lipids, as well as PC and SM are not extracted using MTBE, a hydrogen acceptor as would be expected. MTBE is often used in lipid extraction, as an alternative to the more traditional extraction procedures using chloroform-methanol mixtures [72]. Koulman et al. has shown that using a mixture of water, MeOH, and MTBE (1:2:5) for extraction of lipids from DBS enables detection of a variety of TG, PC, CE, and SM of different acyl-chain lengths. In this procedure two layers are formed, and the organic layer is analyzed after evaporation and re-solving [38]. This could indicate that a higher amount of MTBE is needed for the extraction of lipids.

Creatine, guanidinoacetic acid, and succinic acid all have hydrogen donor and acceptor groups, as well as permanent dipoles. Acylcarnitine C2 has a permanent dipole and is a hydrogen acceptor. Acylcarnitine C12 and C16 have these functional groups as well as a hydrophobic tail. All the compounds in the metabolome standard have functional groups that can interact with the chosen organic solvents and could be the reason that the coverage is so similar for the different solvents, especially for extraction of the spotted standard.

A problem when using the Snyder solvent selectivity triangle for choosing a solvent, is the fact that the model does not consider the solvents ability to form dispersion interactions. Dispersion interactions are weak interactions, but the strength increases with a compounds and solvents amount of unsaturated bonds [50], which is a common structural feature for most lipids. Other models that include a wider set of parameters for solvent selectivity classifications have been published since this model was first introduced [73], and could possibly be more appropriate for selecting solvents.

Surprisingly, the compounds being extracted were not the same for standards spotted to filter paper and standards spiked to DBS. For instance, with the extraction of the spotted standard the lipids PC (15:0/18:1 (d7)) and CE (18:1 (d7)) were not detected for any of the extraction solutions. When the standards were spiked to DBS, Cer (d18:1/15:0), DG (15:0/18:1) and PE (15:0/18:1) were not detected for any of the extraction solutions. The reason for this strong dependence on the matrix on the compound's extractability is not obvious. Further, the lipid coverage of the different extraction solutions differed for the two approaches. Lipid coverage

for spotted standards was best using high percentage iso-propanol, 1-propanol and 1-butanol/MeOH. For the spiked DBS, the high percentage of ACN, iso-propanol, 1-propanol, and 1-butanol/MeOH gave the best coverage regarding the lipidome standards. The extraction solutions that gave the best lipid coverage for the two approaches were iso-propanol, 1-propanol, and 1-butanol/MeOH.

To summarize: Lipid and metabolite coverage was affected by altering the extraction solution of DBS. The amount of organic solvent used had a greater impact on coverage than that of the type of organic solvent. Increasing the amount of organic solvent increased both lipid and metabolite coverage. The best coverage for the extraction of the lipidome standard spiked to DBS was found using 80% ACN, 80% iso-propanol, 80% 1-propanol and 40% 1-butanol/40% MeOH. The best coverage for the metabolome standard was found using 80% MeOH, 80% ACN, and 80% iso-propanol.

4.2.3 Dried blood spot metabolome differently affected by the extraction solutions in positive and negative ionization

The software Compound Discoverer was used to perform principle component analysis (PCA) for visualization the variance between the metabolomes of DBS extracted using the different extraction solutions. Each point in the PCA plot represent one sample, and all identified metabolites in that sample. The distance between the points represent the variation between them. This means that points that are close to each other are similar, and points far from each other are more different [9]. The axis represents principal components (PC), where the x-axis is represented by PC 1 (40.7% for positive ionization and 41.4% for negative ionization) which represent the highest variation, and the y-axis is represented by PC 2 (8.3% for positive ionization and 13.1% negative ionization), which has the second most variation. **Figure 29** shows the PCA plot of the spiked DBS extracted using the different extraction solutions, in positive (left) and negative (right) ionization.

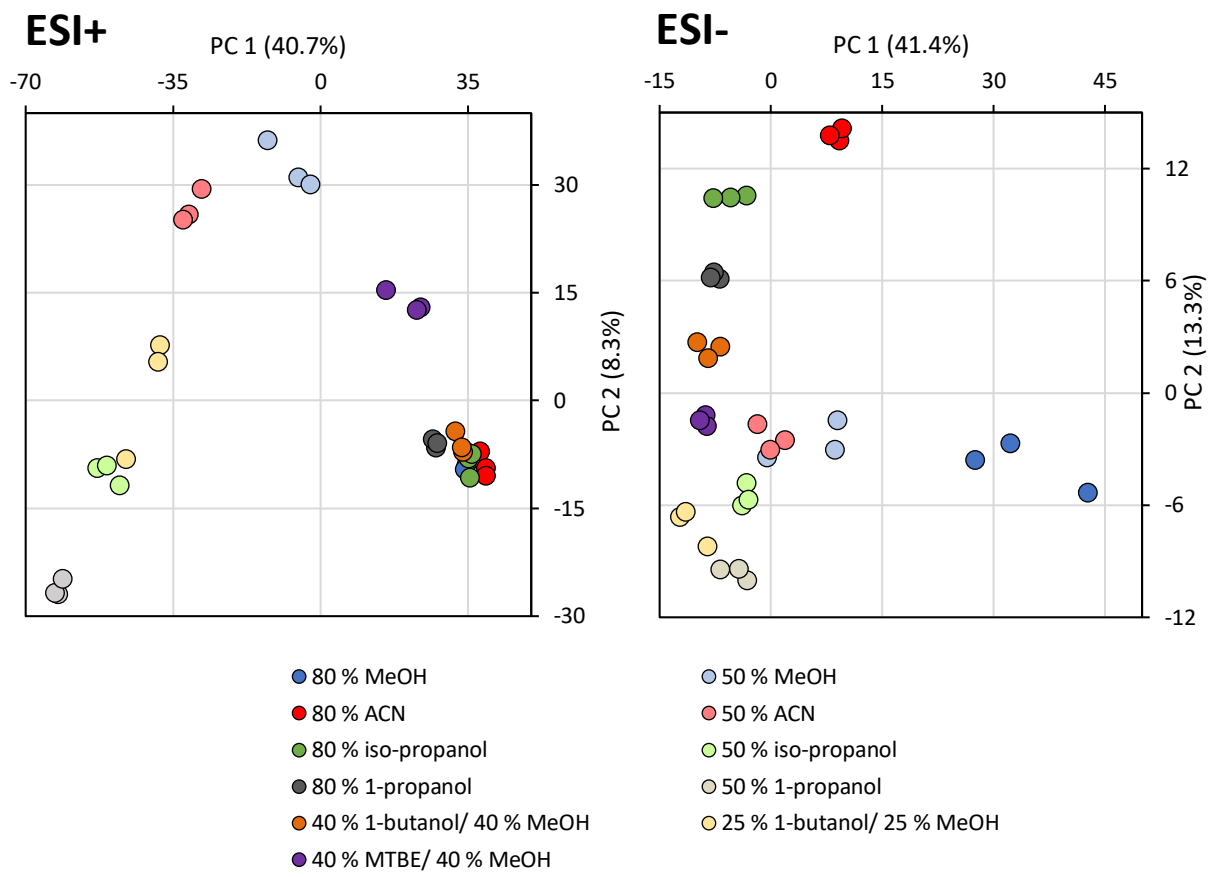

Figure 29: Principle component analysis (PCA) plot of dried blood spots (DBS) from one healthy volunteer extracted using different extraction solutions, in positive ionization (left) and negative ionization (right). The different colors represent the DBS extracted with different extraction solutions, each analyzed in three replicates. Each circle represents all identified metabolites in the sample.

The PCA plot for positive ionization shows that the DBS extracted using high amount of organic solvent are clustered together, while the DBS extracted by the medium amount of organic solvent are more spread out across the plot. This indicates that the metabolomes extracted using high organic solvents solutions are more similar than those extracted using the medium organic solvent solutions.

Compared to the positive ionization results, the PCA plot for the negative ionization results show no clear clustering of samples based on extraction by high or medium percent organic solvent. This could indicate that for negative ionization results, the metabolome is more influenced by type and percentage of organic solvent, than that found with positive ionization. The DBS metabolome extracted using 80% MeOH show large variance also for the different replicates, compared to the other metabolomes.

The difference between the metabolomes in positive and negative ionization could be because different compounds are better ionized in the different ionization modes. Typically, basic

compounds are easily ionized in positive ionization, and acids in negative ionization. However, many metabolites are found in both modes [74].

Molecular features are ions with a given *m/z* value and retention time, and not an identified metabolite [74]. In negative ionization mode, the number of molecular features identified was lower than that in positive ionization mode, shown in **Appendix**, section 6.3.5 **Table 59**. The difference is likely because fewer metabolites ionized and thus detected in negative ionization, but also because in negative ionization there is less adduct formation compared to that usually seen for positive ionization [74]. This also means that the PCA plot for negative ionization is based on fewer metabolites than that of the positive, and that could be the reason why the two PCA plots show so different results.

Combining the fact that the PCA plot for the DBS metabolome showed that there was no variance in the metabolomes extracted using high percentage of organic solvent, and that there was not a big difference in lipid coverage in spiked DBS between the original extraction solution (80% MeOH) and the high percentage iso-propanol, 1-propanol, and 1-butanol/MeOH, it was chosen to use 80% MeOH for the extraction of DBS in future experiments. It has also been shown that using 80% MeOH for DBS extraction is repeatable [61].

To summarize: For positive ionization, the DBS metabolome showed the most variance between extraction using high or medium amount of organic solvent. For the negative ionization, the type and amount of organic solvent seemed to be of greater importance.

4.3 The method revealed exercise induced changes in the metabolome and the lipidome

During exercise, all aspects of metabolism is affected. The muscles energy requirements increase, stimulating catabolic pathways, like glycolysis and fatty-acid oxidation, while energy demanding pathways, like the synthesis of fatty acids, cholesterols and proteins are not favored [75]. This metabolic shift affects the metabolome and lipidome and can be seen by studying different biofluids. Energy metabolites, such as carbohydrates and lipids are mobilized, utilized and converted, to meet the increased adenosine 5´-triphosphate (ATP) demand [76]. ATP is the body´s energy currency, carrying chemical energy between metabolic pathways [77]. Because exercise has such an immediate impact on the metabolome

and lipidome, it is a great way to assess whether the metabolic platform can pick up immediate metabolic changes.

Seven healthy volunteers participated in a high intensity exercise, that lasted for twenty minutes. The exercise consisted of four different exercises, repeated in three sets. The exercises were carried out for thirty seconds, with a twenty second break in between. Following this, three sets of as many push-ups as possible in thirty seconds were completed, with a twenty second break in between sets. Ten different DBS were collected from the participant, from the day prior to the exercise, the day of the exercise, and the morning after. The full sampling schedule is shown in **Figure 30**.

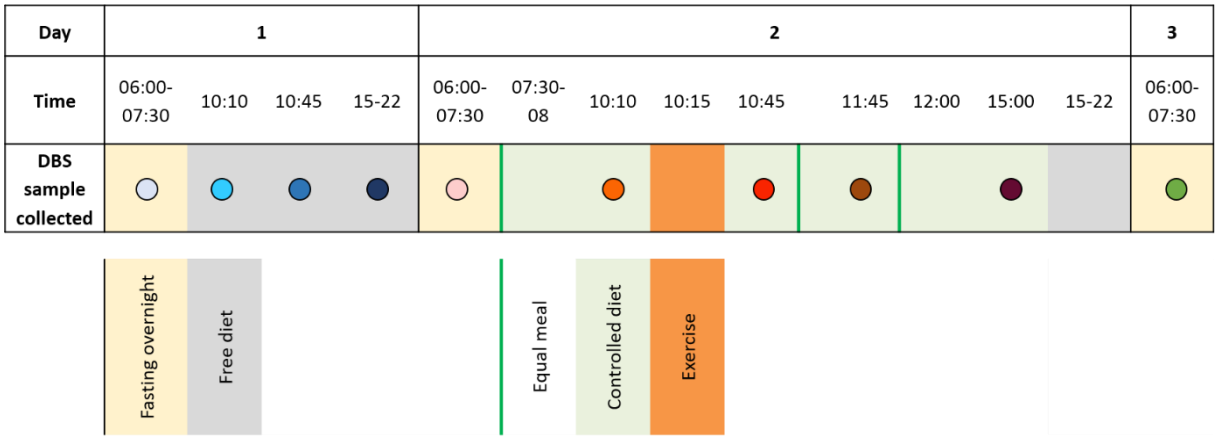

Figure 30: Sampling schedule. Samples were collected at ten different time point for three days, marked by different colored circles. Three overnight fasting samples, three during free diet and four during controlled diet were collected.

During day one (D1), an overnight fasting sample was taken, as well as three during free diet. Day two (D2), one overnight fasting sample was taken, as well as four under controlled diet. Day three (D3) only one overnight fasting sample was taken. More details about the controlled diet can be found in **Appendix**, section 6.4.2. Samples were taken the day prior as well as the day of the exercise to avoid comparing any metabolic changes caused by the circadian rhythm of metabolism [78], to exercise induced changes. The DBS were extracted with the original extraction solution, (80% MeOH with 0.1% FA), and the samples were analyzed using the original method in both positive and negative ionization. **Figure 31** shows the PCA plot for all samples taken during the project as well as PQCs, in positive ionization.

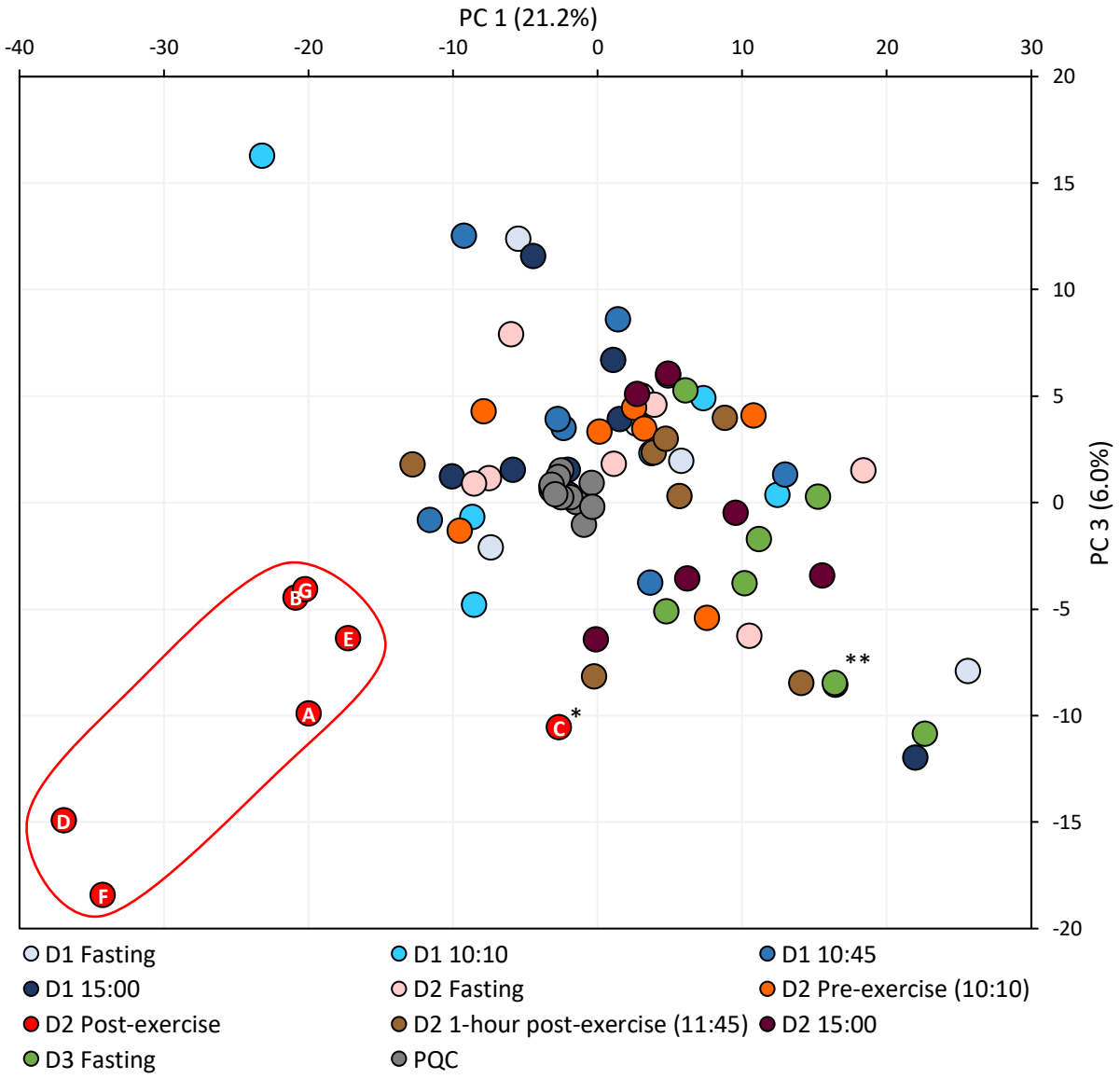

Figure 31: Principle component analysis (PCA) plot of samples taken of the participants (A-F), colored according to sampling time. The plot shows the variation in the metabolome of DBS samples collected at the different times on day one (D1) of free diet, day two (D2) of controlled diet and exercise, and day three with overnight fasting. Each point represents all metabolites detected in that sample. The samples taken immediately after the exercise are colored red and circled, showing the largest variation from the other samples. *Person C participated in an alternative exercise on ergometer bike. **Two points (D1 15:00 and D3 Fasting) with the same coordinates.

As shown in **Figure 31**, the PQCs cluster tightly in comparison to the total variance and are close to the origin of the PCA scores plot. This is a strong indicator the data acquired by LC-MS analysis were precise [58], and provided confidence in the interpretation of the metabolomics data obtained from all the samples.

The samples taken immediately after the exercise are colored in red and show the biggest variance from the other samples. Person C participated in an alternative interval exercise on

ergometer bike, which could be the reason why it did not cluster closer to the other samples taken after the exercise.

Things that could affect how metabolism is affected by a high intensity exercise depends several factors, like age, gender, and fitness level among other things. The sample taken one-hour post exercise (D2 11:45) is clustered among the rest of the samples, indicating that the changes induced by exercise on the metabolome is not long lasting.

Volcano plots are used for visualizing the difference in relative abundance of metabolites between two groups. The x-axis shows the difference in relative abundance between the two groups as the fold change, and the y-axis shows the P-value from a significance test comparing the relative abundance of the given metabolite in the two groups. Metabolites with unchanged abundance in the two groups are plotted near the origin of the x-axis. Metabolites that are located in the upper left and right corners of the graph show a significant change in relative abundance between the two groups [79]. **Figure 32** shows the volcano plot comparing the samples immediately after the exercise (D2 10:45) and the samples taken at the same time the day prior (D1 10:45), for positive and negative ionization, respectively. The threshold for significance was set to $P<0.05$, and fold change higher and lower than one. Statistical significance was calculated using ANOVA and Tukey honest significance test post-hoc by the software.

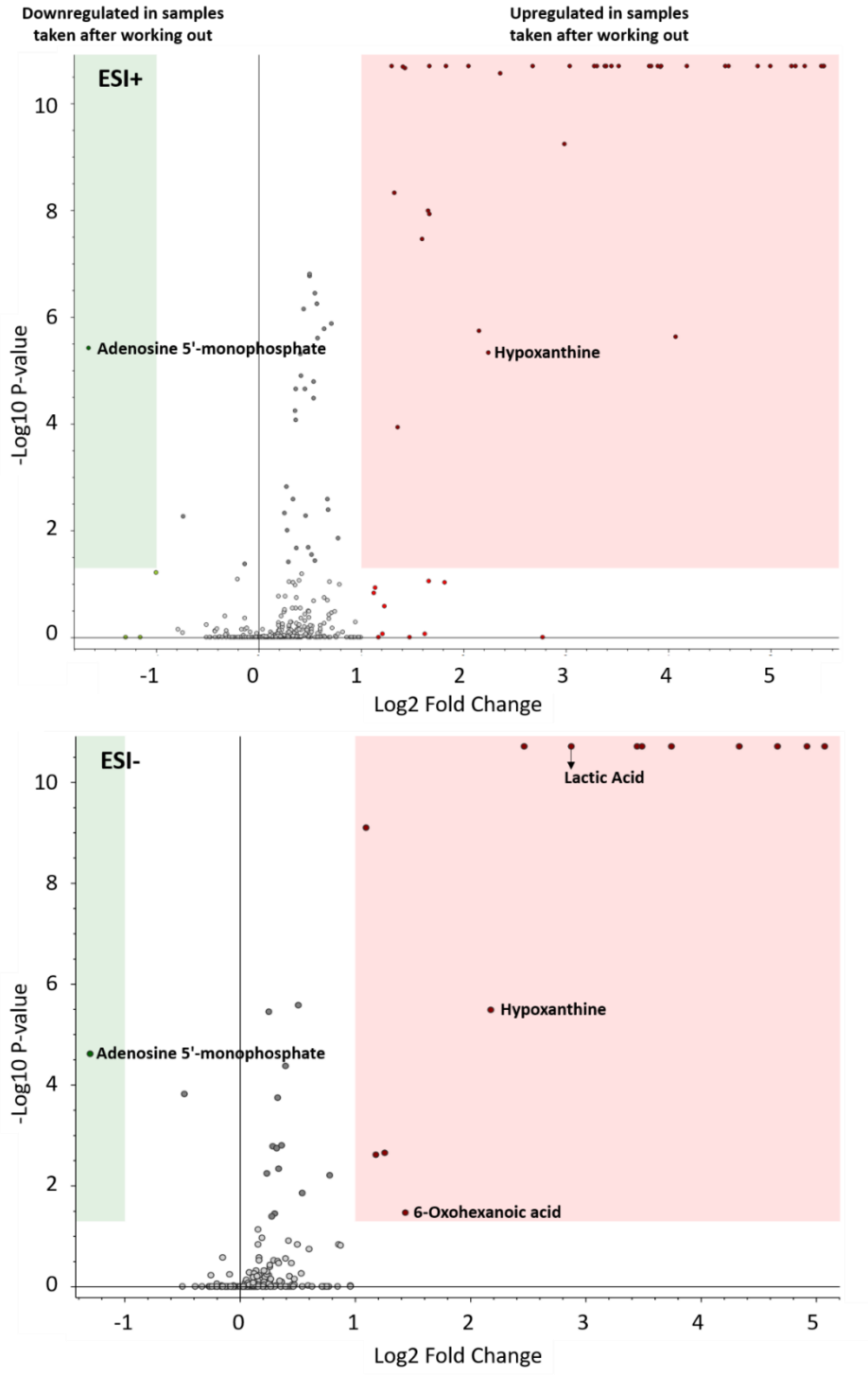

Figure 32: Volcano plot comparing the metabolome after exercise (D2 10:45) and the metabolome during a normal day of office work (D1 10:45), for positive ionization (top) and negative ionization (bottom). Each point represents a metabolite that is present in both groups, and metabolites in the shaded regions are statistically significant for the specified p-value and fold change threshold. The green region shows significantly downregulated metabolites, and the red region significantly upregulated metabolites. Adenosine 5'-monophosphate was significantly downregulated, and hypoxanthine was significantly upregulated in samples taken after exercise in both the positive and negative ionization. In negative ionization, lactic acid and 6-oxohexanoic acid was found to be significantly upregulated after exercise. Log2 Fold Change (after workout/ normal day) > 1 (red) and <-1 (green) and $P<0.05$.

Only metabolites who had a well-established connection to exercise induced change was included with name in the volcano plot. AMP was the only metabolite that was found to be significantly downregulated after exercising. In **Appendix**, section **6.4.3**, more information about the identification of AMP in negative ionization can be found. In short, the software used for metabolite identification and statistical analysis identified the significantly downregulated metabolite in negative ionization as deoxy-guanosine 5'-monophosphate (dGMP), and the metabolite significantly downregulated in positive ionization was identified as AMP. The retention time and fragmentation of the metabolite identified as dGMP by the software was compared to a standard of AMP, and it was found that the metabolite was most likely AMP, also in the negative ionization results.

Hypoxanthine was found to be significantly increased after exercising, in both the positive and negative ionization results. Lactic acid was also found to be significantly increased in samples taken after exercise in the negative ionization results.

To summarize: Participating in high intensity exercise had an immediate effect on the metabolome, which was detected by the global metabolomics platform.

4.3.1 Metabolites associated with adenine nucleotide catabolism affected by exercise

The two metabolites AMP and hypoxanthine, whose abundance found to be significantly altered in the volcano plot (**Figure 32**), are intermediates and products of adenine nucleotide catabolism. During exercise, there is a net hydrolysis of ATP to adenosine 5'-diphosphate (ADP) and AMP. ADP can be regenerated to ATP, and AMP is catabolized. AMP is deaminated to inosine-5'-monophosphate (IMP), which is dephosphorylated to inosine, and further oxidized to hypoxanthine, xanthine and uric acid, as shown in **Figure 33** [80, 81].

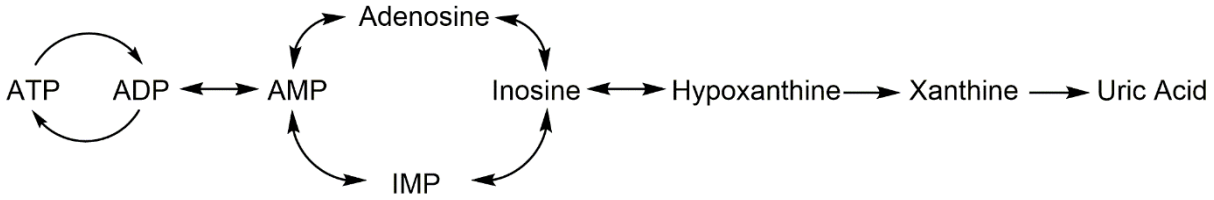

Figure 33: Adenine nucleotide catabolism. ATP catabolism occurs when the rate of hydrolysis exeeds the rate of resynthesis, for instance during anaerobic exercise. Adenine nucleotide catabolism end with accumultation of hypoxanthine, xanthine and uric acid in the blood stream and are excreted via urine [80, 81].

The box-whisker plot is a five-number summary of a set of data for a given metabolite. The median of the data is represented as the line in the middle of the bar, and the top and bottom of the bar represents the upper and lower quartile of the data, respectively. The upper and lower whiskers represent the highest and lowest value of the data. **Figure 34** shows the relative abundance of AMP, hypoxanthine, and uric acid in all samples.

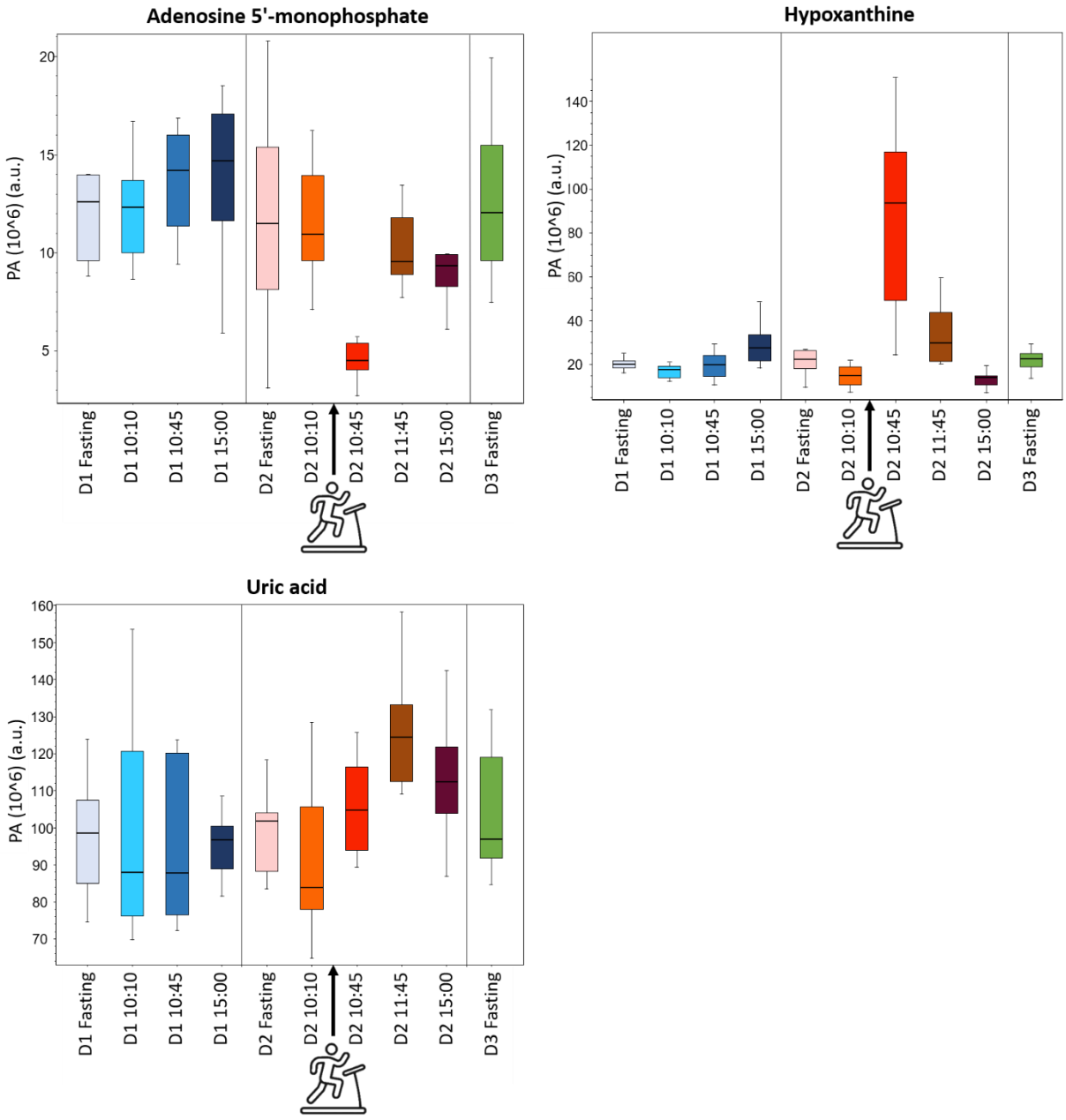

Figure 34: Adenosine 5'-monophosphate (AMP) (top left), hypoxanthine (top right) and uric acid (bottom left). Measured peak area (PA) of AMP, hypoxanthine, and uric acid in samples from seven healthy volunteers, taken for three days at different times during the day. Day one (D1) the participants had a normal workday with a free diet. Day two (D2) the participants had a controlled diet and participated in a high intensity exercise (indicated by the running man). Day 3 (D3) only a fasting sample was collected. The results shown are from positive ionization. AMP was found to be significantly downregulated in samples taken immediately after the exercise, and hypoxanthine was significantly upregulated.

AMP and hypoxanthine were as already mentioned significantly down and upregulated, respectively, after exercise. Uric acid, the end-product of adenine nucleotide catabolism was also identified. The box-whiskers plot show an increase in uric acid immediately after exercise (D2 10:45) and an hour after exercise (D2 11:45) compared to the sample taken right before exercise (D2 10:10), but the change in relative abundance was not statistically significant with $P<0.05$.

4.3.2 Lactic acid increased after exercise

Lactic acid was found to be significantly upregulated in the samples taken immediately after the exercise, as shown in the volcano plot in **Figure 32**. Lactic acid is quite commonly known to be increased after intense muscle work, and lactate concentrations in blood, the conjugate base of lactic acid, is widely used as a marker for exercise intensity [82]. **Figure 35** shows the box and whisker plot of lactic acid abundance in all samples, and the increase in lactic acid levels in the samples taken immediately after the exercise.

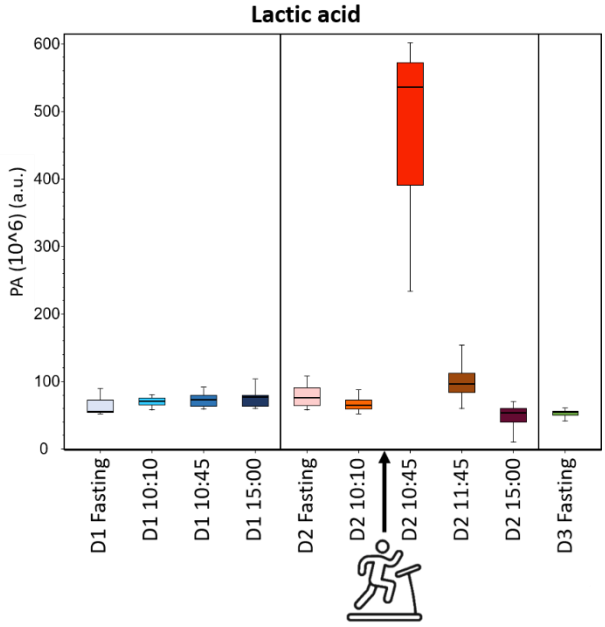

Figure 35: Lactic acid. Measured peak area (PA) of lactic acid in samples from seven healthy volunteers, taken for three days at different times during the day. Day one (D1) the participants had a normal workday with a free diet. Day two (D2) the participants had a controlled diet and participated in a high intensity exercise (indicated by the running man). Day 3 (D3) only a fasting sample was collected. The results shown are from negative ionization. Lactic acid was significantly increased after exercise.

Lactic acid is formed by reduction of pyruvate under anaerobic conditions. Pyruvate is the product of glycolysis where glucose is consumed, and ATP produced. Under aerobic

conditions, pyruvate is reduced to lactic acid to regenerate the electron acceptor nicotinamide adenine dinucleotide (NAD^+) needed to continue glycolysis. Lactic acid can be regenerated into glycose during rest, which again can take part in glycolysis [83]. The presence if lactic acid in the samples taken after the exercise indicate that the exercise was anaerobic.

To summarize: Adenosine 5'-monophosphate, hypoxanthine, and lactic acid were significantly increased after exercise, which corresponds with established knowledge about the physiological change exercise has on metabolism.

4.3.3 Lipids affected by exercise

As the overall goal of this work was to better understand the lipid coverage of the global metabolomics platform, special attention was placed to the lipids and lipid-derived metabolites that were identified. 6-oxohexanoic acid, a medium chain fatty acid, was found to be significantly increased in the samples taken immediately after exercising, as shown in **Figure 36**.

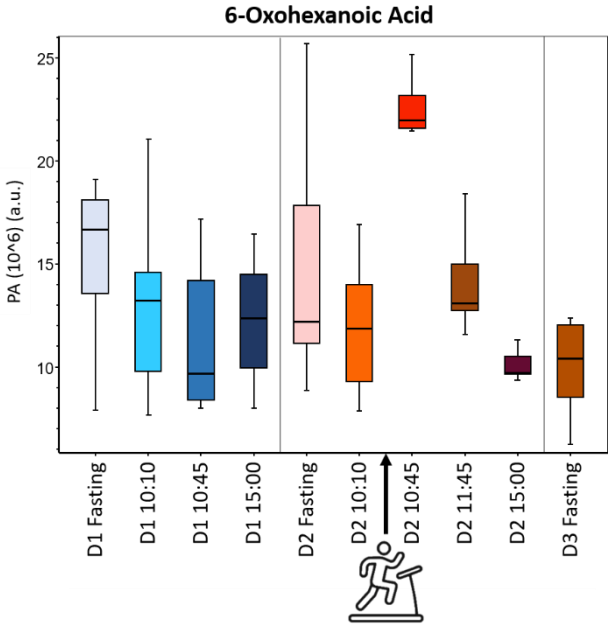

Figure 36: 6-Oxohexanoic acid. Measured peak area (PA) of 6-oxohexanoic acid in samples from seven healthy volunteers, taken for three days at different times during the day. Day one (D1) the participants had a normal workday with a free diet. Day two (D2) the participants had a controlled diet and participated in a high intensity exercise (indicated by the running man). Day 3 (D3) only a fasting sample was collected. The results shown are for negative ionization.

The relative abundance of the fatty acids oleic acid linoleic acid is shown in **Figure 37**. Both fatty acids

The two fatty acids oleic acid and linoleic acid were also identified, and the relative abundance in all samples is show in Figure 33. There was an increase in the relative abundance of these two lipids, but it was not statistically significant ($p<0.05$).

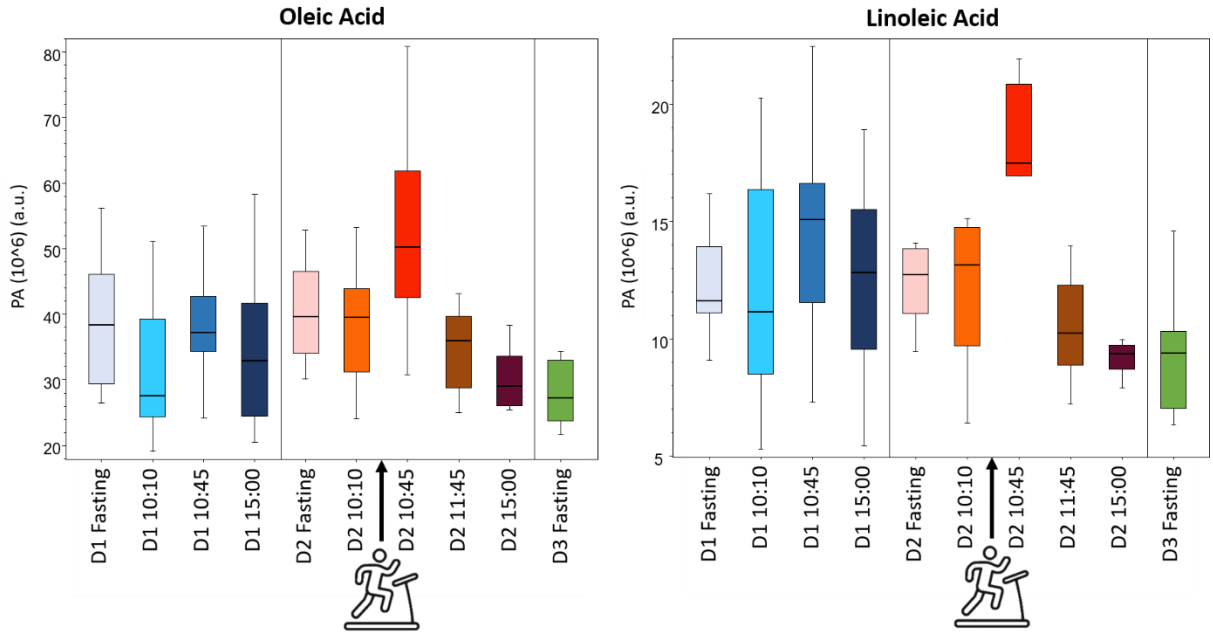

Figure 37: Oleic acid (right) and linoleic acid (left). Measured peak area (PA) of oleic acid (left) and linoleic acid (right) in samples from seven healthy volunteers, taken for three days at different times during the day. Day one (D1) the participants had a normal workday with a free diet. Day two (D2) the participants had a controlled diet and participated in a high intensity exercise (indicated by the running man). Day 3 (D3) only a fasting sample was collected. The results shown are from negative ionization.

Fatty acids are next to glucose, a major fuel for muscles during exercise, as the oxidation of fatty acids to acetyl-CoA is a central energy-yielding pathway. The electrons removed through oxidation pass through the respiratory chain, diving ATP synthesis. Because of this it is expected to find an increase in fatty acids in blood after exercise, and it is immediate [84].

The metabolites acylcarnitine C2 and acylcarnitine C16 were identified and their relative abundance are shown in **Figure 38**.

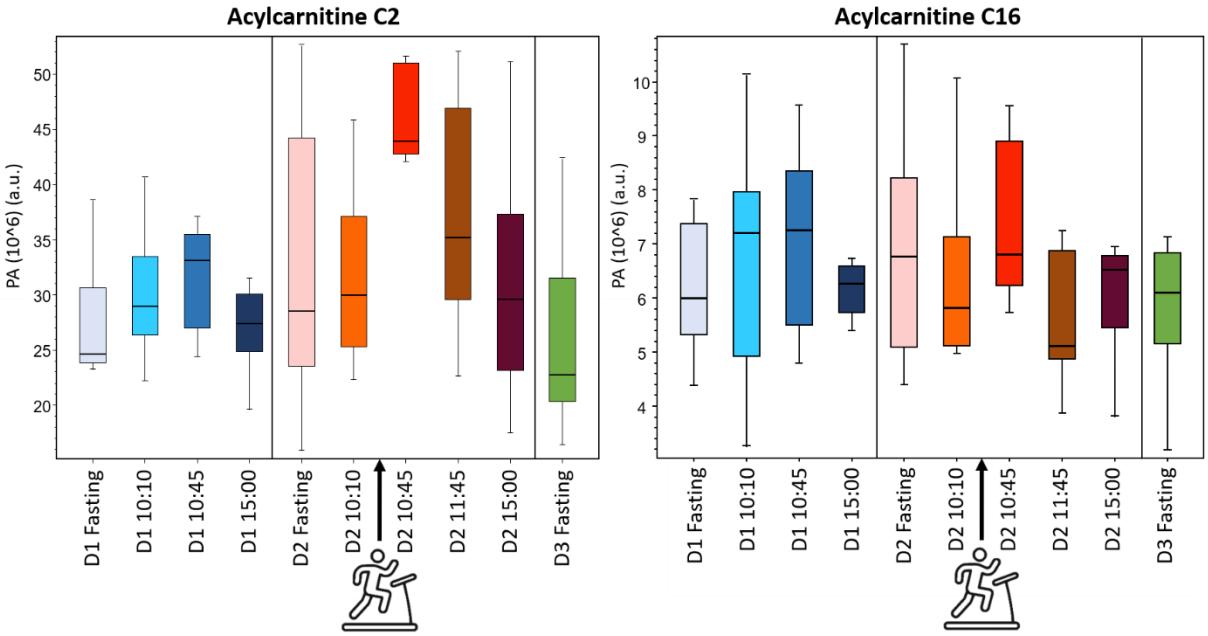

Figure 38: Acylcarnitine C2 and C16. Measured peak area (PA) of acylcarnitine C2 (left) and acylcarnitine C16 (right) in samples from seven healthy volunteers, taken for three days at different times during the day. Day one (D1) the participants had a normal workday with a free diet. Day two (D2) the participants had a controlled diet and participated in a high intensity exercise (indicated by the running man). Day 3 (D3) only a fasting sample was collected. The results shown are from positive ionization.

The acylcarnitines showed no statistically significant increase in samples taken post exercise, compared to samples taken the day prior at the same time (D1 10:45 vs D2 10:45). Acylcarnitines are fatty acids bound to carnitine, intermediates made for transporting fatty acids into the mitochondria. Acylcarnitines can leave the cells to appear in blood and other biofluids [13]. Similar to the fatty acids, the relative abundance of acylcarnitines is expected to increase and the effect is seen early after.

The glycerophospholipids PE of different acyl chain length and saturation were detected, and their abundance is shown in **Figure 39**.

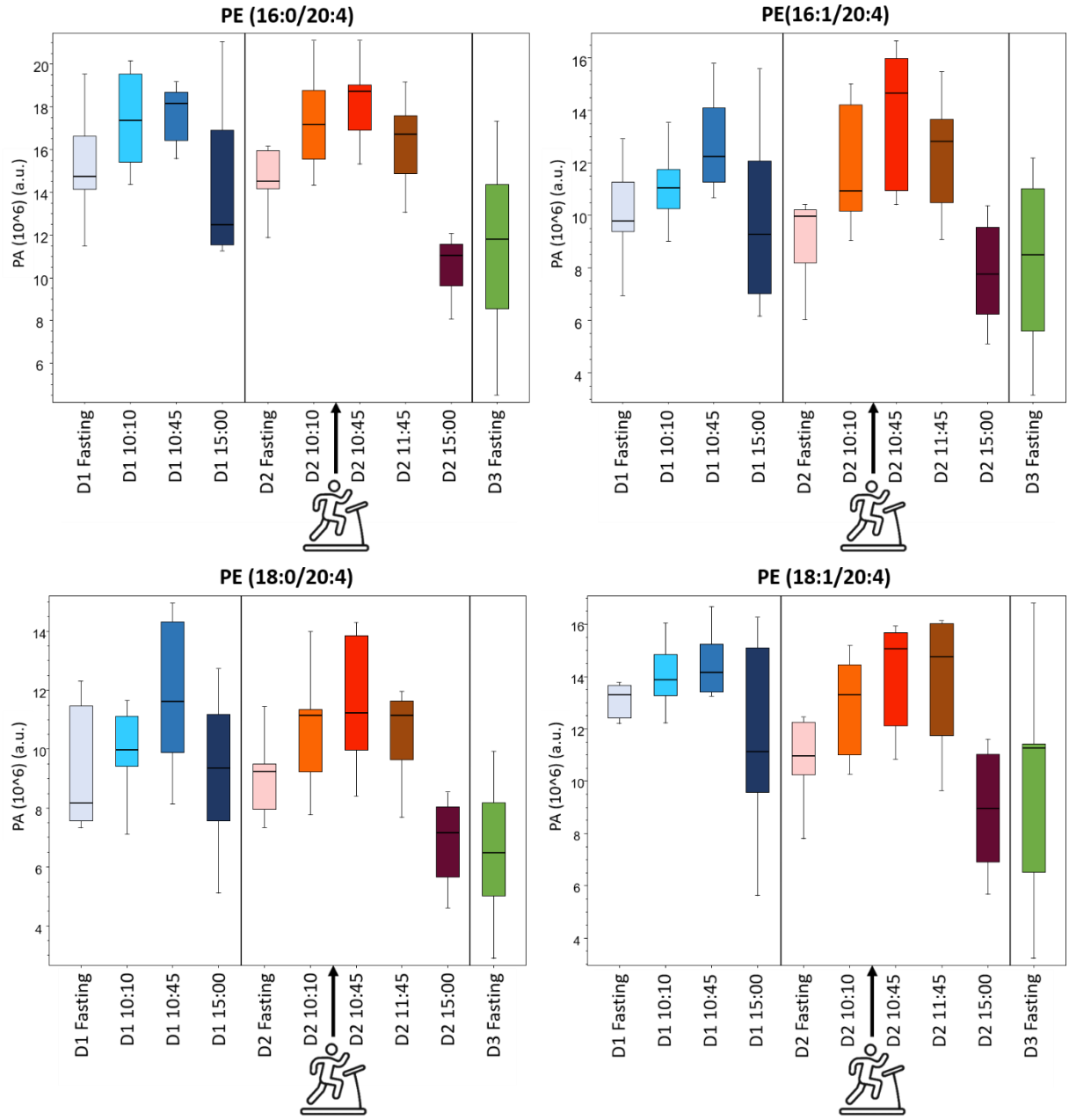

Figure 39: PE (16:0/20:4) and PE (16:1/20:4) (top), and PE (18:0/20:4) and PE (18:1/20:4) (bottom). Measured peak area (PA) of PE (16:0/20:4) and PE (16:1/20:4) (top), and PE (18:0/20:4) and PE (18:1/20:4) (bottom) in samples from seven healthy volunteers, taken for three days at different times during the day. Day one (D1) the participants had a normal workday with a free diet. Day two (D2) the participants had a controlled diet and participated in a high intensity exercise (indicated by the running man). Day 3 (D3) only a fasting sample was collected. The results shown are from negative ionization.

For these four lipids, there was no statistically significant difference between relative abundance in samples taken immediately after exercise and samples taken the day prior at the same time.

The retention time of lipids belonging to the same class or subclass has been shown to be dependent on the length of the acyl carbon chain and degree of unsaturation when using RP-

LC. A longer acyl carbon chain has shown to increase retention, and double bond saturation decrease retention [85]. This was also found to be the case for the different PE lipids detected using this method, as illustrated in **Figure 40**.

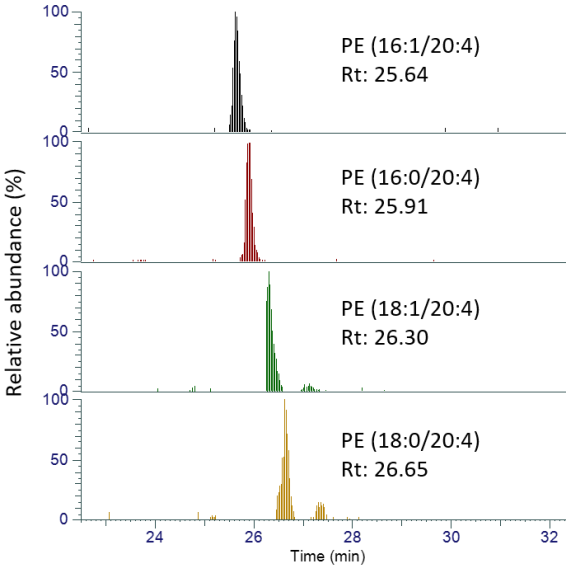

Figure 40: Extracted ion chromatogram (EIC) showing the retention of phosphatidylethanolamine (PE) of different chain length and saturation. This shows that the retention time of lipids of the same subclass is related to the carbon length of the acyl chain and saturation. This shows the different PE in the pooled quality control (PQC) in positive ionization.

Sphingolipids are like PE, membrane lipids. sphingosine 1-phosphate and palmitoyl sphingomyelin were identified, and their relative abundance is shown in **Figure 41**.

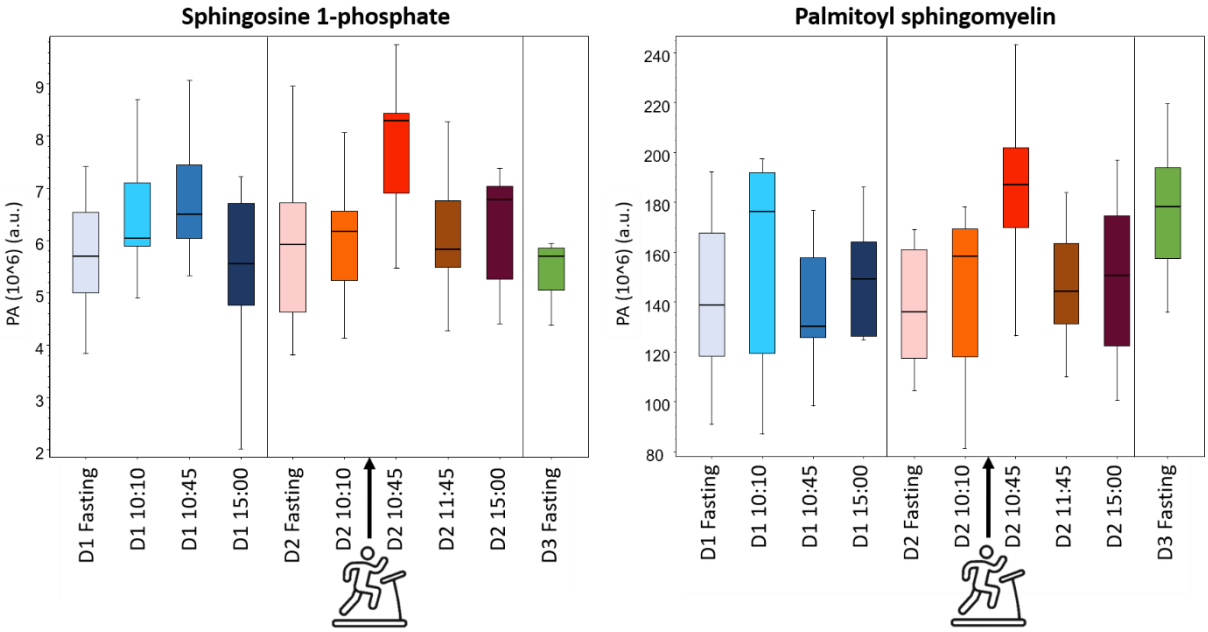

Figure 41: Sphingosine 1-phosphate and palmitoyl sphingomyelin. Measured peak area (PA) of sphingosine 1-phosphate (left) and palmitoyl sphingomyelin (right) in samples from seven healthy volunteers, taken for three days at different times during the day. Day one (D1) the participants had a normal workday with a free diet. Day two (D2) the participants had a controlled diet and participated in a high intensity exercise (indicated by the running man). Day 3 (D3) only a fasting sample was collected. The results shown are from positive ionization.

There was no statistically significant increase after exercise, but the relative abundance increased somewhat for both sphingolipids. Others have found that membrane lipids like sphingolipids and PE decreased after a bout of exercise, but the intensity and length of the exercise done was not comparable to that done in this work [13, 86].

3-Hydroxybutyric acid was identified and the relative abundance in the different samples is shown in **Figure 42**.

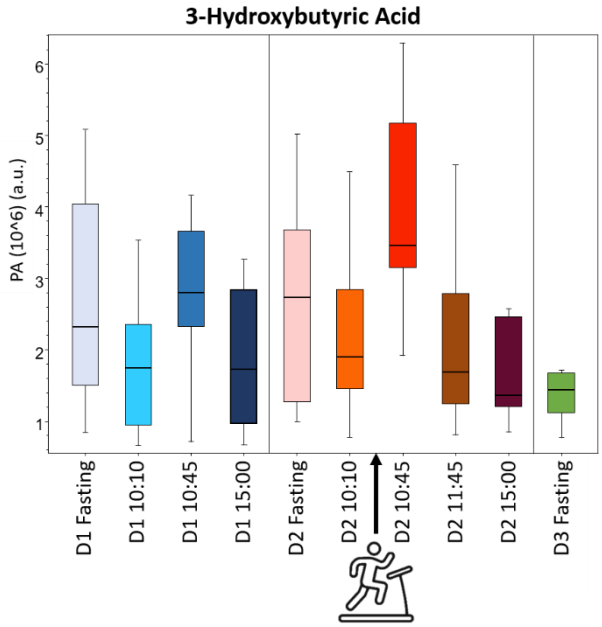

Figure 42: 3-Hyrdoxybutyric acid. Measured peak area (PA) of 3-hydroxybutyric acid in samples from seven healthy volunteers, taken for three days at different times during the day. Day one (D1) the participants had a normal workday with a free diet. Day two (D2) the participants had a controlled diet and participated in a high intensity exercise (indicated by the running man). Day 3 (D3) only a fasting sample was collected. The results shown are from negative ionization.

3-Hydroxybutyric acid is a is a ketone body, which is a lipid-derived compound. Ketone bodies are energy metabolites synthesized from acetyl-CoA or ketogenic amino acids in the liver. An increase in these are usually found when carbohydrates are limited, like during fasting or during exercise [13, 87]. Although there was no statistically significant increase in fasting or the exercise sample was found this lipid-derived metabolite, there was an increase in the sample taken after exercise.

To summarize: Lipids like fatty acids, acylcarnitines, phosphatidylethanolamines, sphingolipids, and a ketone body were detected and identified using the global metabolomics approach. Only 6-oxohexanoic acid was found to be significantly increased as a result of the exercise.

4.3.4 Diluted pooled quality controls show a linear relationship between signal intensity and metabolite concentration

In data interpretation, there is an inherent assumption that there is a positive, linear correlation between observed signal and metabolite concentration [58]. To investigate this, a series of the PQC were diluted, and the peak area of a selection of metabolites: alanine, uracil, tryptophan,

LPC (16:0), and acylcarnitine C16, was found and is shown in **Figure 43**. The metabolites were identified using Compound Discoverer.

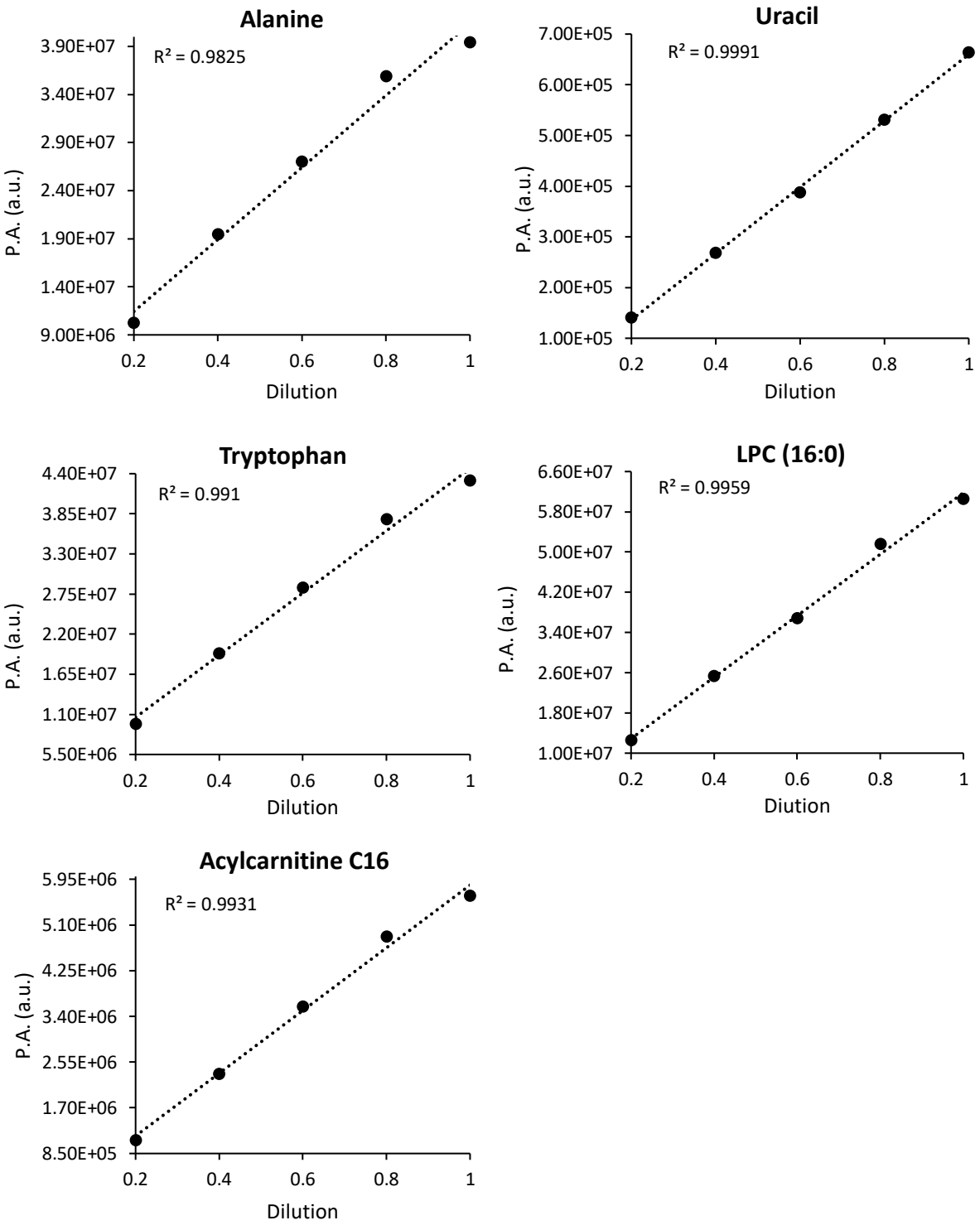

Figure 43: Peak area of alanine, uracil, tryptophan, acylcarnitine C16 and LPC (16:0) in the diluted PQCs, with R^2 value. All metabolites follow a linear regression for the signal intensity and dilution, with R^2>0.98 for all metabolites.

All the given metabolites follow linear correlation between signal intensity, represented by peak area, and dilution. This cannot be done for all metabolites, but it indicates that the assumption of a linear correlation between signal intensity and concentration is correct for some metabolites. This approach does not take into consideration that some metabolites may give non-linear signal intensity to concentration relationship, and it does not measure signal intensities over the concentration of the non-diluted PQC [58].

To summarize: dilution of the PQC showed that there was a linear relationship between signal intensity and concentration, with $R^2 > 0.98$ *for a set of metabolites.*

5 Conclusions and Future Work

The global metabolomics method described in this thesis was able to detect a variety of lipids. Extraction of lipids from DBS was found to be mostly influenced by amount of organic solvent, rather than the type of organic solvent used. The original extraction solution containing 80% MeOH with 0.1% FA was deemed appropriate for extraction of DBS, as the metabolome and lipidome coverage of this and the other high organic solvent extraction solutions were not considerably different. There was no clear indication of extraction being different for solvents of different groups in the Snyder's solvent selectivity diagram. Increasing the logP value of the solvent did slightly improve lipid coverage, but only by a few lipids. This was likely due to the fact that the solvents used were in a too small logP range to make a significant difference in hydrophobicity of the solvents.

The lipid coverage using the global metabolomics method was also found to be dependent on chromatographic and ESI-MS factors. Ionization was also found to influence the detection of lipids, and some lipids were only detectable in negative ionization with an alternative mobile phase with pH of approximately 7.

The global metabolomics method could detect changes in the metabolome and lipidome after exercise. The abundance of metabolites that are known to be affected by hard physical activity was found to be significantly altered. A variety of lipids were also found to be affected, but only 6-oxohexanoic acid had a statistically significant increase. Using PQCs was a useful indicator of data quality, and the diluted PQCs showed that there was a linear relationship between signal intensity and metabolite concentration, with R^2>0.98 for a selection of metabolites.

5.1 Future work

The global metabolomics method described in this work is used for research and is implemented as a supplementary diagnostic tool at the National Unit for Screening and Diagnosis of Congenital Pediatric Metabolic Disorders at Oslo university hospital. Even though it is in use, the method can be further optimized and adapted.

The ionization of metabolites and lipids in the negative mode can be improved by using a mobile phase that promotes ionization of acidic compounds.

The extraction of the DBS metabolome can be further investigated by use of even more hydrophobic solvents than that was done here, for instance by using chloroform or MTBE in higher amounts.

Identification of lipids was difficult. As lipids within a group or subgroup often share a common structural feature, identification of these groups could be made easier by employing other fragmentation methods than DDA topN, for instance by using product ion scanning.

The use of quality controls, and PQCs should be further investigated, and implemented in the global metabolomics workflow.

Although comprehensive, developing a LC-MS method purely for the analysis of lipids, would provide a more comprehensive lipid coverage than that of a global metabolomics method.

References

[1] J.T.R. Clarke, *General Principles, A clinical guide to inherited metabolic diseases*, Cambridge University Press, Cambridge, 2006, pp. 1-21.

[2] C.M. Mak, H.C. Lee, A.Y. Chan, C.W. Lam, *Inborn errors of metabolism and expanded newborn screening: review and update*, Crit Rev Clin Lab Sci 50(6) (2013) 142-62.

[3] C.R. Ferreira, C.D.M. van Karnebeek, J. Vockley, N. Blau, *A proposed nosology of inborn errors of metabolism*, Genet Med 21(1) (2019) 102-106.

[4] *Om medfødte stoffskiftesykdommer*. https://oslo-universitetssykehus.no/fag-og-forskning/laboratorietjenester/-medisinsk-biokjemi/seksjon-for-medfodte-metabolske-sykdommer/om-medfodte-stoffskiftesykdommer, 2016 (cited 12.05.2020).

[5] *Newborn Screening*. https://oslo-universitetssykehus.no/avdelinger/barne-og-ungdomsklinikken/nyfodtscreeningen/nyfodtscreening#information-in-english, 2019 (cited 13.01.2020).

[6] I.T. Ismail, M.R. Showalter, O. Fiehn, *Inborn Errors of Metabolism in the Era of Untargeted Metabolomics and Lipidomics*, Metabolites 9(10) (2019).

[7] A. Tebani, L. Abily-Donval, C. Afonso, S. Marret, S. Bekri, *Clinical Metabolomics: The New Metabolic Window for Inborn Errors of Metabolism Investigations in the Post-Genomic Era*, Int J Mol Sci 17(7) (2016) 1167.

[8] F. Lamari, F. Mochel, J.-M. Saudubray, *An overview of inborn errors of complex lipid biosynthesis and remodelling*, Journal of Inherited Metabolic Disease 38(1) (2015) 3-18.

[9] W.B. Dunn, D.I. Broadhurst, H.J. Atherton, R. Goodacre, J.L. Griffin, *Systems level studies of mammalian metabolomes: the roles of mass spectrometry and nuclear magnetic resonance spectroscopy*, Chemical Society Reviews 40(1) (2011) 387-426.

[10] A. Klassen, G.A.B. Canuto, P.L.R. da Cruz, M.F.M. Tavares, H.C. Ribeiro, A. Sussulini, *Metabolomics: Definitions and Significance in Systems Biology*, in: A. Sussulini (Ed.) *Metabolomics: From Fundamentals to Clinical Applications. Advances in Experimental Medicine and Biology*, Springer International Publishing : Imprint: Springer, Cham, 2017, pp. 3-13.

[11] D.C. Harris, *Introduction to Analytical Separations*, in *Quantitative chemical analysis*, Freeman, New York, 2010, pp. 538-542.

[12] M.R. Wenk, *The emerging field of lipidomics*, Nat Rev Drug Discov 4(7) (2005) 594-610.

[13] D. Schranner, G. Kastenmüller, M. Schönfelder, W. Römisch-Margl, H. Wackerhage, *Metabolite Concentration Changes in Humans After a Bout of Exercise: a Systematic Review of Exercise Metabolomics Studies*, Sports Medicine - Open 6(1) (2020) 11.

[14] R. Rennie, J. Law, *A Dictionary of Chemistry*, 7 ed., Oxford University Press2016.

[15] E. Fahy, S. Subramaniam, H.A. Brown, C.K. Glass, A.H. Merrill, Jr., R.C. Murphy, C.R. Raetz, D.W. Russell, Y. Seyama, W. Shaw, T. Shimizu, F. Spener, G. van Meer, M.S. VanNieuwenhze, S.H. White, J.L. Witztum, E.A. Dennis, *A comprehensive classification system for lipids*, J Lipid Res 46(5) (2005) 839-61.

[16] E. Fahy, D. Cotter, M. Sud, S. Subramaniam, *Lipid classification, structures and tools*, Biochim Biophys Acta 1811(11) (2011) 637-47.

[17] *The nomenclature of lipids (Recommendations 1976) IUPAC-IUB Commission on Biochemical Nomenclature*, Biochem J 171(1) (1978) 21-35.

[18] G.A. Nagana Gowda, D. Raftery, *Can NMR solve some significant challenges in metabolomics?*, J Magn Reson 260 (2015) 144-60.

[19] J.H. Gross, *Introduction*, in *Mass Spectrometry : A Textbook*, Springer International Publishing : Imprint: Springer, Cham, 2017, pp. 9-18.

[20] S.A. Goldansaz, A.C. Guo, T. Sajed, M.A. Steele, G.S. Plastow, D.S. Wishart, *Livestock metabolomics and the livestock metabolome: A systematic review*, PLoS One 12(5) (2017) e0177675.

[21] B. Zhou, J.F. Xiao, L. Tuli, H.W. Ressom, *LC-MS-based metabolomics*, Mol Biosyst 8(2) (2012) 470-81.

[22] D.J. Weston, *Ambient ionization mass spectrometry: current understanding of mechanistic theory; analytical performance and application areas*, Analyst 135(4) (2010) 661-668.

[23] P. Begley, S. Francis-McIntyre, W.B. Dunn, D.I. Broadhurst, A. Halsall, A. Tseng, J. Knowles, R. Goodacre, D.B. Kell, *Development and Performance of a Gas Chromatography−Time-of-Flight Mass Spectrometry Analysis for Large-Scale Nontargeted Metabolomic Studies of Human Serum*, Analytical Chemistry 81(16) (2009) 7038-7046.

[24] O. Fiehn, J. Kopka, R.N. Trethewey, L. Willmitzer, *Identification of Uncommon Plant Metabolites Based on Calculation of Elemental Compositions Using Gas Chromatography and Quadrupole Mass Spectrometry*, Analytical Chemistry 72(15) (2000) 3573-3580.

[25] J.H. Gross, *Isotopic Composition and Accurate Mass*, in *Mass Spectrometry : A Textbook*, Springer International Publishing : Imprint: Springer, Cham, 2017, pp. 85-145.

[26] M. Krauss, H. Singer, J. Hollender, *LC-high resolution MS in environmental analysis: from target screening to the identification of unknowns*, Anal Bioanal Chem 397(3) (2010) 943-51.

[27] D.S. Wishart, *Advances in metabolite identification*, Bioanalysis 3(15) (2011) 1769-1782.

[28] J.H. Gross, *4.8 Orbitrap Analyzers*, in *Mass Spectrometry : A Textbook*, Springer International Publishing : Imprint: Springer, Cham, 2017, pp. 246-253.

[29] A. Michalski, E. Damoc, J.P. Hauschild, O. Lange, A. Wieghaus, A. Makarov, N. Nagaraj, J. Cox, M. Mann, S. Horning, *Mass spectrometry-based proteomics using Q Exactive, a high-performance benchtop quadrupole Orbitrap mass spectrometer*, Mol Cell Proteomics 10(9) (2011) M111 011015.

[30] J.V. Olsen, L.M. de Godoy, G. Li, B. Macek, P. Mortensen, R. Pesch, A. Makarov, O. Lange, S. Horning, M. Mann, *Parts per million mass accuracy on an Orbitrap mass spectrometer via lock mass injection into a C-trap*, Mol Cell Proteomics 4(12) (2005) 2010-21.

[31] A. Makarov, *Electrostatic axially harmonic orbital trapping: a high-performance technique of mass analysis*, Anal Chem 72(6) (2000) 1156-62.

[32] J.H. Gross, *Electrospray Ionization*, J.H. Gross (Ed.) in *Mass Spectrometry: A Textbook*, Springer Berlin Heidelberg, Berlin, Heidelberg, 2011, pp. 561-620.

[33] H. Awad, M.M. Khamis, A. El-Aneed, *Mass Spectrometry, Review of the Basics: Ionization*, Applied Spectroscopy Reviews 50(2) (2015) 158-175.

[34] D.C. Harris, *Mass Spectrometry*, in *Quantitative chemical analysis*, Freeman, New York, 2010, pp. 502-521.

[35] W.B. Dunn, D. Broadhurst, P. Begley, E. Zelena, S. Francis-McIntyre, N. Anderson, M. Brown, J.D. Knowles, A. Halsall, J.N. Haselden, A.W. Nicholls, I.D. Wilson, D.B. Kell, R. Goodacre, C. Human Serum Metabolome, *Procedures for large-scale metabolic profiling of serum and plasma using gas chromatography and liquid chromatography coupled to mass spectrometry*, Nat Protoc 6(7) (2011) 1060-83.

[36] A. Makarov, M. Scigelova, *Coupling liquid chromatography to Orbitrap mass spectrometry*, J Chromatogr A 1217(25) (2010) 3938-45.

[37] E. Lundanes, L. Reubsaet, T. Greibrokk, *High-Performance Liquid Chromatography (HPLC)*, in *Chromatography : basic principles, sample preparations and related methods*, Wiley-VCH, Weinheim, 2014, pp. 47-104.

[38] A. Koulman, P. Prentice, M.C.Y. Wong, L. Matthews, N.J. Bond, M. Eiden, J.L. Griffin, D.B. Dunger, *The development and validation of a fast and robust dried blood spot based lipid profiling method to study infant metabolism*, Metabolomics : Official journal of the Metabolomic Society 10(5) (2014) 1018-1025.

[39] B.L. Therrell, C.D. Padilla, J.G. Loeber, I. Kneisser, A. Saadallah, G.J. Borrajo, J. Adams, *Current status of newborn screening worldwide: 2015*, Semin Perinatol 39(3) (2015) 171-87.

[40] V. Moreira, E. Brasili, J. Fiamoncini, F. Marini, A. Miccheli, H. Daniel, J.J.H. Lee, N.M.A. Hassimotto, F.M. Lajolo, *Orange juice affects acylcarnitine metabolism in healthy volunteers as revealed by a mass-spectrometry based metabolomics approach*, Food Res Int 107 (2018) 346-352.

[41] J. Dénes, E. Szabó, S.L. Robinette, I. Szatmári, L. Szőnyi, J.G. Kreuder, E.W. Rauterberg, Z. Takáts, *Metabonomics of Newborn Screening Dried Blood Spot Samples: A Novel Approach in the Screening and Diagnostics of Inborn Errors of Metabolism*, Analytical Chemistry 84(22) (2012) 10113-10120.

[42] A. Acharjee, P. Prentice, C. Acerini, J. Smith, I.A. Hughes, K. Ong, J.L. Griffin, D. Dunger, A. Koulman, *The translation of lipid profiles to nutritional biomarkers in the study of infant metabolism*, Metabolomics : Official journal of the Metabolomic Society 13(3) (2017) 25.

[43] A. Sharma, S. Jaiswal, M. Shukla, J. Lal, *Dried blood spots: Concepts, present status, and future perspectives in bioanalysis*, Drug Testing and Analysis 6(5) (2014) 399-414.

[44] W. Li, F.L.S. Tse, *Dried blood spot sampling in combination with LC-MS/MS for quantitative analysis of small molecules*, 24(1) (2010) 49-65.

[45] R. Fingerhut, R. Ensenauer, W. Röschinger, R. Arnecke, B. Olgemöller, A.A. Roscher, *Stability of Acylcarnitines and Free Carnitine in Dried Blood Samples: Implications for Retrospective Diagnosis of Inborn Errors of Metabolism and Neonatal Screening for Carnitine Transporter Deficiency*, Analytical Chemistry 81(9) (2009) 3571-3575.

[46] Y. Enderle, K. Foerster, J. Burhenne, *Clinical feasibility of dried blood spots: Analytics, validation, and applications*, Journal of Pharmaceutical and Biomedical Analysis 130 (2016) 231-243.

[47] D.C. Lehotay, P. Hall, J. Lepage, J.C. Eichhorst, M.L. Etter, C.R. Greenberg, *LC–MS/MS progress in newborn screening*, Clinical Biochemistry 44(1) (2011) 21-31.

[48] S.G. Oliver, M.K. Winson, D.B. Kell, F. Baganz, *Systematic functional analysis of the yeast genome*, Trends Biotechnol 16(9) (1998) 373-8.

[49] S. Pedersen-Bjergaard, A. Gjelstad, T. Halvorsen Grønhaug, *Sample preparation*, S. Honoré Hansen, S. Pedersen-Bjergaard (Eds.) in *Bioanalysis of pharmaceuticals : sample preparation, separation techniques, and mass spectrometry*, Wiley, West Sussex, England, 2015, pp. 73-113.

[50] V.J. Barwick, *Strategies for solvent selection — a literature review*, TrAC Trends in Analytical Chemistry 16(6) (1997) 293-309.

[51] S.B. Milne, T.P. Mathews, D.S. Myers, P.T. Ivanova, H.A. Brown, *Sum of the parts: mass spectrometry-based metabolomics*, Biochemistry 52(22) (2013) 3829-40.

[52] P. Yin, G. Xu, *Current state-of-the-art of nontargeted metabolomics based on liquid chromatography-mass spectrometry with special emphasis in clinical applications*, J Chromatogr A 1374 (2014) 1-13.

[53] L.R. Snyder, *Classification of the Solvent Properties of Common Liquids*, Journal of Chromatographic Science 16(6) (1978) 223-234.

[54] E. Lundanes, L. Reubsaet, T. Greibrokk, *Sample Preparation*, in *Chromatography : basic principles, sample preparations and related methods*, Wiley-VCH Verlag GmbH & Co. KGaA, Weinheim, 2014, pp. 161-188.

[55] L.R. Snyder, P.W. Carr, S.C. Rutan, *Solvatochromically Based Solvent-Selectivity Triangle*, J Chromatogr A 656(1-2) (1993) 537-547.

[56] T. Nemkov, K.C. Hansen, L.J. Dumont, A. D'Alessandro, *Metabolomics in transfusion medicine*, Transfusion 56(4) (2016) 980-93.

[57] Y. Tang, Z. Li, L. Lazar, Z. Fang, C. Tang, J. Zhao, *Metabolomics workflow for lung cancer: Discovery of biomarkers*, Clin Chim Acta 495 (2019) 436-445.

[58] D. Broadhurst, R. Goodacre, S.N. Reinke, J. Kuligowski, I.D. Wilson, M.R. Lewis, W.B. Dunn, *Guidelines and considerations for the use of system suitability and quality control samples in mass spectrometry assays applied in untargeted clinical metabolomic studies*, Metabolomics : Official journal of the Metabolomic Society 14(6) (2018) 72.

[59] A.C. Schrimpe-Rutledge, S.G. Codreanu, S.D. Sherrod, J.A. McLean, *Untargeted Metabolomics Strategies-Challenges and Emerging Directions*, J Am Soc Mass Spectrom 27(12) (2016) 1897-1905.

[60] W.B. Dunn, I.D. Wilson, A.W. Nicholls, D. Broadhurst, *The importance of experimental design and QC samples in large-scale and MS-driven untargeted metabolomic studies of humans*, Bioanalysis 4(18) (2012) 2249-2264.

[61] E.M. Sandås, *Liquid chromatography - Orbitrap mass spectrometry is a useful tool in untargeted metabolomics analysis of dried blood spots in clinical chemistry [Master thesis]*, *Department of Chemistry*, Universety of Oslo, 2018.
[62] H.B. Skogvold, *Laboratory diagnostics: Maximizing sensitivity of a Q-Exactive Orbitrap mass spectrometer for untargeted metabolomics of dried blood spots [Master thesis]*, *Department of Chemistry*, University of Oslo, 2017.
[63] C.E. Arnesen, *Optimization of liquid chromatographic parameters for untargeted metabolomics of dried blood spots [Master thesis]*, *Department of Chemistry*, University of Oslo, 2017.
[64] S. Naz, M. Vallejo, A. García, C. Barbas, *Method validation strategies involved in non-targeted metabolomics*, J Chromatogr A 1353 (2014) 99-105.
[65] G.A. Theodoridis, H.G. Gika, E.J. Want, I.D. Wilson, *Liquid chromatography–mass spectrometry based global metabolite profiling: A review*, Analytica Chimica Acta 711 (2012) 7-16.
[66] D.S. Wishart, Y.D. Feunang, A. Marcu, A.C. Guo, K. Liang, R. Vazquez-Fresno, T. Sajed, D. Johnson, C. Li, N. Karu, Z. Sayeeda, E. Lo, N. Assempour, M. Berjanskii, S. Singhal, D. Arndt, Y. Liang, H. Badran, J. Grant, A. Serra-Cayuela, Y. Liu, R. Mandal, V. Neveu, A. Pon, C. Knox, M. Wilson, C. Manach, A. Scalbert, *HMDB 4.0: the human metabolome database for 2018*, Nucleic Acids Res 46(D1) (2018) D608-d617.
[67] S. Kim, J. Chen, T. Cheng, A. Gindulyte, J. He, S. He, Q. Li, B.A. Shoemaker, P.A. Thiessen, B. Yu, L. Zaslavsky, J. Zhang, E.E. Bolton, *PubChem 2019 update: improved access to chemical data*, Nucleic Acids Research 47(D1) (2018) D1102-D1109.
[68] O.L. Knittelfelder, B.P. Weberhofer, T.O. Eichmann, S.D. Kohlwein, G.N. Rechberger, *A versatile ultra-high performance LC-MS method for lipid profiling*, J Chromatogr B Analyt Technol Biomed Life Sci 951-952(100) (2014) 119-128.
[69] P.J. Schoenmakers, S. Vanmolle, C.M.G. Hayes, L.G.M. Uunk, *Effects of pH in Reversed-Phase Liquid-Chromatography*, Analytica Chimica Acta 250(1) (1991) 1-19.
[70] E. Balashova, O. Trifonova, D. Maslov, P. Lokhov, *Application of dried blood spot for analysis of low molecular weight fraction (metabolome) of blood*, Health and Primary Care 2 (2018).
[71] S. Keunchkarian, M. Reta, L. Romero, C. Castells, *Effect of sample solvent on the chromatographic peak shape of analytes eluted under reversed-phase liquid chromatogaphic conditions*, J Chromatogr A 1119(1) (2006) 20-28.

[72] J. Folch, M. Lees, G.H.S. Stanley, *A Simple Method for The Isolation and Purification of Total Lipides From Animal Tissues*, Journal of Biological Chemistry 226(1) (1957) 497-509.
[73] E. Lesellier, *Sigmapider diagram: a universal and versatile approach for system comparison and classification: application to solvent properties*, J Chromatogr A 1389 (2015) 49-64.
[74] S. Gao, Z.-P. Zhang, H.T. Karnes, *Sensitivity enhancement in liquid chromatography/atmospheric pressure ionization mass spectrometry using derivatization and mobile phase additives*, Journal of Chromatography B 825(2) (2005) 98-110.
[75] D.G. Hardie, J.W. Scott, D.A. Pan, E.R. Hudson, *Management of cellular energy by the AMP-activated protein kinase system*, FEBS Lett 546(1) (2003) 113-20.
[76] J.A. Hawley, M. Hargreaves, M.J. Joyner, J.R. Zierath, *Integrative biology of exercise*, Cell 159(4) (2014) 738-49.
[77] D.L. Nelson, A.L. Lehninger, M.M. Cox, *Nucleotides and Nucleic Acids*, in *Lehninger Principles of Biochemistry*, W.H. Freeman, New York, 2013, pp. 281-308.
[78] H. Reinke, G. Asher, *Crosstalk between metabolism and circadian clocks*, Nature Reviews Molecular Cell Biology 20(4) (2019) 227-241.
[79] M. Hur, A.A. Campbell, M. Almeida-de-Macedo, L. Li, N. Ransom, A. Jose, M. Crispin, B.J. Nikolau, E.S. Wurtele, *A global approach to analysis and interpretation of metabolic data for plant natural product discovery*, Natural Product Reports 30(4) (2013) 565-583.
[80] K. Sahlin, M. Tonkonogi, K. Soderlund, *Plasma hypoxanthine and ammonia in humans during prolonged exercise*, Eur J Appl Physiol Occup Physiol 80(5) (1999) 417-22.
[81] L.H. Ketai, R.H. Simon, J.W. Kreit, C.M. Grum, *Plasma hypoxanthine and exercise*, Am Rev Respir Dis 136(1) (1987) 98-101.
[82] S.P. Cairns, *Lactic Acid and Exercise Performance*, Sports Medicine 36(4) (2006) 279-291.
[83] D.L. Nelson, A.L. Lehninger, M.M. Cox, *Glycolysis, Gluconeogenesis, and the Pentose Phosphate Pathway*, in *Lehninger Principles of Biochemistry*, W.H. Freeman, New York, 2013, pp. 543-580.
[84] J.W. Starnes, T.L. Parry, S.K. O'Neal, J.R. Bain, M.J. Muehlbauer, A. Honcoop, A. Ilaiwy, P.M. Christopher, C. Patterson, M.S. Willis, *Exercise-Induced Alterations in Skeletal Muscle, Heart, Liver, and Serum Metabolome Identified by Non-Targeted Metabolomics Analysis*, Metabolites 7(3) (2017) 40.
[85] A. Fauland, H. Köfeler, M. Trötzmüller, A. Knopf, J. Hartler, A. Eberl, C. Chitraju, E. Lankmayr, F. Spener, *A comprehensive method for lipid profiling by liquid chromatography-*

ion cyclotron resonance mass spectrometry, Journal of lipid research 52(12) (2011) 2314-2322.

[86] J.P. Karl, L.M. Margolis, N.E. Murphy, C.T. Carrigan, J.W. Castellani, E.H. Madslien, H.-K. Teien, S. Martini, S.J. Montain, S.M. Pasiakos, *Military training elicits marked increases in plasma metabolomic signatures of energy metabolism, lipolysis, fatty acid oxidation, and ketogenesis*, Physiological Reports 5(17) (2017) e13407.

[87] D.L. Nelson, A.L. Lehninger, M.M. Cox, *Fatty Acid Catabolism*, in *Lehninger Principles of Biochemistry*, W.H. Freeman, New York, 2013, pp. 667-688.

[88] W.B. Dunn, D. Broadhurst, P. Begley, E. Zelena, S. Francis-McIntyre, N. Anderson, M. Brown, J.D. Knowles, A. Halsall, J.N. Haselden, A.W. Nicholls, I.D. Wilson, D.B. Kell, R. Goodacre, C. The Human Serum Metabolome, *Procedures for large-scale metabolic profiling of serum and plasma using gas chromatography and liquid chromatography coupled to mass spectrometry*, Nature Protocols 6(7) (2011) 1060-1083.

6 Appendix

6.1 List of positive and negative ions for the lipidome and metabolome standards

The positive and negative ions used for making extracted ion chromatograms for the compounds in the lipidome and metabolome standards are shown in **Table 17-19**.

Table 17: Positive and negative adducts, with *m/z* values for the compounds in the isotopically labeled lipidome standard.

Compound	Positive adduct	*m/z*	Negative adduct	*m/z*
PC (15:0/18:1 (d7))	$[M+H]^+$	753.6134	$[M+COO]^-$	797.6043
LPC (18:1 (d7))	$[M+H]^+$	529.3994	$[M+COO]^-$	573.3903
PE (15:0/18:1 (d7))	$[M+H]^+$	711.5664	$[M-H]^-$	709.5519
LPE (18:1 (d7))	$[M+H]^+$	487.3524	$[M-H]^-$	485.3378
PG (15:0/18:1(d7))	-	-	$[M-H]^-$	740.5464
PI (15:0/18:1(d7))	-	-	$[M-H]^-$	828.5625
PS (15:0/18:1(d7))	-	-	$[M-H]^-$	753.5417
TG (15:0/18:1 (d7)/15:0)	$[M+Na]^+$	834.7538	-	-
DG (15:0/18:1 (d7))	$[M+H]^+$	588.5579	$[M+COO]^-$	632.5488
MG (18:1 (d7))	$[M+H]^+$	364.3439	$[M+COO]^-$	408.3348
CE (18:1 (d7))	$[M+Na]^+$	680.6333	-	-
SM (d18:1/18:1 (d9))	$[M+H]^+$	738.647	$[M+COO]^-$	782.6379
Cer (d18:1 (d7)/15:0)	$[M+H]^+$	531.5477	$[M+COO]^-$	575.5386

Table 18: Positive and negative adducts, with *m/z* values for the compounds in the lipidome standard.

Compound	Positive adduct	*m/z*	Negative adduct	*m/z*
PC (15:0/18:1)	$[M+H]^+$	746.5694	$[M+COO]^-$	790.5604
LPC (18:1)	$[M+H]^+$	522.3554	$[M+COO]^-$	566.3463
PE (15:0/18:1)	$[M+H]^+$	704.5225	$[M-H]^-$	702.5079
LPE (18:1)	$[M+H]^+$	480.3085	$[M-H]^-$	478.2939
PG (15:0/18:1)	-	-	$[M-H]^-$	733.5025
PI (15:0/18:1)	-	-	$[M-H]^-$	821.5186
PS (15:0/18:1)	-	-	$[M-H]^-$	746.4978
TG (15:0/18:1 /15:0)	$[M+Na]^+$	827.7099	-	-
DG (15:0/18:1)	$[M+H]^+$	581.514	$[M+COO]^-$	625.5049
MG (18:1)	$[M+H]^+$	357.2999	$[M+COO]^-$	401.2909
CE (18:1)	$[M+Na]^+$	673.5894	-	-
SM (d18:1/18:1)	$[M+H]^+$	729.5905	$[M+COO]^-$	773.5814
Cer (d18:1/15:0)	$[M+H]^+$	524.5037	$[M+COO]^-$	568.4946

Table 19: Positive and negative adducts, with *m/z* values for the compounds in the metabolome standard.

Compound	Positive adduct	*m/z*	Negative adduct	*m/z*
D3 acylcarnitine C2	$[M+H]^+$	207.1419	$[M+COO]^-$	251.1328
D3 acylcarnitine C12	$[M+H]^+$	347.2984	$[M+COO]^-$	345.2838
D3 acylcarnitine C16	$[M+H]^+$	403.361	$[M+COO]^-$	447.3519
^{13}C creatine	$[M+H]^+$	133.0801	-	-
^{13}C2 guanidinoacetic acid	$[M+H]^+$	120.0678	-	-
D4 succinic acid	$[M+H]^+$	123.059	-	-

6.2 Average and relative standard deviation for peak areas and retention times of each compound in the experiments

The average and % relative standard deviation (% RSD) of all peak areas and retention times for were calculated for all observed compounds, shown in **Table 20-56**.

Table 20: Isotopically labeled lipidome standard (ESI+). Average and relative standard deviation in % (% RSD) of the peak areas (PA) and retention times (Rt) of compounds in the isotopically labeled lipidome standard analyzed three times (N=3), in positive ionization.

Compound	Average PA (a.u.) N=3	% RSD PA (a.u.) N=3	Average Rt (min) N=3	% RSD Rt (min) N=3
PC (15:0/18:1(d7))	1.11E+07	5%	27.98	0.03%
PC (0:0/18:1 (d7))	2.02E+07	1%	19.06	0.1%
PC (18:1 (d7)/0:0)	1.48E+08	0.1%	19.57	0.04%
PE (15:0/18:1 (d7))	1.72E+07	1%	24.74	0.05%
PE (0:0/18:1 (d7))	1.61E+07	2%	17.15	0.04%
PE (18:1 (d7)/0:0)	1.91E+08	0.1%	17.55	0%
PG (15:0/18:1 (d7))	N.D.*	N.D.*	N.D.*	N.D.*
PI (15:0/18:1 (d7))	N.D.*	N.D.*	N.D.*	N.D.*
PS (15:0/18:1)	N.D.*	N.D.*	N.D.*	N.D.*
TG (15:0/18:1 (d7)/15:0)	2.28E+07	2%	30.17	0.04%
DG (15:0/18:1 (d7))	5.35E+06	2%	26.22	0.06%
MG (0:0/18:1 (d7)/0:0)	1.09E+07	3%	18.46	0.1%
MG (18:1(d7)/0:0/0:0)	1.18E+08	2%	18.81	0.03%
CE (18:1 (d7))	2.20E+07	2%	31.20	0.05%
SM (d18:1/18:1 (d9))	1.77E+07	2%	25.80	0.09%
Cer (d18:1 (d7)/15:0)	4.29E+07	3%	23.01	0.1%

*N.D. = Not detectable.

Table 21: Isotopically labeled lipidome standard (ESI-). Average and relative standard deviation in % (% RSD) of peak areas (PA) and retention times (Rt) of compounds in the isotopically labeled lipidome standard analyzed three times (N=3), in negative ionization.

Compound	Average PA (a.u.) N=3	% RSD PA (a.u.) N=3	Average Rt (min) N=3	% RSD Rt (min) N=3
PC (15:0/18:1 (d7))	6.39E+06	1%	27.94	0.07%
PC (0:0/18:1 (d7))	1.37E+07	2%	19.04	0.04%
PC (18:1 (d7)/0:0)	8.88E+07	1%	19.54	0.07%
PE (15:0/18:1 (d7))	1.62E+07	3%	24.74	0.09%
PE (0:0/18:1 (d7))	1.67E+07	2%	17.16	0.04%
PE (18:1 (d7)/0:0)	1.78E+08	2%	17.58	0.09%
PG (15:0/18:1 (d7))	N.D.*	N.D.*	N.D.*	N.D.*
PI (15:0/18:1 (d7))	N.D.*	N.D.*	N.D.*	N.D.*
PS (15:0/18:1)	N.D.*	N.D.*	N.D.*	N.D.*
TG (15:0/18:1 (d7)/15:0)	N.D.*	N.D.*	N.D.*	N.D.*
DG (15:0/18:1(d7))	N.D.*	N.D.*	N.D.*	N.D.*
MG (0:0/18:1 (d7)/0:0)	1.35E+07	2%	18.46	0.04%
MG (18:1 (d7)/0:0/0:0)	7.51E+07	2%	18.81	0.05%
CE (18:1 (d7))	N.D.*	N.D.*	N.D.*	N.D.*
SM (d18:1/18:1((d9))	1.31E+07	2%	25.76	0.07%
Cer (d18:1 (d7)/15:0)	6.19E+07	1%	23.01	0.04%

*N.D. = Not detectable.

Table 22: Metabolome standard (ESI+). Average and relative standard deviation in % (% RSD) of the peak areas (PA) and retention times (Rt) of compounds in the metabolome standard, analyzed three times (N=3) in positive ionization.

Compound	**Average PA (a.u.) N=3**	**% RSD PA (a.u.) N=3**	**Average Rt (min) N=3**	**% RSD Rt (min) N=3**
D3 acylcarnitine C2	4.37E+08	0.3%	3.34	0.1%
D3 acylcarnitine C12	8.44E+08	1.4%	12.78	0.1%
D3 acylcarnitine C16	2.98E+08	7.7%	13.79	0.0%
^{13}C creatine	1.50E+08	0.8%	2.39	0.1%
^{13}C2 guanidinoacetic acid	2.29E+08	0.1%	2.11	0.2%
D4 succinic acid	3.88E+06	0.8%	4.46	0.1%

Table 23: Metabolome standard (ESI-). Average and relative standard deviation in % (% RSD) of the peak areas (PA) and retention times (Rt) of compounds in the metabolome standard, analyzed three times (N=3) in negative ionization.

Compound	**Average PA (a.u.) N=3**	**% RSD PA (a.u.) N=3**	**Average Rt (min) N=3**	**% RSD Rt (min) N=3**
D3 acylcarnitine C2	1.56E+06	1%	3.34	0.3%
D3 acylcarnitine C12	2.48E+07	1%	12.79	0.0%
D3 acylcarnitine C16	8.93E+06	46%	13.80	0.1%
^{13}C creatine	N.D.*	N.D.*	N.D.*	N.D.*
^{13}C2 guanidinoacetic acid	N.D.*	N.D.*	N.D.*	N.D.*
D4 succinic acid	N.D.*	N.D.*	N.D.*	N.D.*

Table 24: Isotopically labeled lipidome standard analyzed after removal of the column (ESI-): Average and relative standard deviation in % (% RSD) of the peak area (PA) and retention time (Rt) of compounds in the isotopically labeled lipidome standard after removal of the column (N=1) in negative ionization.

Compound	PA (a.u.) N=1	Rt (min) N=1
PC (15:0/18:1 (d7))	9.81E+06	4.82
LPC (18:1 (d7))	1.85E+07	0.07
PE (15:0/18:1 (d7))	1.55E+07	4.83
LPE (18:1 (d7)))	2.91E+07	0.07
PG (15:0/18:1 (d7))	3.15E+07	5.02
PI (15:0/18:1 (d7))	2.74E+07	4.97
PS (15:0/18:1)	1.89E+07	5.02
TG (15:0/18:1 (d7)/15:0)	N.D.*	N.D.*
DG (15:0/18:1 (d7))	N.D.*	N.D.*
MG (18:1 (d7)/0:0/0:0)	6.37E+06	4.48
CE (18:1 (d7))	N.D.*	N.D.*
SM (d18:1/18:1 (d9))	1.12E+07	4.77
Cer (d18:1 (d7)/15:0)	4.21E+07	4.77

*N.D. = Not detectable.

Table 25: Isotopically labeled lipidome standard analyzed using the alternative mobile phase (ESI+): Average and relative standard deviation in % (% RSD) of the peak area (PA) and retention time (Rt) of the compounds in the isotopically labeled lipidome standard analyzed three times (N=3) with the alternative mobile phase, in positive ionization.

Compound	Average PA (a.u.) N=3	% RSD PA (a.u.) N=3	Average Rt (min) N=3	% RSD Rt (min) N=3
PC (15:0/18:1 (d7))	N.D.*	N.D.*	N.D.*	N.D.*
PC (0:0/18:1 (d7))	2.85E+07	1%	22.66	0.05%
PC (18:1 (d7)/0:0)	2.20E+08	1%	23.31	0.08%
PE (15:0/18:1 (d7))	N.D.*	N.D.*	N.D.*	N.D.*
PE (0:0/18:1 (d7))	2.45E+07	1%	21.81	0.02%
PE (18:1 (d7)/0:0)	1.53E+08	2%	22.48	0.02%
PG (15:0/18:1 (d7))	N.D.*	N.D.*	N.D.*	N.D.*
PI (15:0/18:1 (d7))	N.D.*	N.D.*	N.D.*	N.D.*
PS (15:0/18:1 (d7))	N.D.*	N.D.*	N.D.*	N.D.*
TG (15:0/18:1 (d7)/15:0)	N.D.*	N.D.*	N.D.*	N.D.*
DG (15:0/18:1 (d7))	N.D.*	N.D.*	N.D.*	N.D.*
MG (0:0/18:1 (d7)/0:0)	1.22E+07	2%	24.23	0.02%
MG (18:1 (d7)/0:0/0:0)	4.43E+07	3%	24.75	0.01%
CE (18:1 (d7))	N.D.*	N.D.*	N.D.*	N.D.*
SM (d18:1/18:1 (d9))	3.78E+07	1%	31.86	0.08%
Cer (d18:1 (d7)/15:0)	1.14E+08	2%	30.14	0.9%

*N.D. = Not detectable.

Table 26: Isotopically labeled lipidome standard analyzed using the alternative mobile phase (ESI-): Average and relative standard deviation in % (% RSD) of the peak area (PA) and retention time (Rt) of the compounds in the isotopically labeled lipidome standard analyzed three times (N=3) with the alternative mobile phase, in negative ionization.

Compound	Average PA (a.u.) N=3	% RSD PA (a.u.) N=3	Average Rt (min) N=3	% RSD Rt (min) N=3
PC (15:0/18:1 (d7))	N.D.*	N.D.*	N.D.*	N.D.*
PC (0:0/18:1 (d7))	N.D.*	N.D.*	N.D.*	N.D.*
PC (18:1 (d7)/0:0)	4.88E+06	9%	24.07	0.03%
PE (15:0/18:1 (d7))	3.07E+07	1%	31.21	0.04%
PE (0:0/18:1 (d7))	6.15E+06	2%	20.61	0.03%
PE (18:1 (d7)/0:0)	7.17E+07	0%	21.26	0%
PG (15:0/18:1 (d7))	3.26E+07	2%	28.59	0.06%
PS (15:0/18:1 (d7))	2.01E+07	3%	28.55	0.04%
PI (15:0/18:1 (d7))	2.23E+07	2%	28.24	0.03%
TG (15:0/18:1 (d7)/15:0)	N.D.*	N.D.*	N.D.*	N.D.*
DG (15:0/18:1 (d7))	N.D.*	N.D.*	N.D.*	N.D.*
MG (0:0/18:1 (d7)/0:0)	2.10E+06	8%	22.67	0.06%
MG (18:1 (d7)/0:0/0:0)	2.20E+07	5%	23.17	0.08%
CE (18:1 (d7))	N.D.*	N.D.*	N.D.*	N.D.*
SM (d18:1/18:1 (d9))	N.D.*	N.D.*	N.D.*	N.D.*
Cer (d18:1 (d7)/15:0)	5.46E+07	5%	28.91	0.04%

*N.D. = Not detectable.

Table 27: Extraction of the isotopically labeled lipidome and metabolome standards spotted to filter cards, using 0.1% FA. Average and relative standard deviation in % (% RSD) of the peak area (PA) and retention time (Rt) for the compounds in the isotopically labeled lipidome and metabolome standard analyzed five times (N=5), in positive ionization.

Water + 0.1% FA				
Compound	**Average PA (a.u.) N=5**	**% RSD PA (a.u.) N=5**	**Average Rt (min) N=5**	**% RSD Rt (min) N=5**
PC (15:0/18:1 (d7))	N.D.*	N.D.*	N.D.*	N.D.*
PC (0:0/18:1 (d7))	N.D.*	N.D.*	N.D.*	N.D.*
PC (18:1 (d7)/0:0)	N.D.*	N.D.*	N.D.*	N.D.*
PE (15:0/18:1 (d7))	N.D.*	N.D.*	N.D.*	N.D.*
PE (0:0/18:1 (d7))	N.D.*	N.D.*	N.D.*	N.D.*
PE (18:1 (d7)/0:0)	N.D.*	N.D.*	N.D.*	N.D.*
TG (15:0/18:1 (d7)/15:0)	N.D.*	N.D.*	N.D.*	N.D.*
DG (15:0/18:1 (d7))	N.D.*	N.D.*	N.D.*	N.D.*
MG (0:0/18:1 (d7)/0:0)	N.D.*	N.D.*	N.D.*	N.D.*
MG (18:1 (d7)/0:0/0:0)	N.D.*	N.D.*	N.D.*	N.D.*
CE (18:1 (d7))	N.D.*	N.D.*	N.D.*	N.D.*
SM (d18:1/18:1 (d9))	N.D.*	N.D.*	N.D.*	N.D.*
Cer (d18:1 (d7)/15:0)	N.D.*	N.D.*	N.D.*	N.D.*
D3 acylcarnitine C2	6.74E+06	5%	3.43	0.5%
D3 acylcarnitine C12	1.89E+07	16%	12.88	0.1%
D3 acylcarnitine C16	3.30E+05	59%	13.68	1.3%
^{13}C creatine	1.84E+06	2%	2.40	0.4%
^{13}C2 guanidinoacetic acid	2.54E+06	4%	2.11	0.0%

Table 28: Extraction of the isotopically labeled lipidome and metabolome standards spotted to filter cards, using 80% MeOH with 0.1% FA. Average and relative standard deviation in % (% RSD) of the peak area (PA) and retention time (Rt) for the compounds in the isotopically labeled lipidome and metabolome standard analyzed five times (N=5), in positive ionization.

80% MeOH + 0.1% FA				
Compound	**Average PA (a.u.) N=5**	**% RSD PA (a.u.) N=5**	**Average Rt (min) N=5**	**% RSD Rt (min) N=5**
PC (15:0/18:1 (d7))	N.D.*	N.D.*	N.D.*	N.D.*
PC (0:0/18:1 (d7))	N.D.*	N.D.*	N.D.*	N.D.*
PC (18:1 (d7)/0:0)	8.81E+05	14%	19.65	0.1%
PE (15:0/18:1 (d7))	4.68E+05	22%	24.70	0.1%
PE (0:0/18:1 (d7))	N.D.*	N.D.*	N.D.*	N.D.*
PE (18:1 (d7)/0:0)	9.47E+05	15%	17.54	0.1%
TG (15:0/18:1 (d7)/15:0)	5.44E+05**	-	30.14	-
DG (15:0/18:1 (d7))	1.89E+06	9%	26.18	0.1%
MG (0:0/18:1 (d7)/0:0)	N.D.*	N.D.*	N.D.*	N.D.*
MG (18:1 (d7)/0:0/0:0)	1.05E+06	7%	18.76	0.1%
CE (18:1 (d7))	N.D.*	N.D.*	N.D.*	N.D.*
SM (d18:1/18:1 (d9))	N.D.*	N.D.*	N.D.*	N.D.*
Cer (d18:1 (d7)/15:0)	1.47E+06	9%	22.96	0.1%
D3 acylcarnitine C2	3.01E+06	5%	3.32	0.7%
D3 acylcarnitine C12	7.31E+07	4%	12.87	0.1%
D3 acylcarnitine C16	4.59E+07	67%	13.91	0.3%
^{13}C creatine	2.58E+06	3%	2.39	0.2%
^{13}C2 guanidinoacetic acid	3.40E+06	1%	2.12	0.2%

*N.D. = Not detectable. **Only detected in one replicate

Table 29: Extraction of the isotopically labeled lipidome and metabolome standards spotted to filter cards, using 50% MeOH with 0.1% FA. Average and relative standard deviation in % (% RSD) of the peak area (PA) and retention time (Rt) for the compounds in the isotopically labeled lipidome and metabolome standard analyzed five times (N=5), in positive ionization.

50% MeOH + 0.1% FA				
Compound	**Average PA (a.u.) N=5**	**% RSD PA (a.u.) N=5**	**Average Rt (min) N=5**	**% RSD Rt (min) N=5**
PC (15:0/18:1 (d7))	N.D.*	N.D.*	N.D.*	N.D.*
PC (0:0/18:1 (d7))	N.D.*	N.D.*	N.D.*	N.D.*
PC (18:1 (d7)/0:0)	1.05E+06	18%	19.71	0.1%
PE (15:0/18:1 (d7))	N.D.*	N.D.*	N.D.*	N.D.*
PE (0:0/18:1 (d7))	N.D.*	N.D.*	N.D.*	N.D.*
PE (18:1 (d7)/0:0)	1.34E+06	25%	17.55	0.1%
TG (15:0/18:1 (d7)/15:0)	N.D.*	N.D.*	N.D.*	N.D.*
DG (15:0/18:1 (d7))	N.D.*	N.D.*	N.D.*	N.D.*
MG (0:0/18:1 (d7)/0:0)	N.D.*	N.D.*	N.D.*	N.D.*
MG (18:1 (d7)/0:0/0:0)	1.11E+06	30%	18.79	0.1%
CE (18:1 (d7))	N.D.*	N.D.*	N.D.*	N.D.*
SM (d18:1/18:1 (d9))	N.D.*	N.D.*	N.D.*	N.D.*
Cer (d18:1 (d7)/15:0)	N.D.*	N.D.*	N.D.*	N.D.*
D3 acylcarnitine C2	4.27E+06	2%	3.40	0.4%
D3 acylcarnitine C12	5.48E+07	7%	12.89	0.1%
D3 acylcarnitine C16	5.04E+07	14%	13.93	0.2%
^{13}C creatine	2.17E+06	3%	2.39	0.1%
^{13}C2 guanidinoacetic acid	3.11E+06	3%	2.12	0.1%

*N.D. = Not detectable.

Table 30: Extraction of the isotopically labeled lipidome and metabolome standards spotted to filter cards, using 20% MeOH with 0.1% FA. Average and relative standard deviation in % (% RSD) of the peak area (PA) and retention time (Rt) for the compounds in the isotopically labeled lipidome and metabolome standard analyzed five times (N=5), in positive ionization.

20% MeOH + 0.1% FA				
Compound	**Average PA (a.u.) N=5**	**% RSD PA (a.u.) N=5**	**Average Rt (min) N=5**	**% RSD Rt (min) N=5**
PC (15:0/18:1 (d7))	N.D.*	N.D.*	N.D.*	N.D.*
PC (0:0/18:1 (d7))	N.D.*	N.D.*	N.D.*	N.D.*
PC (18:1 (d7)/0:0)	N.D.*	N.D.*	N.D.*	N.D.*
PE (15:0/18:1 (d7))	N.D.*	N.D.*	N.D.*	N.D.*
PE (0:0/18:1 (d7))	N.D.*	N.D.*	N.D.*	N.D.*
PE (18:1 (d7)/0:0)	N.D.*	N.D.*	N.D.*	N.D.*
TG (15:0/18:1 (d7)/15:0)	N.D.*	N.D.*	N.D.*	N.D.*
DG (15:0/18:1 (d7))	N.D.*	N.D.*	N.D.*	N.D.*
MG (0:0/18:1 (d7)/0:0)	N.D.*	N.D.*	N.D.*	N.D.*
MG (18:1 (d7)/0:0/0:0)	N.D.*	N.D.*	N.D.*	N.D.*
CE (18:1 (d7))	N.D.*	N.D.*	N.D.*	N.D.*
SM (d18:1/18:1 (d9))	N.D.*	N.D.*	N.D.*	N.D.*
Cer (d18:1 (d7)/15:0)	N.D.*	N.D.*	N.D.*	N.D.*
D3 acylcarnitine C2	8.63E+06	1%	3.40	0.5%
D3 acylcarnitine C12	5.43E+07	2%	12.87	0.1%
D3 acylcarnitine C16	1.31E+07	27%	13.90	0.3%
^{13}C creatine	2.35E+06	3%	2.40	0.2%
^{13}C2 guanidinoacetic acid	3.42E+06	5%	2.11	0.2%

*N.D. = Not detectable.

Table 31: Extraction of the isotopically labeled lipidome and metabolome standards spotted to filter cards, using 80% ACN with 0.1% FA. Average and relative standard deviation in % (% RSD) of the peak area (PA) and retention time (Rt) for the compounds in the isotopically labeled lipidome and metabolome standard analyzed five times (N=5), in positive ionization.

80% ACN + 0.1% FA				
Compound	**Average PA (a.u.) N=5**	**% RSD PA (a.u.) N=5**	**Average Rt (min) N=5**	**% RSD Rt (min) N=5**
PC (15:0/18:1 (d7))	N.D.*	N.D.*	N.D.*	N.D.*
PC (0:0/18:1 (d7))	N.D.*	N.D.*	N.D.*	N.D.*
PC (18:1 (d7)/0:0)	1.34E+06	13%	19.68	0.1%
PE (15:0/18:1 (d7))	6.88E+05	9%	24.71	0.1%
PE (0:0/18:1 (d7))	N.D.*	N.D.*	N.D.*	N.D.*
PE (18:1 (d7)/0:0)	1.53E+06	13%	17.55	0.1%
TG (15:0/18:1 (d7)/15:0)	8.24E+05	17%	30.11	0.1%
DG (15:0/18:1 (d7))	2.64E+06	8%	26.17	0.1%
MG (0:0/18:1 (d7)/0:0)	N.D.*	N.D.*	N.D.*	N.D.*
MG (18:1 (d7)/0:0/0:0)	1.51E+06	1%	18.78	0.2%
CE (18:1 (d7))	N.D.*	N.D.*	N.D.*	N.D.*
SM (d18:1/18:1 (d9))	3.30E+05**	-	25.94	-
Cer (d18:1 (d7)/15:0)	2.30E+06	3%	22.96	0.1%
D3 acylcarnitine C2	2.11E+07	5%	3.38	0.1%
D3 acylcarnitine C12	1.39E+08	5%	12.87	0.2%
D3 acylcarnitine C16	1.75E+08	1%	13.90	0.3%
^{13}C creatine	5.60E+06	5%	2.40	0.2%
^{13}C2 guanidinoacetic acid	8.22E+06	6%	2.12	0.01%

*N.D. = Not detectable. **Only detected in one replicate

Table 32: Extraction of the isotopically labeled lipidome and metabolome standards spotted to filter cards, using 50% ACN with 0.1% FA. Average and relative standard deviation in % (% RSD) of the peak area (PA) and retention time (Rt) for the compounds in the isotopically labeled lipidome and metabolome standard analyzed five times (N=5), in positive ionization.

50% ACN + 0.1% FA				
Compound	**Average PA (a.u.) N=5**	**% RSD PA (a.u.) N=5**	**Average Rt (min) N=5**	**% RSD Rt (min) N=5**
PC (15:0/18:1 (d7))	N.D.*	N.D.*	N.D.*	N.D.*
PC (0:0/18:1 (d7))	N.D.*	N.D.*	N.D.*	N.D.*
PC (18:1 (d7)/0:0)	2.07E+06	42%	19.66	0.2%
PE (15:0/18:1 (d7))	N.D.*	N.D.*	N.D.*	N.D.*
PE (0:0/18:1 (d7))	N.D.*	N.D.*	N.D.*	N.D.*
PE (18:1 (d7)/0:0)	2.16E+06	39%	17.54	0.2%
TG (15:0/18:1 (d7)/15:0)	2.49E+05	45%	30.15	0.1%
DG (15:0/18:1 (d7))	3.09E+06	1%	17.51	0.1%
MG (0:0/18:1 (d7)/0:0)	N.D.*	N.D.*	N.D.*	N.D.*
MG (18:1 (d7)/0:0/0:0)	2.02E+06	36%	18.79	0.2%
CE (18:1 (d7))	N.D.*	N.D.*	N.D.*	N.D.*
SM (d18:1/18:1 (d9))	2.96E+05	1%	25.96	0.1%
Cer (d18:1 (d7)/15:0)	9.41E+05	76%	22.95	0.2%
D3 acylcarnitine C2	1.04E+07	41%	3.33	0.1%
D3 acylcarnitine C12	1.09E+08	9%	12.88	0.2%
D3 acylcarnitine C16	1.55E+08	5%	13.90	0.3%
^{13}C creatine	3.30E+06	7%	2.40	0.4%
^{13}C2 guanidinoacetic acid	4.97E+06	9%	2.12	0.2%

*N.D. = Not detectable.

Table 33: Extraction of the isotopically labeled lipidome and metabolome standards spotted to filter cards, using 20% ACN with 0.1% FA. Average and relative standard deviation in % (% RSD) of the peak area (PA) and retention time (Rt) for the compounds in the isotopically labeled lipidome and metabolome standard analyzed five times (N=5), in positive ionization.

20% ACN + 0.1% FA				
Compound	**Average PA (a.u.) N=5**	**% RSD PA (a.u.) N=5**	**Average Rt (min) N=5**	**% RSD Rt (min) N=5**
PC (15:0/18:1 (d7))	N.D.*	N.D.*	N.D.*	N.D.*
PC (0:0/18:1 (d7))	N.D.*	N.D.*	N.D.*	N.D.*
PC (18:1 (d7)/0:0)	N.D.*	N.D.*	N.D.*	N.D.*
PE (15:0/18:1 (d7))	N.D.*	N.D.*	N.D.*	N.D.*
PE (0:0/18:1 (d7))	N.D.*	N.D.*	N.D.*	N.D.*
PE (18:1 (d7)/0:0)	N.D.*	N.D.*	N.D.*	N.D.*
TG (15:0/18:1 (d7)/15:0)	N.D.*	N.D.*	N.D.*	N.D.*
DG (15:0/18:1 (d7))	N.D.*	N.D.*	N.D.*	N.D.*
MG (0:0/18:1 (d7)/0:0)	N.D.*	N.D.*	N.D.*	N.D.*
MG (18:1 (d7)/0:0/0:0)	N.D.*	N.D.*	N.D.*	N.D.*
CE (18:1 (d7))	N.D.*	N.D.*	N.D.*	N.D.*
SM (d18:1/18:1 (d9))	N.D.*	N.D.*	N.D.*	N.D.*
Cer (d18:1 (d7)/15:0)	N.D.*	N.D.*	N.D.*	N.D.*
D3 acylcarnitine C2	9.50E+06	2%	3.40	0.4%
D3 acylcarnitine C12	4.89E+07	1%	12.87	0.2%
D3 acylcarnitine C16	4.06E+07	10%	13.91	0.2%
^{13}C creatine	2.76E+06	2%	2.40	0.3%
^{13}C2 guanidinoacetic acid	3.64E+06	4%	2.12	0.1%

*N.D. = Not detectable.

Table 34: Extraction of the isotopically labeled lipidome and metabolome standards spotted to filter cards, using 80% iso-propanol with 0.1% FA. Average and relative standard deviation in % (% RSD) of the peak area (PA) and retention time (Rt) for the compounds in the isotopically labeled lipidome and metabolome standard analyzed five times (N=5), in positive ionization.

80% iso-propanol + 0.1% FA				
Compound	**Average PA (a.u.) N=5**	**% RSD PA (a.u.) N=5**	**Average Rt (min) N=5**	**% RSD Rt (min) N=5**
PC (15:0/18:1 (d7))	N.D.*	N.D.*	N.D.*	N.D.*
PC (0:0/18:1 (d7))	N.D.*	N.D.*	N.D.*	N.D.*
PC (18:1 (d7)/0:0)	9.77E+05	6%	19.68	0.1%
PE (15:0/18:1 (d7))	5.44E+05	16%	24.70	0.1%
PE (0:0/18:1 (d7))	N.D.*	N.D.*	N.D.*	N.D.*
PE (18:1 (d7)/0:0)	1.14E+06	10%	17.54	0.1%
TG (15:0/18:1 (d7)/15:0)	6.65E+05	15%	30.10	0.01%
DG (15:0/18:1 (d7))	2.08E+06	5%	26.18	0.01%
MG (0:0/18:1 (d7)/0:0)	N.D.*	N.D.*	N.D.*	N.D.*
MG (18:1 (d7)/0:0/0:0)	1.13E+06	14%	18.79	0.2%
CE (18:1 (d7))	N.D.*	N.D.*	N.D.*	N.D.*
SM (d18:1/18:1 (d9))	2.46E+05	24%	25.93	0.2%
Cer (d18:1 (d7)/15:0)	1.58E+06	9%	22.97	0.1%
D3 acylcarnitine C2	7.53E+06	3%	3.36	0.2%
D3 acylcarnitine C12	6.68E+07	10%	12.89	0.1%
D3 acylcarnitine C16	8.52E+07	76%	13.94	0.2%
^{13}C creatine	2.13E+06	4%	2.40	0.1%
^{13}C2 guanidinoacetic acid	3.07E+06	5%	2.12	0.4%

*N.D. = Not detectable.

Table 35: Extraction of the isotopically labeled lipidome and metabolome standards spotted to filter cards, using 50% iso-propanol with 0.1% FA. Average and relative standard deviation in % (% RSD) of the peak area (PA) and retention time (Rt) for the compounds in the isotopically labeled lipidome and metabolome standard analyzed five times (N=5), in positive ionization.

50% iso-propanol + 0.1% FA				
Compound	**Average PA (a.u.) N=5**	**% RSD PA (a.u.) N=5**	**Average Rt (min) N=5**	**% RSD Rt (min) N=5**
PC (15:0/18:1 (d7))	N.D.*	N.D.*	N.D.*	N.D.*
PC (0:0/18:1 (d7))	N.D.*	N.D.*	N.D.*	N.D.*
PC (18:1 (d7)/0:0)	7.82E+05	18%	19.66	0.1%
PE (15:0/18:1 (d7))	4.00E+05	32%	24.70	0.1%
PE (0:0/18:1 (d7))	N.D.*	N.D.*	N.D.*	N.D.*
PE (18:1 (d7)/0:0)	8.53E+05	19%	17.55	0.1%
TG (15:0/18:1 (d7)/15:0)	4.78E+05	26%	30.12	0.1%
DG (15:0/18:1 (d7))	1.73E+06	15%	26.18	0.1%
MG (0:0/18:1 (d7)/0:0)	N.D.*	N.D.*	N.D.*	N.D.*
MG (18:1 (d7)/0:0/0:0)	8.81E+05	22%	18.78	0.1%
CE (18:1 (d7))	N.D.*	N.D.*	N.D.*	N.D.*
SM (d18:1/18:1 (d9))	1.48E+05	52%	25.91	0.1%
Cer (d18:1 (d7)/15:0)	1.24E+06	18%	22.96	0.1%
D3 acylcarnitine C2	7,15E+06	2%	3.39	0.5%
D3 acylcarnitine C12	5,95E+07	3%	12.88	0.2%
D3 acylcarnitine C16	5,90E+07	5%	13.91	0.4%
^{13}C creatine	1,94E+06	2%	2.40	0.2%
^{13}C2 guanidinoacetic acid	2,92E+06	3%	2.12	0.01%

*N.D. = Not detectable.

Table 36: Extraction of the isotopically labeled lipidome and metabolome standards spotted to filter cards, using 20% iso-propanol with 0.1% FA. Average and relative standard deviation in % (% RSD) of the peak area (PA) and retention time (Rt) for the compounds in the isotopically labeled lipidome and metabolome standard analyzed five times (N=5), in positive ionization.

20% iso-Propanol + 0.1% FA				
Compound	**Average PA (a.u.) N=5**	**% RSD PA (a.u.) N=5**	**Average Rt (min) N=5**	**% RSD Rt (min) N=5**
PC (15:0/18:1 (d7))	N.D.*	N.D.*	N.D.*	N.D.*
PC (0:0/18:1 (d7))	N.D.*	N.D.*	N.D.*	N.D.*
PC (18:1 (d7)/0:0)	N.D.*	N.D.*	N.D.*	N.D.*
PE (15:0/18:1 (d7))	N.D.*	N.D.*	N.D.*	N.D.*
PE (0:0/18:1 (d7))	N.D.*	N.D.*	N.D.*	N.D.*
PE (18:1 (d7)/0:0)	N.D.*	N.D.*	N.D.*	N.D.*
TG (15:0/18:1 (d7)/15:0)	N.D.*	N.D.*	N.D.*	N.D.*
DG (15:0/18:1 (d7))	N.D.*	N.D.*	N.D.*	N.D.*
MG (0:0/18:1 (d7)/0:0)	N.D.*	N.D.*	N.D.*	N.D.*
MG (18:1 (d7)/0:0/0:0)	N.D.*	N.D.*	N.D.*	N.D.*
CE (18:1 (d7))	N.D.*	N.D.*	N.D.*	N.D.*
SM (d18:1/18:1 (d9))	N.D.*	N.D.*	N.D.*	N.D.*
Cer (d18:1 (d7)/15:0)	N.D.*	N.D.*	N.D.*	N.D.*
D3 acylcarnitine C2	7.70E+06	2%	3.41	0.1%
D3 acylcarnitine C12	7.31E+07	1%	12.88	0.2%
D3 acylcarnitine C16	2.27E+07	26%	13.90	0.3%
^{13}C creatine	2.14E+06	2%	2.41	0.2%
^{13}C2 guanidinoacetic acid	3.10E+06	3%	2.11	0.2%

Table 37: Extraction of the isotopically labeled lipidome and metabolome standards spotted to filter cards, using 80% 1-propanol with 0.1% FA. Average and relative standard deviation in % (% RSD) of the peak area (PA) and retention time (Rt) for the compounds in the isotopically labeled lipidome and metabolome standard analyzed five times (N=5), in positive ionization.

80% 1-propanol + 0.1% FA				
Compound	**Average PA (a.u.) N=5**	**% RSD PA (a.u.) N=5**	**Average Rt (min) N=5**	**% RSD Rt (min) N=5**
PC (15:0/18:1 (d7))	N.D.*	N.D.*	N.D.*	N.D.*
PC (0:0/18:1 (d7))	N.D.*	N.D.*	N.D.*	N.D.*
PC (18:1 (d7)/0:0)	8.77E+05	7%	19.67	0.2%
PE (15:0/18:1 (d7))	5.19E+05	10%	24.70	0.1%
PE (0:0/18:1 (d7))	N.D.*	N.D.*	N.D.*	N.D.*
PE (18:1 (d7)/0:0)	9.98E+05	8%	17.55	0.01%
TG (15:0/18:1 (d7)/15:0)	6.86E+05	15%	30.12	0.01%
DG (15:0/18:1 (d7))	2.10E+06	2%	26.17	0.01%
MG (0:0/18:1 (d7)/0:0)	N.D.*	N.D.*	N.D.*	N.D.*
MG (18:1 (d7)/0:0/0:0)	9.92E+05	23%	18.79	0.1%
CE (18:1 (d7))	N.D.*	N.D.*	N.D.*	N.D.*
SM (d18:1/18:1 (d9))	3.12E+05	12%	25.96	0.2%
Cer (d18:1 (d7)/15:0)	1.54E+06	10%	22.97	0.1%
D3 acylcarnitine C2	7.84E+06	1%	3.39	0%
D3 acylcarnitine C12	6.71E+07	3%	12.88	0.2%
D3 acylcarnitine C16	1.17E+08	3%	13.92	0.3%
^{13}C creatine	2.21E+06	1%	2.40	0.2%
^{13}C2 guanidinoacetic acid	3.12E+06	1%	2.12	0.2%

*N.D. = Not detectable.

Table 38: Extraction of the isotopically labeled lipidome and metabolome standards spotted to filter cards, using 50% 1-propanol with 0.1% FA. Average and relative standard deviation in % (% RSD) of the peak area (PA) and retention time (Rt) for the compounds in the isotopically labeled lipidome and metabolome standard analyzed five times (N=5), in positive ionization.

50% 1-propanol + 0.1% FA				
Compound	**Average PA (a.u.) N=5**	**% RSD PA (a.u.) N=5**	**Average Rt (min) N=5**	**% RSD Rt (min) N=5**
PC (15:0/18:1 (d7))	N.D.*	N.D.*	N.D.*	N.D.*
PC (0:0/18:1 (d7))	N.D.*	N.D.*	N.D.*	N.D.*
PC (18:1 (d7)/0:0)	8.70E+05	10%	19.66	0.1%
PE (15:0/18:1 (d7))	4.81E+05	18%	24.70	0.1%
PE (0:0/18:1 (d7))	N.D.*	N.D.*	N.D.*	N.D.*
PE (18:1 (d7)/0:0)	1.06E+06	10%	17.56	0.1%
TG (15:0/18:1 (d7)/15:0)	6.30E+05	20%	30.12	0.1%
DG (15:0/18:1 (d7))	2.03E+06	5%	26.18	0.01%
MG (0:0/18:1 (d7)/0:0)	N.D.*	N.D.*	N.D.*	N.D.*
MG (18:1 (d7)/0:0/0:0)	9.61E+05	34%	18.79	0.1%
CE (18:1 (d7))	N.D.*	N.D.*	N.D.*	N.D.*
SM (d18:1/18:1 (d9))	1.80E+05	25%	25.95	0.1%
Cer (d18:1 (d7)/15:0)	1.58E+06	12%	22.97	0.1%
D3 acylcarnitine C2	9.04E+06	1%	3.41	0.3%
D3 acylcarnitine C12	6.38E+07	2%	12.88	0.2%
D3 acylcarnitine C16	1.03E+08	1%	13.91	0.2%
^{13}C creatine	2.49E+06	3%	2.41	0.3%
^{13}C2 guanidinoacetic acid	3.71E+06	3%	2.12	0.01%

*N.D. = Not detectable.

Table 39: Extraction of the isotopically labeled lipidome and metabolome standards spotted to filter cards, using 20% 1-propanol with 0.1% FA. Average and relative standard deviation in % (% RSD) of the peak area (PA) and retention time (Rt) for the compounds in the isotopically labeled lipidome and metabolome standard analyzed five times (N=5), in positive ionization.

20% 1-Propanol + 0.1% FA				
Compound	**Average PA (a.u.) N=5**	**% RSD PA (a.u.) N=5**	**Average Rt (min) N=5**	**% RSD Rt (min) N=5**
PC (15:0/18:1 (d7))	N.D.*	N.D.*	N.D.*	N.D.*
PC (0:0/18:1 (d7))	N.D.*	N.D.*	N.D.*	N.D.*
PC (18:1 (d7)/0:0)	N.D.*	N.D.*	N.D.*	N.D.*
PE (15:0/18:1 (d7))	N.D.*	N.D.*	N.D.*	N.D.*
PE (0:0/18:1 (d7))	N.D.*	N.D.*	N.D.*	N.D.*
PE (18:1 (d7)/0:0)	N.D.*	N.D.*	N.D.*	N.D.*
TG (15:0/18:1 (d7)/15:0)	N.D.*	N.D.*	N.D.*	N.D.*
DG (15:0/18:1 (d7))	N.D.*	N.D.*	N.D.*	N.D.*
MG (0:0/18:1 (d7)/0:0)	N.D.*	N.D.*	N.D.*	N.D.*
MG (18:1 (d7)/0:0/0:0)	N.D.*	N.D.*	N.D.*	N.D.*
CE (18:1 (d7))	N.D.*	N.D.*	N.D.*	N.D.*
SM (d18:1/18:1 (d9))	N.D.*	N.D.*	N.D.*	N.D.*
Cer (d18:1 (d7)/15:0)	N.D.*	N.D.*	N.D.*	N.D.*
D3 acylcarnitine C2	7.42E+06	2%	3.42	0.4%
D3 acylcarnitine C12	5.08E+07	1%	12.88	0.1%
D3 acylcarnitine C16	2.68E+07	19%	13.90	0.3%
^{13}C creatine	2.08E+06	3%	2.40	0.2%
^{13}C2 guanidinoacetic acid	2.99E+06	4%	2.12	0.2%

*N.D. = Not detectable.

Table 40: Extraction of the isotopically labeled lipidome and metabolome standards spotted to filter cards, using 40% 1-butanol/ 40% MeOH with 0.1% FA. Average and relative standard deviation in % (% RSD) of the peak area (PA) and retention time (Rt) for the compounds in the isotopically labeled lipidome and metabolome standard analyzed five times (N=5), in positive ionization.

40% 1-butanol/40% MeOH + 0.1% FA				
Compound	**Average PA (a.u.) N=5**	**% RSD PA (a.u.) N=5**	**Average Rt (min) N=5**	**% RSD Rt (min) N=5**
PC (15:0/18:1 (d7))	N.D.*	N.D.*	N.D.*	N.D.*
PC (0:0/18:1 (d7))	N.D.*	N.D.*	N.D.*	N.D.*
PC (18:1 (d7)/0:0)	5.58E+05	14%	19.68	0.1%
PE (15:0/18:1 (d7))	5.68E+05	18%	24.71	0.1%
PE (0:0/18:1 (d7))	N.D.*	N.D.*	N.D.*	N.D.*
PE (18:1 (d7)/0:0)	1.17E+06	14%	17.53	0.1%
TG (15:0/18:1 (d7)/15:0)	7.88E+05	12%	30.11	0.01%
DG (15:0/18:1 (d7))	2.17E+06	10%	26.17	0.01%
MG (0:0/18:1 (d7)/0:0)	N.D.*	N.D.*	N.D.*	N.D.*
MG (18:1 (d7)/0:0/0:0)	1.07E+06	12%	18.79	0.1%
CE (18:1 (d7))	N.D.*	N.D.*	N.D.*	N.D.*
SM (d18:1/18:1 (d9))	2.98E+05	28%	25.94	0.1%
Cer (d18:1 (d7)/15:0)	1.52E+06	11%	22.97	0.1%
D3 acylcarnitine C2	5.95E+06	3%	3.36	0.1%
D3 acylcarnitine C12	7.45E+07	5%	12.88	0.2%
D3 acylcarnitine C16	1.32E+08	1%	13.92	0.2%
^{13}C creatine	2.32E+06	2%	2.40	0.4%
^{13}C2 guanidinoacetic acid	3.44E+06	2%	2.12	0.4%

*N.D. = Not detectable.

Table 41: Extraction of the isotopically labeled lipidome and metabolome standards spotted to filter cards, using 25% 1-butanol/ 25% MeOH with 0.1% FA. Average and relative standard deviation in % (% RSD) of the peak area (PA) and retention time (Rt) for the compounds in the isotopically labeled lipidome and metabolome standard analyzed five times (N=5), in positive ionization.

25% 1-butanol/25% MeOH + 0.1% FA				
Compound	**Average PA (a.u.) N=5**	**% RSD PA (a.u.) N=5**	**Average Rt (min) N=5**	**% RSD Rt (min) N=5**
PC (15:0/18:1 (d7))	N.D.*	N.D.*	N.D.*	N.D.*
PC (0:0/18:1 (d7))	N.D.*	N.D.*	N.D.*	N.D.*
PC (18:1 (d7)/0:0)	5.58E+05	14%	19.68	0.1%
PE (15:0/18:1 (d7))	3.68E+05	16%	24.71	0.1%
PE (0:0/18:1 (d7))	N.D.*	N.D.*	N.D.*	N.D.*
PE (18:1 (d7)/0:0)	7.63E+05	14%	17.57	0.2%
TG (15:0/18:1 (d7)/15:0)	5.20E+05	17%	30.11	0.1%
DG (15:0/18:1 (d7))	1.78E+06	10%	26.18	0.1%
MG (0:0/18:1 (d7)/0:0)	N.D.*	N.D.*	N.D.*	N.D.*
MG (18:1 (d7)/0:0/0:0)	7.16E+05	16%	18.79	0.1%
CE (18:1 (d7))	N.D.*	N.D.*	N.D.*	N.D.*
SM (d18:1/18:1 (d9))	N.D.*	N.D.*	N.D.*	N.D.*
Cer (d18:1 (d7)/15:0)	1.28E+06	8%	22.99	0.1%
D3 acylcarnitine C2	7.73E+06	3%	3.39	0.2%
D3 acylcarnitine C12	6.54E+07	2%	12.88	0.2%
D3 acylcarnitine C16	1.02E+08	1%	13.92	0.2%
^{13}C creatine	2.22E+06	2%	2.40	0.2%
^{13}C2 guanidinoacetic acid	3.24E+06	2%	2.12	0.2%

*N.D. = Not detectable.

Table 42: Extraction of the isotopically labeled lipidome and metabolome standards spotted to filter cards, using 40% MTBE/40% MeOH with 0.1% FA. Average and relative standard deviation in % (% RSD) of the peak area (PA) and retention time (Rt) for the compounds in the isotopically labeled lipidome and metabolome standard analyzed five times (N=5), in positive ionization.

40% MTBE+ 40% MeOH + 0.1% FA				
Compound	**Average PA (a.u.) N=5**	**% RSD PA (a.u.) N=5**	**Average Rt (min) N=5**	**% RSD Rt (min) N=5**
PC (15:0/18:1 (d7))	N.D.*	N.D.*	N.D.*	N.D.*
PC (0:0/18:1 (d7))	N.D.*	N.D.*	N.D.*	N.D.*
PC (18:1 (d7)/0:0)	1.02E+06	7%	19.69	0.1%
PE (15:0/18:1 (d7))	5.52E+05	19%	24.71	0.1%
PE (0:0/18:1 (d7))	N.D.*	N.D.*	N.D.*	N.D.*
PE (18:1 (d7)/0:0)	1.25E+06	14%	17.56	0.1%
TG (15:0/18:1 (d7)/15:0)	6.16E+05	38%	30.12	0.1%
DG (15:0/18:1 (d7))	2.31E+06	12%	26.18	0.1%
MG (0:0/18:1 (d7)/0:0)	N.D.*	N.D.*	N.D.*	N.D.*
MG (18:1 (d7)/0:0/0:0)	1.22E+06	5%	18.80	0.1%
CE (18:1 (d7))	N.D.*	N.D.*	N.D.*	N.D.*
SM (d18:1/18:1 (d9))	N.D.*	N.D.*	N.D.*	N.D.*
Cer (d18:1 (d7)/15:0)	1.67E+06	10%	22.98	0.1%
D3 acylcarnitine C2	4.25E+06	5%	3.35	1%
D3 acylcarnitine C12	8.20E+07	6%	12.88	0.1%
D3 acylcarnitine C16	1.03E+08	7%	13.91	0.2%
^{13}C creatine	2.90E+06	8%	2.40	0.2%
^{13}C2 guanidinoacetic acid	4.10E+06	9%	2.11	0.2%

*N.D. = Not detectable.

Table 43: Extraction of lipidome and metabolome standards from spiked dried blood spots, using 80% MeOH with 0.1% FA. Average and relative standard deviation in % (% RSD) of the peak area (PA) and retention time (Rt) for the compounds in the lipidome and metabolome standard analyzed three times (N=3), in positive ionization.

80% MeOH + 0.1% FA				
Compound	**Average PA (a.u.) N=3**	**% RSD PA (a.u.) N=3**	**Average Rt (min) N=3**	**% RSD Rt (min) N=3**
PC (15:0/18:1)	4.54E+06	4%	26.66	0.04%
PC (0:0/18:1)	2.40E+06	9%	18.82	0.1%
PC (18:1/0:0)	2.09E+07	2%	19.37	0.02%
PE (15:0/18:1)	N.D.*	N.D.*	N.D.*	N.D.*
PE (0:0/18:1)	3.37E+06	5%	17.74	0.06%
PE (18:1/0:0)	4.79E+06	5%	18.18	0.01%
TG (15:0/18:1/15:0)	9.62E+05	35%	31.11	0.04%
DG (15:0/18:1)	N.D.*	N.D.*	N.D.*	N.D.*
MG (0:0/18:1/0:0)	1.24E+06	8%	19.26	0.07%
MG (18:1/0:0/0:0)	2.08E+06	8%	19.63	0.06%
CE (18:1)	N.D.*	N.D.*	N.D.*	N.D.*
SM (d18:1/18:1)	9.13E+06	2%	25.78	0.1%
Cer (d18:1/15:0)	N.D.*	N.D.*	N.D.*	N.D.*
D3 acylcarnitine C2	3.61E+05	1%	2.76	0.2%
D3 acylcarnitine C12	9.81E+05	9%	13.04	0.04%
D3 acylcarnitine C16	3.85E+05	20%	14.20	0.1%
^{13}C creatine	9.00E+06	5%	2.44	0.1%
^{13}C2 guanidinoacetic acid	N.D.*	N.D.*	N.D.*	N.D.*

*N.D. = Not detectable.

Table 45: Extraction of lipidome and metabolome standards from spiked dried blood spots, using 50% MeOH with 0.1% FA. Average and relative standard deviation in % (% RSD) of the peak area (PA) and retention time (Rt) for the compounds in the lipidome and metabolome standard analyzed three times (N=3), in positive ionization.

50% MeOH + 0.1% FA				
Compound	**Average PA (a.u.) N=3**	**% RSD PA (a.u.) N=3**	**Average Rt (min) N=3**	**% RSD Rt (min) N=3**
PC (15:0/18:1)	N.D.*	N.D.*	N.D.*	N.D.*
PC (0:0/18:1)	1.22E+06**	33%	18.82	0.03%
PC (18:1/0:0)	1.20E+07	1%	19.35	0.04%
PE (15:0/18:1)	N.D.*	N.D.*	N.D.*	N.D.*
PE (0:0/18:1)	1.32E+06	7%	17.74	0.1%
PE (18:1/0:0)	2.15E+06	4%	18.17	0.01%
TG (15:0/18:1/15:0)	5.86E+05**	69%	31.13	0.06%
DG (15:0/18:1)	N.D.*	N.D.*	N.D.*	N.D.*
MG (0:0/18:1/0:0)	N.D.*	N.D.*	N.D.*	N.D.*
MG (18:1/0:0/0:0)	N.D.*	N.D.*	N.D.*	N.D.*
CE (18:1)	N.D.*	N.D.*	N.D.*	N.D.*
SM (d18:1/18:1)	2.11E+06	14%	25.06	0.08%
Cer (d18:1/15:0)	N.D.*	N.D.*	N.D.*	N.D.*
D3 acylcarnitine C2	N.D.*	N.D.*	N.D.*	N.D.*
D3 acylcarnitine C12	6.97E+05	9%	13.03	0.1%
D3 acylcarnitine C16	8.21E+04	0.1%	14.22	0.01%
^{13}C creatine	7.80E+06	8%	2.44	0.1%
^{13}C2 guanidinoacetic acid	N.D.*	N.D.*	N.D.*	N.D.*

*N.D. = Not detectable. **Only eight points across the chromatographic peak.

Table 46: Extraction of lipidome and metabolome standards from spiked dried blood spots, using 80% ACN with 0.1% FA. Average and relative standard deviation in % (% RSD) of the peak area (PA) and retention time (Rt) for the compounds in the lipidome and metabolome standard analyzed three times (N=3), in positive ionization.

80% ACN + 0.1% FA				
Compound	**Average PA (a.u.) N=3**	**% RSD PA (a.u.) N=3**	**Average Rt (min) N=3**	**% RSD Rt (min) N=3**
PC (15:0/18:1)	5.26E+06	6%	26.65	0.01%
PC (0:0/18:1)	2.09E+06	7%	18.84	0.07%
PC (18:1/0:0)	1.91E+07	4%	19.36	0.1%
PE (15:0/18:1)	N.D.*	N.D.*	N.D.*	N.D.*
PE (0:0/18:1)	2.83E+06	5%	17.73	0.01%
PE (18:1/0:0)	4.08E+06	3%	18.17	0.07%
TG (15:0/18:1/15:0)	8.58E+05**	73%	31.08	0.05%
DG (15:0/18:1)	N.D.*	N.D.*	N.D.*	N.D.*
MG (0:0/18:1/0:0)	1.46E+06	10%	19.25	0.07%
MG (18:1/0:0/0:0)	2.22E+06	7%	19.61	0.06%
CE (18:1)	1.45E+07	7%	32.45	0.05%
SM (d18:1/18:1)	7.14E+06	20%	25.77	0.09%
Cer (d18:1/15:0)	N.D.*	N.D.*	N.D.*	N.D.*
D3 acylcarnitine C2	2.93E+05	1%	3.43	0.3%
D3 acylcarnitine C12	1.01E+06	1%	13.01	0.01%
D3 acylcarnitine C16	3.61E+05	19%	14.20	0.02%
^{13}C creatine	7.93E+06	3%	2.45	0.1%
^{13}C2 guanidinoacetic acid	N.D.*	N.D.*	N.D.*	N.D.*

*N.D. = Not detectable. ** 6 points across the chromatographic peak.

Table 47: Extraction of lipidome and metabolome standards from spiked dried blood spots, using 50% ACN with 0.1% FA. Average and relative standard deviation in % (% RSD) of the peak area (PA) and retention time (Rt) for the compounds in the lipidome and metabolome standard analyzed three times (N=3), in positive ionization.

50% ACN + 0.1% FA				
Compound	**Average PA (a.u.) N=3**	**% RSD PA (a.u.) N=3**	**Average Rt (min) N=3**	**% RSD Rt (min) N=3**
PC (15:0/18:1)	N.D.*	N.D.*	N.D.*	N.D.*
PC (0:0/18:1)	1.36E+06	14%	18.82	0.07%
PC (18:1/0:0)	1.38E+07	3%	19.37	0.1%
PE (15:0/18:1)	N.D.*	N.D.*	N.D.*	N.D.*
PE (0:0/18:1)	1.49E+06	10%	17.74	0.03%
PE (18:1/0:0)	2.53E+06	4%	18.20	0.05%
TG (15:0/18:1/15:0)	N.D.*	N.D.*	N.D.*	N.D.*
DG (15:0/18:1)	N.D.*	N.D.*	N.D.*	N.D.*
MG (0:0/18:1/0:0)	7.06E+05	6%	19.26	0.1%
MG (18:1/0:0/0:0)	1.15E+06	13%	19.62	0.02%
CE (18:1)	N.D.*	N.D.*	N.D.*	N.D.*
SM (d18:1/18:1)	N.D.*	N.D.*	N.D.*	N.D.*
Cer (d18:1/15:0)	N.D.*	N.D.*	N.D.*	N.D.*
D3 acylcarnitine C2	2.78E+05	2%	3.46	0.3%
D3 acylcarnitine C12	5.47E+05	9%	13.01	0.04%
D3 acylcarnitine C16	N.D.*	N.D.*	N.D.*	N.D.*
^{13}C creatine	8.28E+06	1%	2.45	0.1%
^{13}C2 guanidinoacetic acid	N.D.*	N.D.*	N.D.*	N.D.*

*N.D. = Not detectable.

Table 48: Extraction of lipidome and metabolome standards from spiked dried blood spots, using 80% iso-propanol with 0.1% FA. Average and relative standard deviation in % (% RSD) of the peak area (PA) and retention time (Rt) for the compounds in the lipidome and metabolome standard analyzed three times (N=3), in positive ionization.

80% iso-propanol + 0.1% FA				
Compound	**Average PA (a.u.) N=3**	**% RSD PA (a.u.) N=3**	**Average Rt (min) N=3**	**% RSD Rt (min) N=3**
PC (15:0/18:1)	5.55E+06	8%	26.65	0.03%
PC (0:0/18:1)	1.83E+06	7%	18.83	0.04%
PC (18:1/0:0)	1.75E+07	4%	19.37	0.06%
PE (15:0/18:1)	N.D.*	N.D.*	N.D.*	N.D.*
PE (0:0/18:1)	2.02E+06	5%	17.73	0.09%
PE (18:1/0:0)	3.63E+06	6%	18.19	0.02%
TG (15:0/18:1/15:0)	2.96E+06	4%	31.05	0.09%
DG (15:0/18:1)	N.D.*	N.D.*	N.D.*	N.D.*
MG (0:0/18:1/0:0)	1.17E+06	3%	19.25	0.05%
MG (18:1/0:0/0:0)	1.77E+06	10%	19.64	0.03%
CE (18:1)	4.94E+07	5%	32.39	0.05%
SM (d18:1/18:1)	8.11E+06	5%	25.78	0.06%
Cer (d18:1/15:0)	N.D.*	N.D.*	N.D.*	N.D.*
D3 acylcarnitine C2	2.63E+05	9%	3.45	0.3%
D3 acylcarnitine C12	8.92E+05	2%	13.00	0.03%
D3 acylcarnitine C16	3.63E+05	7%	14.15	0.1%
^{13}C creatine	7.39E+06	4%	2.44	0.1%
^{13}C2 guanidinoacetic acid	N.D.*	N.D.*	N.D.*	N.D.*

*N.D. = Not detectable.

Table 49: Extraction of lipidome and metabolome standards from spiked dried blood spots, using 50% iso-propanol with 0.1% FA. Average and relative standard deviation in % (% RSD) of the peak area (PA) and retention time (Rt) for the compounds in the lipidome and metabolome standard analyzed three times (N=3), in positive ionization.

50% iso-propanol + 0.1% FA				
Compound	**Average PA (a.u.) N=3**	**% RSD PA (a.u.) N=3**	**Average Rt (min) N=3**	**% RSD Rt (min) N=3**
PC (15:0/18:1)	5.20E+06	2%	26.63	0.05%
PC (0:0/18:1)	1.54E+06	4%	18.81	0.06%
PC (18:1/0:0)	1.53E+07	2%	19.35	0.06%
PE (15:0/18:1)	N.D.*	N.D.*	N.D.*	N.D.*
PE (0:0/18:1)	1.45E+06	5%	17.74	0.06%
PE (18:1/0:0)	2.89E+06	7%	18.19	0.06%
TG (15:0/18:1/15:0)	1.06E+06	24%	31.11	0.04%
DG (15:0/18:1)	N.D.*	N.D.*	N.D.*	N.D.*
MG (0:0/18:1/0:0)	8.92E+05	3%	19.26	0.03%
MG (18:1/0:0/0:0)	1.36E+06	4%	19.63	0.01%
CE (18:1)	2.07E+06	6%	32.50	0.02%
SM (d18:1/18:1)	6.79E+06	15%	25.72	0.03%
Cer (d18:1/15:0)	N.D.*	N.D.*	N.D.*	N.D.*
D3 acylcarnitine C2	2.86E+05	11%	3.47	0.1%
D3 acylcarnitine C12	N.D.*	N.D.*	N.D.*	N.D.*
D3 acylcarnitine C16	N.D.*	N.D.*	N.D.*	N.D.*
^{13}C creatine	8.26E+06	3%	2.45	0.2%
^{13}C2 guanidinoacetic acid	N.D.*	N.D.*	N.D.*	N.D.*

*N.D. = Not detectable.

Table 50: Extraction of lipidome and metabolome standards from spiked dried blood spots, using 80% 1-propanol with 0.1% FA. Average and relative standard deviation in % (% RSD) of the peak area (PA) and retention time (Rt) for the compounds in the lipidome and metabolome standard analyzed three times (N=3), in positive ionization.

80% 1-propanol + 0.1% FA				
Compound	**Average PA (a.u.) N=3**	**% RSD PA (a.u.) N=3**	**Average Rt (min) N=3**	**% RSD Rt (min) N=3**
PC (15:0/18:1)	5.44E+06	3%	26.65	0.03%
PC (0:0/18:1)	1.76E+06	5%	18.84	0.1%
PC (18:1/0:0)	1.63E+07	1%	19.37	0.05%
PE (15:0/18:1)	N.D.*	N.D.*	N.D.*	N.D.*
PE (0:0/18:1)	1.94E+06	4%	17.74	0.01%
PE (18:1/0:0)	3.59E+06	1%	18.19	0.06%
TG (15:0/18:1/15:0)	3.05E+06	5%	31.07	0.03%
DG (15:0/18:1)	N.D.*	N.D.*	N.D.*	N.D.*
MG (0:0/18:1/0:0)	1.11E+06	5%	19.25	0.03%
MG (18:1/0:0/0:0)	1.82E+06	7%	19.62	0.04%
CE (18:1)	4.86E+07	2%	32.39	0.04%
SM (d18:1/18:1)	7.65E+06	2%	25.76	0.1%
Cer (d18:1/15:0)	N.D.*	N.D.*	N.D.*	N.D.*
D3 acylcarnitine C2	2.22E+05	10%	3.48	0.4%
D3 acylcarnitine C12	8.55E+05	6%	12.99	0.02%
D3 acylcarnitine C16	2.92E+05	44% **	14.13	0.1%
^{13}C creatine	7.37E+06	3%	2.45	0.1%
^{13}C2 guanidinoacetic acid	N.D.*	N.D.*	N.D.*	N.D.*

*N.D. = Not detectable. **6 points across chromatographic peak.

Table 51: Extraction of lipidome and metabolome standards from spiked dried blood spots, using 50% 1-propanol with 0.1% FA. Average and relative standard deviation in % (% RSD) of the peak area (PA) and retention time (Rt) for the compounds in the lipidome and metabolome standard analyzed three times (N=3), in positive ionization.

50% 1-propanol + 0.1% FA				
Compound	**Average PA (a.u.) N=3**	**% RSD PA (a.u.) N=3**	**Average Rt (min) N=3**	**% RSD Rt (min) N=3**
PC (15:0/18:1)	5.52E+06	7%	26.62	0.05%
PC (0:0/18:1)	1.12E+06	24%	18.84	0.01%
PC (18:1/0:0)	1.54E+07	1%	19.36	0.2%
PE (15:0/18:1)	N.D.*	N.D.*	N.D.*	N.D.*
PE (0:0/18:1)	1.59E+06	9%	17.74	0.03%
PE (18:1/0:0)	3.04E+06	6%	18.19	0.07%
TG (15:0/18:1/15:0)	1.72E+06	4%	31.07	0.1%
DG (15:0/18:1)	N.D.*	N.D.*	N.D.*	N.D.*
MG (0:0/18:1/0:0)	9.84E+05	6%	19.25	0.08%
MG (18:1/0:0/0:0)	1.62E+06	3%	19.63	0.05%
CE (18:1)	2.06E+07	8%	32.42	0.1%
SM (d18:1/18:1)	7.55E+06	19%	25.72	0.09%
Cer (d18:1/15:0)	N.D.*	N.D.*	N.D.*	N.D.*
D3 acylcarnitine C2	1.62E+05	69% **	3.47	0.7%
D3 acylcarnitine C12	N.D.*	N.D.*	N.D.*	N.D.*
D3 acylcarnitine C16	N.D.*	N.D.*	N.D.*	N.D.*
^{13}C creatine	8.52E+06	4%	2.45	0.2%
^{13}C2 guanidinoacetic acid	N.D.*	N.D.*	N.D.*	N.D.*

*N.D. = Not detectable. **6 points across chromatographic peak.

Table 52: Extraction of lipidome and metabolome standards from spiked dried blood spots, using 40% 1-butanol/40% MeOH with 0.1% FA. Average and relative standard deviation in % (% RSD) of the peak area (PA) and retention time (Rt) for the compounds in the lipidome and metabolome standard analyzed three times (N=3), in positive ionization.

40% 1-butanol /40% MeOH + 0.1% FA				
Compound	**Average PA (a.u.) N=3**	**% RSD PA (a.u.) N=3**	**Average Rt (min) N=3**	**% RSD Rt (min) N=3**
PC (15:0/18:1)	4.79E+06	12%	26.67	0.04%
PC (0:0/18:1)	1.74E+06	9%	18.85	0.2%
PC (18:1/0:0)	1.65E+07	6%	19.36	0.04%
PE (15:0/18:1)	N.D.*	N.D.*	N.D.*	N.D.*
PE (0:0/18:1)	2.00E+06	6%	17.75	0.1%
PE (18:1/0:0)	3.54E+06	9%	18.19	0.02%
TG (15:0/18:1/15:0)	2.69E+06	16%	31.10	0.07%
DG (15:0/18:1)	N.D.*	N.D.*	N.D.*	N.D.*
MG (0:0/18:1/0:0)	1.01E+06	8%	19.27	0.07%
MG (18:1/0:0/0:0)	1.45E+06	3%	19.63	0.08%
CE (18:1)	4.04E+07	9%	32.42	0.04%
SM (d18:1/18:1)	7.54E+06	6%	25.78	0.04%
Cer (d18:1/15:0)	N.D.*	N.D.*	N.D.*	N.D.*
D3 acylcarnitine C2	N.D.*	N.D.*	N.D.*	N.D.*
D3 acylcarnitine C12	8.25E+05	7%	12.98	0.03%
D3 acylcarnitine C16	3.42E+05	25%	14.13	0.1%
^{13}C creatine	7.65E+06	2%	2.44	0.2%
^{13}C2 guanidinoacetic acid	N.D.*	N.D.*	N.D.*	N.D.*

*N.D. = Not detectable.

Table 53: Extraction of lipidome and metabolome standards from spiked dried blood spots, using 25% 1-butanol/25% MeOH with 0.1% FA. Average and relative standard deviation in % (% RSD) of the peak area (PA) and retention time (Rt) for the compounds in the lipidome and metabolome standard analyzed three times (N=3), in positive ionization.

25% 1-butanol /25% MeOH + 0.1% FA				
Compound	**Average PA (a.u.) N=3**	**% RSD PA (a.u.) N=3**	**Average Rt (min) N=3**	**% RSD Rt (min) N=3**
PC (15:0/18:1)	4.65E+06	15%	26.64	0.02%
PC (0:0/18:1)	1.11E+06	8%	18.84	0.01%
PC (18:1/0:0)	1.33E+07	5%	19.36	0.04%
PE (15:0/18:1)	N.D.*	N.D.*	N.D.*	N.D.*
PE (0:0/18:1)	1.49E+06	11%	17.73	0.06
PE (18:1/0:0)	2.59E+06	4%	18.20	0.05
TG (15:0/18:1/15:0)	1.45E+06	1%	31.10	0.01%
DG (15:0/18:1)	N.D.*	N.D.*	N.D.*	N.D.*
MG (0:0/18:1/0:0)	9.17E+05	9%	19.25	0.06%
MG (18:1/0:0/0:0)	1.65E+06	8%	19.64	0.08%
CE (18:1)	5.05E+06**	47%	32.46	0.07%
SM (d18:1/18:1)	7.30E+06	10%	25.76	0.03%
Cer (d18:1/15:0)	N.D.*	N.D.*	N.D.*	N.D.*
D3 acylcarnitine C2	N.D.*	N.D.*	N.D.*	N.D.*
D3 acylcarnitine C12	N.D.*	N.D.*	N.D.*	N.D.*
D3 acylcarnitine C16	N.D.*	N.D.*	N.D.*	N.D.*
^{13}C creatine	7.57E+06	7%	2.44	0.1%
^{13}C2 guanidinoacetic acid	N.D.*	N.D.*	N.D.*	N.D.*

*N.D. = Not detectable. ** 7 points across the chromatographic peak.

Table 54: Extraction of lipidome and metabolome standards from spiked dried blood spots, using 40% MTBE/40% MeOH with 0.1% FA. Average and relative standard deviation in % (% RSD) of the peak area (PA) and retention time (Rt) for the compounds in the lipidome and metabolome standard analyzed three times (N=3), in positive ionization.

40% MTBE/40% MeOH + 0.1% FA				
Compound	**Average PA (a.u.) N=3**	**% RSD PA (a.u.) N=3**	**Average Rt (min) N=3**	**% RSD Rt (min) N=3**
PC (15:0/18:1)	N.D.*	N.D.*	N.D.*	N.D.*
PC (0:0/18:1)	1.67E+06	2%	18.83	0.09%
PC (18:1/0:0)	1.52E+07	2%	19.37	0.06%
PE (15:0/18:1)	N.D.*	N.D.*	N.D.*	N.D.*
PE (0:0/18:1)	2.04E+06	6%	17.75	0.01%
PE (18:1/0:0)	3.24E+06	1%	18.18	0.03%
TG (15:0/18:1/15:0)	7.37E+05	12%	31.13	0.01%
DG (15:0/18:1)	N.D.*	N.D.*	N.D.*	N.D.*
MG (0:0/18:1/0:0)	7.52E+05	17%	19.25	0.04%
MG (18:1/0:0/0:0)	1.37E+06	5%	19.63	0.05%
CE (18:1)	N.D.*	N.D.*	N.D.*	N.D.*
SM (d18:1/18:1)	N.D.*	N.D.*	N.D.*	N.D.*
Cer (d18:1/15:0)	N.D.*	N.D.*	N.D.*	N.D.*
D3 acylcarnitine C2	N.D.*	N.D.*	N.D.*	N.D.*
D3 acylcarnitine C12	8.43E+05	4%	12.97	0.1%
D3 acylcarnitine C16	2.38E+05	0.1%	14.11	0.01%
^{13}C creatine	7.66E+06	3%	2.44	0.2%
^{13}C2 guanidinoacetic acid	N.D.*	N.D.*	N.D.*	N.D.*

*N.D. = Not detectable.

Table 55: Adenosine 5'-monophosphate and guanosine 5'-monophosphate standards (ESI-). Average and relative standard deviation in % (% RSD) of the peak area (PA) and retention time (Rt) of adenosine 5'-monophosphate and guanosine 5'-monophosphate, analyzed three times (N=3) using the original method in negative ionization.

Compound	Average PA (a.u.) N=3	% RSD PA (a.u.) N=3	Average Rt (min) N=3	% RSD Rt (min) N=3
Adenosine 5'-monophosphate	7.98E+08	1%	3.34	0.1%
Guanosine 5'-monophosphate	7.58E+08	0.4%	4.02	0.2%

Table 56: Adenosine 5'-monophosphate and guanosine 5'-monophosphate standards spiked to a pooled quality control (PQC). Average and relative standard deviation in % (% RSD) of the peak area (PA) and retention time (Rt) of adenosine 5'-monophosphate and guanosine 5'-monophosphate in the spiked PQC, analyzed three times (N=3) using the original method in negative ionization.

Compound	Average PA (a.u.) N=3	% RSD PA (a.u.) N=3	Average Rt (min) N=3	% RSD Rt (min) N=3
Adenosine 5'-monophosphate	9.70E+08	0.4%	3.33	0.2%
Guanosine 5'-monophosphate	8.48E+08	1%	4.01	0.3%

Table 57: Peak area (PA) and retention time (Rt) of alanine, uracil, tryptophan, LPC (0:0/16:0), LPC (16:0/0:0), and acylcarnitine C16 in the diluted pooled quality controls (ESI+). Diluted pooled quality controls were analyzed in positive ionization (N=1).

Alanine		
PQC dilution	**PA (a.u.) N=1**	**Rt (min). N=1**
1	3.94E+07	2.14
0.8	3.59E+07	2.14
0.6	2.70E+07	2.15
0.4	1.95E+07	2.14
0.2	1.02E+07	2.14

Uracil		
PQC dilution	**PA (a.u.) N=1**	**Rt (min). N=1**
1	6.64E+05	2.35
0.8	5.30E+05	2.36
0.6	3.87E+05	2.36
0.4	2.69E+05	2.36
0.2	1.41E+05	2.36

Tryptophan		
PQC dilution	**PA (a.u.) N=1**	**Rt (min). N=1**
1	4.31E+07	11.32
0.8	3.78E+07	11.33
0.6	2.84E+07	11.31
0.4	1.93E+07	11.31
0.2	9.67E+06	11.32

Acylcarnitine C16		
PQC dilution	**PA (a.u.) N=1**	**Rt (min). N=1**
1	5.65E+06	14.09
0.8	4.89E+06	14.10
0.6	3.58E+06	14.11
0.4	2.33E+06	14.09
0.2	1.09E+06	14.10

Table 57 continues on the next page.

PC (0:0/16:0)		
PQC dilution	**PA (a.u.) N=1**	**Rt (min). N=1**
1	6.32E+06	17.92
0.8	5.33E+06	17.93
0.6	3.65E+06	17.93
0.4	2.52E+06	17.92
0.2	1.16E+06	17.94

PC (16:0/0:0)		
PQC dilution	**PA (a.u.) N=1**	**Rt (min). N=1**
1	5.42E+07	18.42
0.8	4.62E+07	18.40
0.6	3.31E+07	18.43
0.4	2.28E+07	18.40
0.2	1.13E+07	18.41

Table 58: Peak area (PA) of metabolites and temperature of the capillary in the heated electrospray ion source (HESI). Peak area of alanine, tryptophan, LPC (16:0), acylcarnitine C16, and uracil in the different injections of the pooled quality control (PQC), as the instrument failed to control the temperature of the ion source capillary, in positive ionization, (N=1).

Injection number	Capillary temperature (°C) N=1	Alanine PA (a.u.) N=1	Tryptophan PA (a.u.) N=1	LPC (16:0) PA (a.u.) N=1	Acylcarnitine C16 PA (a.u.) N=1	Uracil PA (a.u.) N=1
1	249.9	8.11E+07	8.56E+07	9.72E+07	7.27E+06	9.02E+05
2	250.1	8.11E+07	8.65E+07	9.32E+07	7.16E+06	1.07E+06
3	250.1	8.60E+07	8.66E+07	9.05E+07	6.87E+06	1.10E+06
4	250.0	8.21E+07	8.09E+07	8.17E+07	6.46E+06	9.52E+05
5	250.1	8.41E+07	7.91E+07	7.95E+07	6.41E+06	1.12E+06
6	60.0	3.26E+07	2.57E+07	3.01E+07	2.14E+06	2.82E+05
7	58.5	3.16E+07	2.54E+07	2.83E+07	2.09E+06	2.67E+05
8	59.8	3.01E+07	2.48E+07	2.70E+07	1.92E+06	2.61E+05
9	59.1	2.98E+07	2.36E+07	2.57E+07	1.91E+06	2.48E+05
10	59.3	2.98E+07	2.47E+07	2.65E+07	1.92E+06	2.33E+05
11	59.8	3.04E+07	2.42E+07	2.70E+07	1.96E+06	2.46E+05
12	60.4	3.04E+07	2.52E+07	2.60E+07	1.97E+06	2.61E+05
13	59.3	3.06E+07	2.51E+07	2.57E+07	1.88E+06	2.49E+05
14	59.6	3.07E+07	2.59E+07	2.57E+07	1.94E+06	2.66E+05
15	59.8	3.30E+07	2.65E+07	2.46E+07	1.89E+06	2.79E+05

6.3 Lipid coverage

6.3.1 Retention times of the spotted lipidome and metabolome standards were consistent

The retention time of the compounds in the isotopically labeled lipidome and metabolome standard were stable even as they were solved in the different extraction solutions. **Figure 44** shows the average retention time for the extracted compounds in the lipidome and metabolome standards, when extracted using the high and medium organic solvent extraction solutions. The values are shown in **Appendix**, Section 6.2 **Table 27-42**.

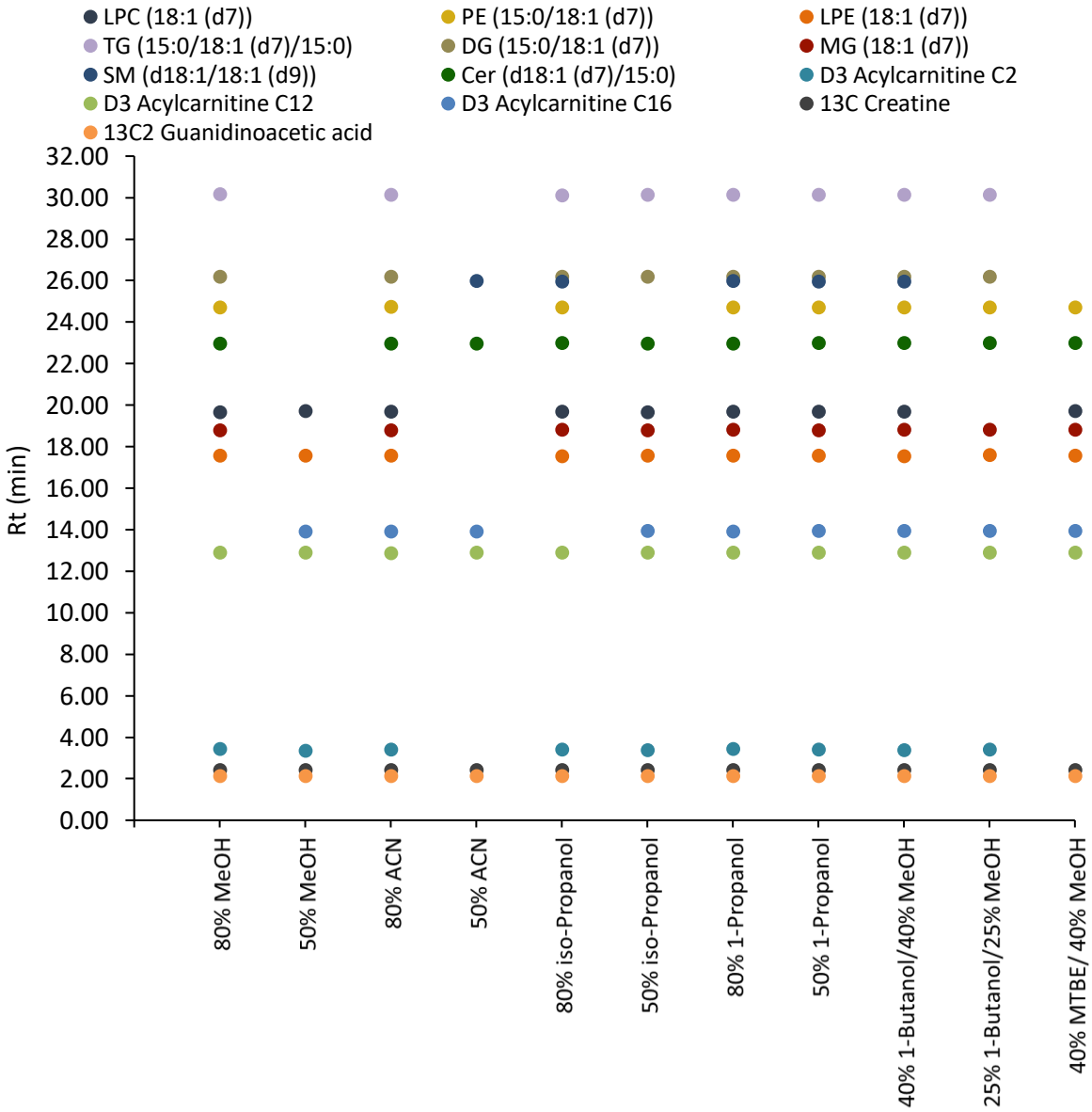

Figure 44: Average retention time (Rt) for all the detected compounds in the isotopically labeled lipidome and metabolome standard, extracted using the different extraction solutions. The relative standard deviation of the retention time was lower than 0.5% for all the compounds in the isotopically labeled lipidome and metabolome standard, despite changing sample solvent.

The figure shows that retention times stayed constant throughout data acquisition even as the sample solvent was altered. The relative standard deviation of the retention time of each of the compounds was lower than 0.5% for all detected compounds in both the isotopically labeled lipidome and metabolome standard for analysis of the different extracts.

Note that only the retention time of the highest chromatographic peak of MG (18:1 (d7)), LPC (18:1 (d7)) and LPE (18:1 (d7)) is shown. This shows that retention was not affected by solving the standards in different extraction solutions.

6.3.2 Retention times of lipidome and metabolome standards in spiked dried blood spots were consistent

The retention time of the detected compounds in the lipidome and metabolome standards, extracted using the different extraction solutions was also found to be stable, as illustrated in **Figure 45**. The values are shown in **Appendix**, Section 6.2 **Table 43-54**.

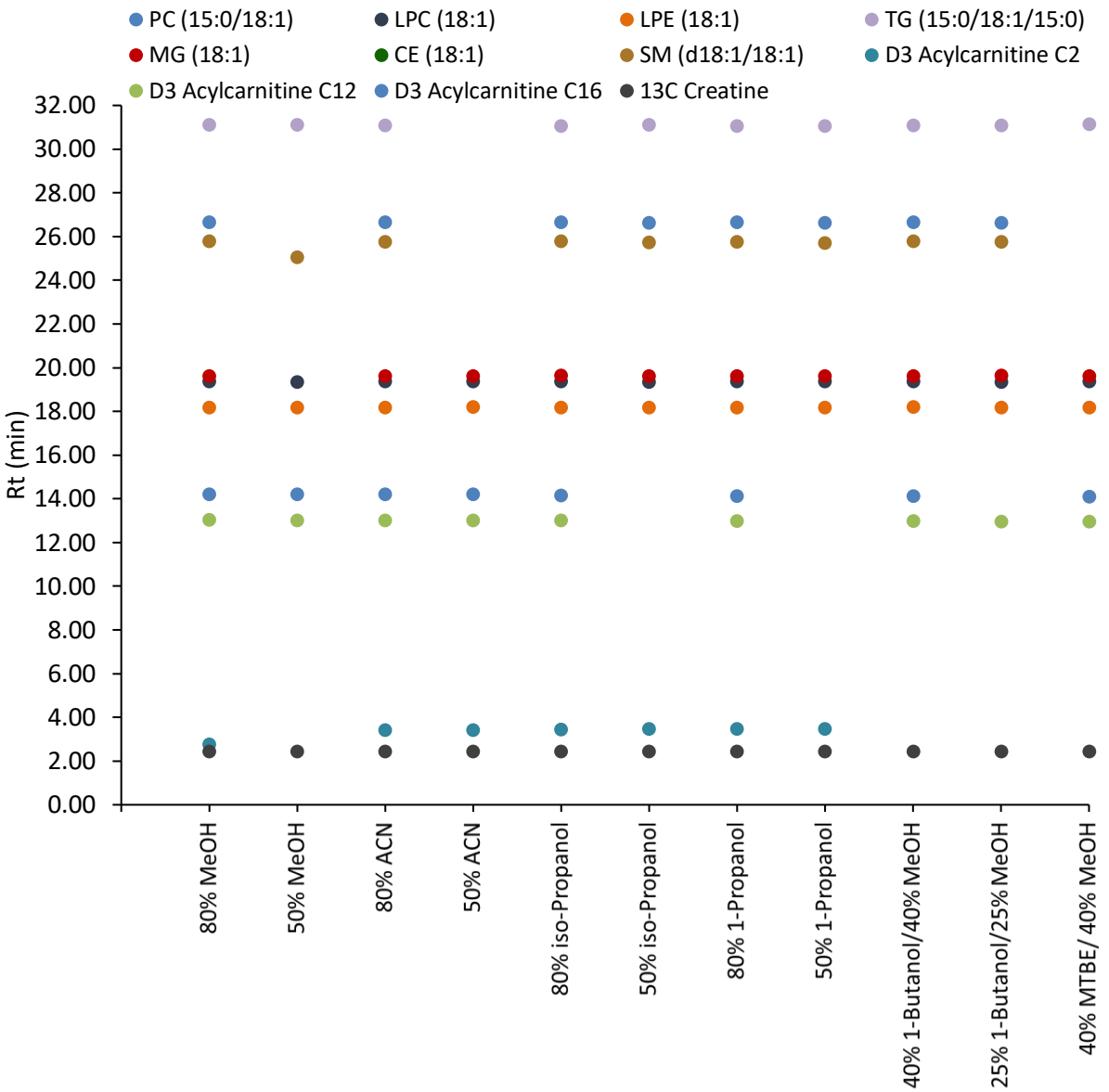

Figure 45: Average retention time of compounds in the lipidome and metabolome standard, extracted using the different extraction solutions. All compounds, except D3 acylcarnitine C2 and SM (d18:1/18.1), had an overall stable retention time with %RSD lower than 0.3%.

The % RSD of the retention times of the metabolome standard was lower than 0.3% for all compounds except for D3 acylcarnitine C2 which had a %RSD of 7%. The retention time %RSD for the lipidome compound was lower than 0.1% for all lipids, except SM (d18:1/18:1) were it was 0.9%.

Conclusion: The retention time of the compounds was not affected by being solved in different extraction solutions.

6.3.3 Number of molecular features in dried blood spot metabolome using different extraction solutions for positive and negative ionization

The number of molecular features detected when extracting the dried blood spot metabolome of one healthy volunteer, using the high and medium organic solvent extraction solutions is shown in **Table 59**.

Table 59: Average and relative standard deviation in % (% RSD) of the number of detected molecular features in the dried blood spot metabolome extracted using the high and medium organic solvent extraction solutions, for positive ionization and negative ionization.

80% MeOH	**Average number of features, N=3**	**%RSD for the number of features, N=3**
Positive ionization	1272	1%
Negative ionization	259	6%
50% MeOH	**Average number of features, N=3**	**%RSD for the number of features, N=3**
Positive ionization	1222	2%
Negative ionization	190	3%
80% ACN	**Average number of features, N=3**	**%RSD for the number of features, N=3**
Positive ionization	1296	1%
Negative ionization	193	2%
50% ACN	**Average number of features, N=3**	**%RSD for the number of features, N=3**
Positive ionization	1323	2%
Negative ionization	180	1%
80% iso-propanol	**Average number of features, N=3**	**%RSD for the number of features, N=3**
Positive ionization	1199	1%
Negative ionization	166	1%

Table 57 continues on the next page.

50% iso-propanol	**Average number of features, N=3**	**%RSD for the number of features, N=3**
Positive ionization	1342	1%
Negative ionization	179	1%
80% 1-propanol	**Average number of features, N=3**	**%RSD for the number of features, N=3**
Positive ionization	1210	1%
Negative ionization	163	2%
50% 1-propanol	**Average number of features, N=3**	**%RSD for the number of features, N=3**
Positive ionization	1411	1%
Negative ionization	171	1%
40% 1-butanol/40% MeOH	**Average number of features, N=3**	**%RSD for the number of features, N=3**
Positive ionization	1369	1%
Negative ionization	168	3%
25% 1-butanol/25% MeOH	**Average number of features, N=3**	**%RSD for the number of features, N=3**
Positive ionization	1300	1%
Negative ionization	161	1%
50% MTBE/40% MeOH	**Average number of features, N=3**	**%RSD for the number of features, N=3**
Positive ionization	1158	1%
Negative ionization	159	1%

6.4 The Exercise Metabolome Project

6.4.1 Regional Committee for Medical and Health Research Ethics informed consent form

An application to the Regional Committee for Medical and Health Research Ethics was applied for investigation of the normal metabolome. The informed consent form given to the participants is described below.

Forespørsel om å avgi biologisk materiale til

KARTLEGGING AV NORMALMETABOLOMET

Bakgrunn og hensikt

Formålet med biobanken er å undersøke sammensetningen av stoffene som kan påvises i kroppsvæsker i en normalbefolkning. Metabolismen er summen av alle kjemiske reaksjoner i kroppen og innebærer nedbrytning og oppbygging av ulike stoffer som inngår i prosessene som skjer i kroppen. Stoffene som deltar i metabolismen kalles metabolitter, og sammensetningen av metabolitter utgjør det som kalles metabolomet. Metabolismen er et dynamisk system, det vil si det er i endring hele tiden, og påvirkes av en rekke naturlige biologiske faktorer slik som alder, kjønn, tid på døgnet, og ytre påvirkninger slik som matinntak/faste, fysisk aktivitet, sykdom, inntak av legemidler m.m.
For å kunne skille variasjoner i metabolomet som skyldes normale prosesser fra avvik som skyldes sykdom er det nødvendig å undersøke metabolomet fra et stort antall friske personer under ulike betingelser (f.eks. tid på døgnet, fødeinntak, fysisk aktivitet).
Forskningsansvarlig er Oslo Universitetssykehus, Avdeling for medisinsk biokjemi ved avdelingsleder. Prosjektleder er Katja B. Prestø Elgstøen ved samme avdeling.
Det biologiske materialet blir oppbevart på ubestemt tid og skal brukes i fremtidig forskning til ulike studier av normalmetabolomet.

Hvilket biologisk materiale skal innsamles?
Vi undersøker i hovedsak blod og/eller urin. I sjeldne tilfeller kan det være aktuelt med hår, spytt, tårevæske, svette eller vev fra deg. Det vil bli et stikk (blodprøve fra armen og/eller stikk i fingeren) i forbindelse med blodprøvetaking. Dersom du gir fibroblaster (hudprøve), vil du få lokalbedøvelse før vi tar en knappenålshode stor prøve fra huden din. Dersom du gir vev, vil dette være i forbindelse med en annen operasjon og du vil ikke oppleve ekstra ubehag pga dette.

Bredt samtykke
Prøvene som du avgir lagres i den generelle forskningsbiobanken 2018/787 «Kartlegging av normalmetabolomet». Når du avgir biologisk materiale til denne forskningsbiobanken gir du også et bredt samtykke til at materiale og relevante helseopplysninger kan brukes til fremtidig forskning som har til hensikt å kartlegge normalmetabolomet, og som normalkontroll i studie av ulike sykdommer.

Innsamling og bruk av helseopplysninger
Biobanken vil inneholde noen opplysninger om deg. Disse er kun tilgjengelige gjennom en koblingsnøkkel som skal beskytte din identitet, men samtidig gjøre det mulig å knytte opplysningene om deg til ditt materiale gjennom en kodeliste dersom det skulle være nødvendig. Oslo Universitetssykehus er ansvarlig for at koblingsnøkkel oppbevares og forvaltes forsvarlig. Materiale og opplysningene om deg lagres permanent og vil analyseres i forbindelse med spesifiserte forskningsprosjekter. Det kan også være ønskelig å registrere annen relevant informasjon enn bare alder og kjønn (kosthold, medisinbruk, kjent sykdom eller liknende). Du står i så fall helt fritt til å oppgi dette.
Det kan være aktuelt å gjøre relevante undersøkelser på gennivå for å bidra til forståelsen av variasjoner i metabolomet.

Genetiske undersøkelser
Det kan være aktuelt å gjøre genetiske analyser på det materialet som er samlet inn for å se på sammenhengen mellom metabolomet og underliggende gener og genvarianter (sekvensering av enkeltgen, grupper av gener eller hele genomet). Genomsekvensen til hvert enkelt menneske er så unik at ingen prøver som inneholder DNA i teorien kan være anonyme. I praksis blir imidlertid alle prøver avidentifiserte og ingen (verken forskere eller personer som deltar i biobanken) informeres om resultater og funn hos enkeltpersoner.

Godkjenning av fremtidige forskningsprosjekter
Alle fremtidige forskningsprosjekter som benytter materialet fra deg skal forhåndsgodkjennes av en regional komité for medisinsk og helsefaglig forskningsetikk, men du vil kun unntaksvis bli spurt på nytt om slik bruk. Det vil derfor kun unntaksvis kunne være behov for å spørre deg på ny om slik bruk av prøvematerialet.

Informasjon om fremtidige prosjekter
Informasjon om forskningsbiobanken 2018/787 kartlegging av normalmetabolomet finnes på Biobankportalen til Oslo Universitetssykehus: https://oslo-universitetssykehus.no/forskningsbiobanker-ved-oslo-universitetssykehus
På denne nettsiden er det lenke videre til forskningsprosjektets nettside hvor informasjon om pågående og framtidige prosjekter er beskrevet.

Utlevering av prøvemateriale
Det kan være aktuelt å sende prøver ut av landet (innad i EU og til USA, data som overføres til USA behandles i henhold til EUs Personverndirektiv), som et ledd i internasjonalt samarbeid. Materialet vil i så fall kun utleveres uten navn, fødselsnummer eller andre personidentifiserbare opplysninger.

Det er frivillig å delta

Å avgi biologisk materiale til Kartlegging av normalmetabolomet er frivillig og krever samtykke. Informasjonen som registreres om deg skal kun brukes slik som beskrevet i hensikten med studien.
Dersom du ønsker å avgi biologisk materiale og godkjenner at prøvene dine lagres for eventuell bruk i fremtidige forskningsprosjekter, undertegner du samtykkeerklæringen på siste side. Der vil det bli spurt spesifikt om a) oppbevaring av din prøve i biobanken til fremtidige studier av normalmetabolomet, b) bruk av prøvene som normalkontroll i andre forskningsprosjekter, og c) om det kan utføres relevante analyser på gennivå knyttet til kartlegging av normalmetabolomet.

Mulighet for å trekke sitt samtykke, innsynsrett, endring og sletting av opplysninger
Du kan til enhver tid få innsyn i hvilket materiale som er lagret fra deg. Du kan når som helst kreve at materialet blir destruert, uten at du må oppgi noen grunn. Destruksjon av materialet vil imidlertid ikke innebære sletting av utledete opplysninger som allerede har inngått i sammenstilling eller analyser.

Kontakt
Biobanken er lokalisert ved Avdeling for medisinsk biokjemi, Rikshospitalet, Oslo Universitetssykehus. Katja B Prestø Elgstøen (kelgstoe@ous-hf.no, tlf. 23073079) er ansvarshavende for biobanken. Dette er en prospektiv biobank, og prøvene vil bli lagret til de eventuelt ønskes fjernet av deg.

OPPLYSNINGER OM DEG

Kode for avidentifisering:_____
Alder:
Kjønn:

Andre opplysninger (frivillig å oppgi):
Faste medisiner:

Andre medisiner tatt siste døgn:

Eventuelle sykdommer:

Kosttilskudd:

Eventuelt spesielt kosthold (f.eks. vegetarianer, laktoseintolerant):

Har du spist i dag? I så fall: hvor lenge er det siden, og hva spiste du?

Røyker eller snuser du?

Annen relevant informasjon:

Samtykke til lagring av biologisk materiale

a) Jeg avgir bredt samtykke til at mitt biologiske materiale kan oppbevares varig i biobanken 2018/787 Kartlegging av normalmetabolomet og kan bli benyttet i fremtidig forskning til ulike studier som omhandler kartlegging av normalmetabolomet

Sted og dato Deltakers signatur

b) Jeg godkjenner at mine prøver kan bli brukt som normalkontroll i andre forskningsprosjekter som er godkjent av Regional komité for medisinsk og helsefaglig forskningsetikk

Sted og dato Deltakers signatur

c) Jeg godkjenner at det kan utføres relevante analyser av mine prøver på gennivå knyttet til kartlegging av normalmetabolomet

Sted og dato	Deltakers signatur
	Deltakers navn med trykte bokstaver

Jeg bekrefter å ha gitt informasjon om prosjektet.

Sted og dato	Signatur
	Rolle i prosjektet

6.4.2 Sampling form given to participants

The volunteers participating in the exercise metabolome project were given a form to fill out, shown in **Table 60**. The form included more detailed information about diet, and it was collected from the participant after the project was completed.

Table 60: Form given to participants for them to fill out actual time of sampling, as well as any comments regarding sampling or diet.

Day	Time	Sample	Note	Actual time	Comments
1	07:00	1	Overnight fasting		
	07:30		Breakfast, done by 08:00 (free diet)		
	10:10	2	Free diet		
	10:45	3	Free diet		
	15:00	4	Free diet		
2	07:00	5	Overnight fasting		
	07:30		Breakfast, done by 08:00 (bread with Norgvegia, 1 cup of coffee)		
	10:10	6	Before workout		
	10:15		Workout		
	10:45	7	After workout		
	10:46		Eat 1 cup of yoghurt (TINE Vanilje)		
	11:45	8	1 h after workout		
	12:00		Lunch (pasta salad, bread, chocolate, coffee)		
	15:00	9			
3	07:00	10	Overnight fasting		

6.4.3 Adenosine 5’-monophosphate was identified as the significantly downregulated metabolite in negative ionization

Compound Discoverer, the software used for statistical analysis and identification of metabolites, identified a metabolite with monoisotopic mass 347.06309 and retention time 3.35 min as deoxy- guanosine 5’-monophosphate (dGMP) in the negative ionization results. This metabolite has the same monoisotopic mass and retention time as the metabolite identified as AMP in the positive results. Both were significantly downregulated in the samples taken immediately after exercise.

AMP and dGMP have the same monoisotopic mass and similar fragmentation in negative ionization, so there was a suspicion that it was in fact AMP, and not dGMP, that was the metabolite downregulated also in the negative ionization results. Unfortunately, a standard of dGMP could not be obtained in time, but the standards of AMP and GMP were obtained. **Table 61** shows the formula, structure, monoisotopic mass and logP of AMP, GMP and dGMP.

Table 61: Formula, structure, monoisotopic mass and logP value of AMP, GMP and dGMP. All values were obtained from PubChem [67].

Name	Formula	Structure	Monoisotopic mass	logP
Adenosine 5'-monophosphate (AMP)	$C_{10}H_{14}N_5O_7P$	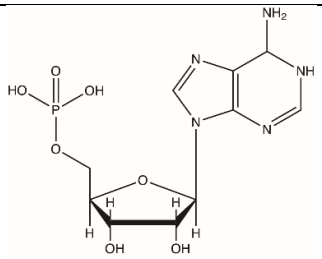	347.06309	-3.5
Guanosine 5'-monophosphate (GMP)	$C_{10}H_{14}N_5O_8P$	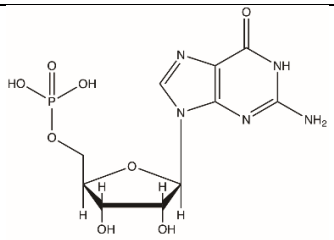	363.05799	-3.5
2'-Deoxyguanosine 5'-monophosphate (dGMP)	$C_{10}H_{14}N_5O_7P$	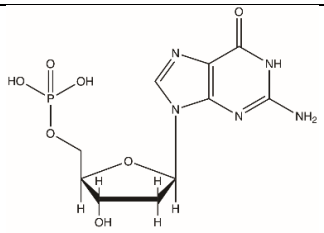	347.06309	-3.0

GMP and dGMP are structurally very similar, the only difference being in the missing hydroxyl group on the ribose of dGMP, and dGMP has slightly higher logP than GMP, as shown in **Table 61**. Because of this, it is likely that dGMP elutes after GMP. The retention time of AMP was found to be 3.35 min, and the retention time of GMP was found to be 4.02 min, as shown in **Figure 46**. AMP and GMP both have fragments with *m/z* 78 and 96.

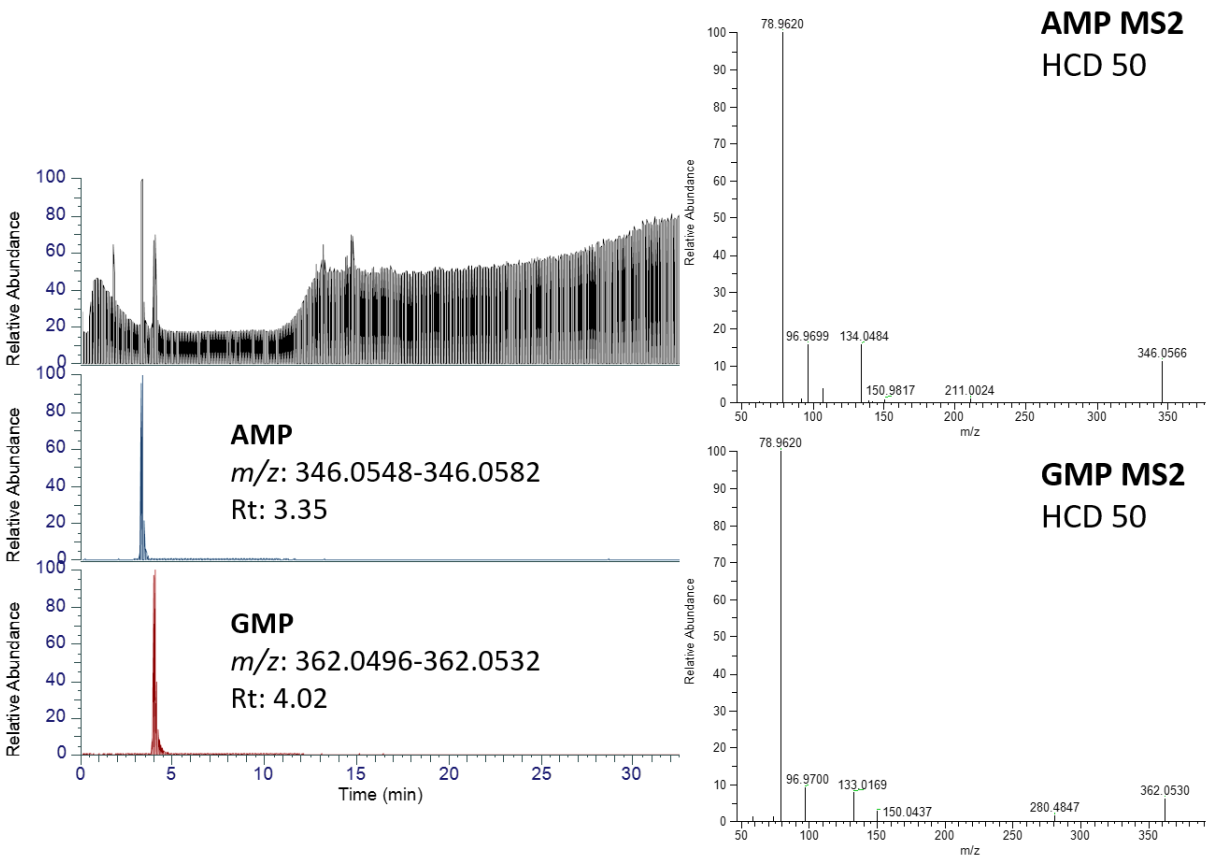

Figure 46: Total ion chromatogram (TIC), extracted ion chromatogram (EIC) and MS2 spectra of adenosine 5'-monophosphate (AMP) and guanosine 5'-monophosphate (GMP), from the analysis of the AMP and GMP standards. Both chromatogram and mass spectra are for the negative ionization mode.

Figure 47 shows the total ion chromatogram (TIC) and the EIC of AMP and GMP in the spiked PQC, as well as the MS2 spectra of the two compounds. It shows that the retention times of the compounds is not affected by the PQC matrix.

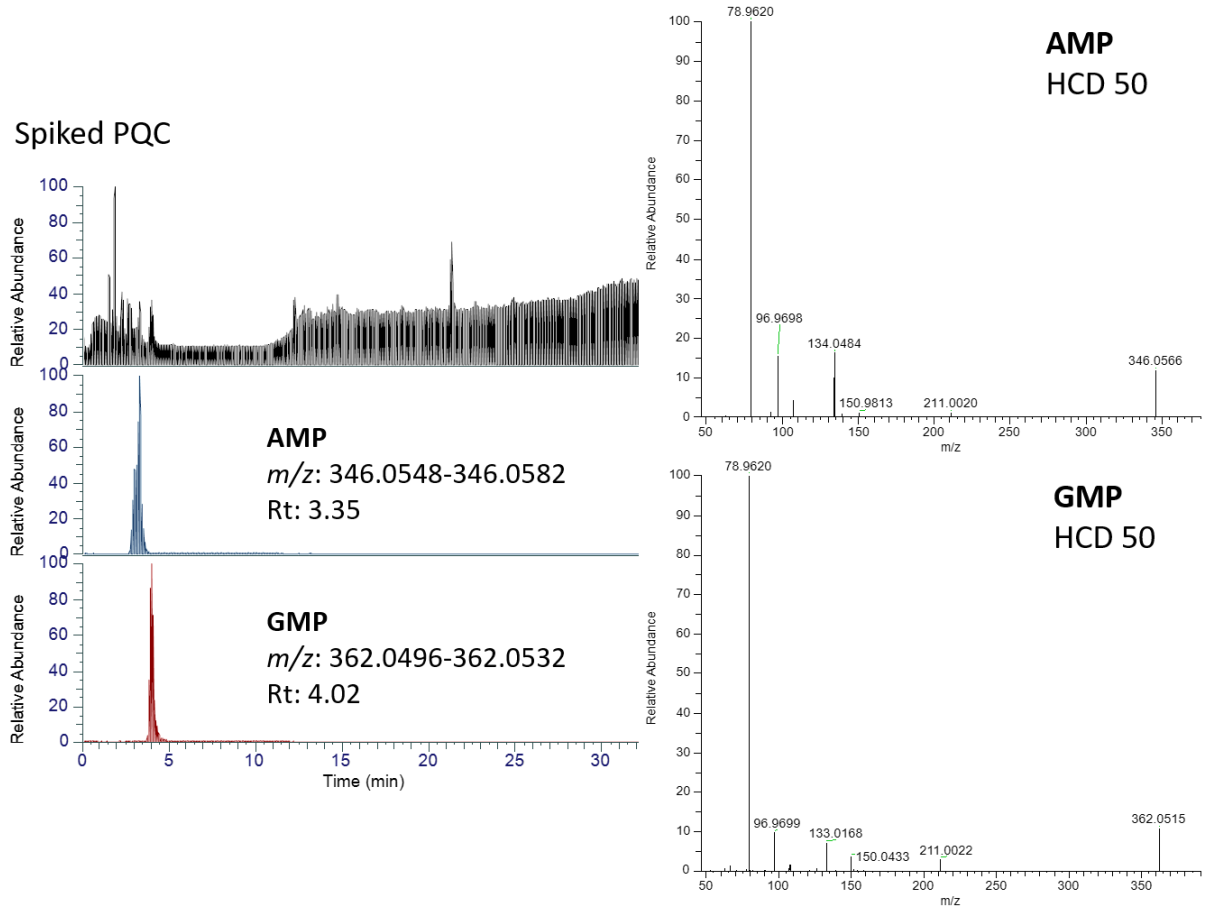

Figure 47: Total ion chromatogram (TIC), extracted ion chromatogram (EIC) and MS2 spectra of adenosine 5'-monophosphate (AMP) and guanosine 5'-monophosphate (GMP) in the spiked-pooled quality control (PQC). Both chromatogram and mass spectra are for the negative ionization mode.

Figure 48 shows the TIC and EIC of AMP, as well as the MS2 spectra in the PQC that was used for identification of metabolites, and GMP was not detected in these samples.

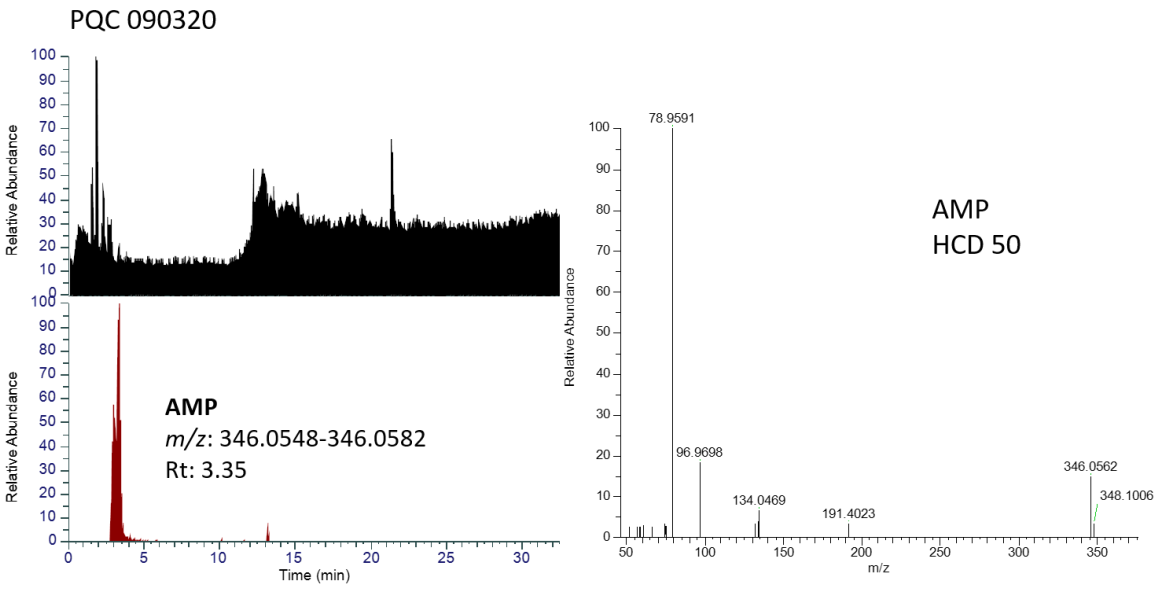

Figure 48: Total ion chromatogram (TIC) and extracted ion chromatogram (EIC) and MS2 spectra of adenosine 5'-monophosphate (AMP) in the pooled quality control (PQC) analyzed in the same batch as the samples from the exercise metabolome project. GMP was not detected in the non-spiked PQC. Both chromatogram and mass spectra are for the negative ionization mode.

The recorded spectra of metabolite with monoisotopic mass 347.06309 and retention time 3.35, was compared to mzCloud library spectra of AMP and dGMP, as shown in **Figure 49**. It shows that both AMP and dGMP match fragment with *m/z* 78, 96 and 346. AMP has a characteristic fragment at *m/z* 134, that is found in all MS2 spectra of the AMP standard. This fragment is also found in the spectra of the metabolite.

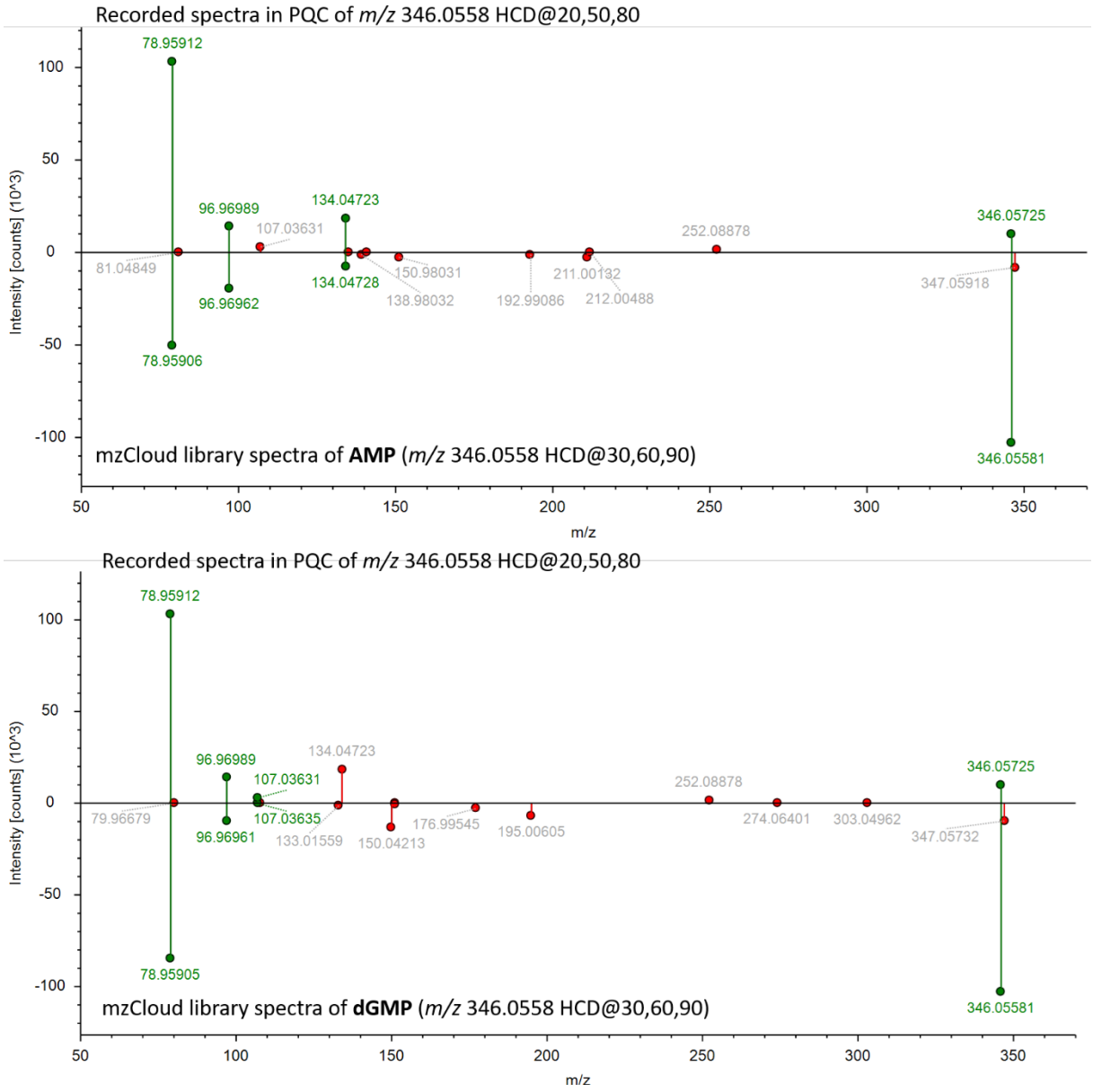

Figure 49: Comparison of the recorded spectra of the metabolite found to have monoisotopic mass 347.06309 and retention time 3.35, to the mzCloud library spectra of adenosine 5´-monophosphate (AMP) (top) and 2'-deoxyguanosine 5'-monophosphate (dGMP) (bottom). Both library spectra of AMP and dGMP matches some of the fragments of the metabolite, but both have a characteristic fragment at *m/z* 134.

As the retention time of the AMP standard was 3.35 min, and that the AMP standard and metabolite with *m/z* 346.0558 had the same fragment at *m/z* 134, indicated that it was AMP and not dGMP, that was significantly decreased also in the negative ionization results.

Conclusion: It was assumed that the metabolite with eluting at 3.35 min and monoisotopic mass 347.06309 was AMP.

6.4.4 Theobromine increased significantly after ingestion of chocolate and coffee

Theobromine, a metabolite of caffeine and present in cocoa beans, was significantly increased in the sample taken three hours after lunch as shown in **Figure 50**.

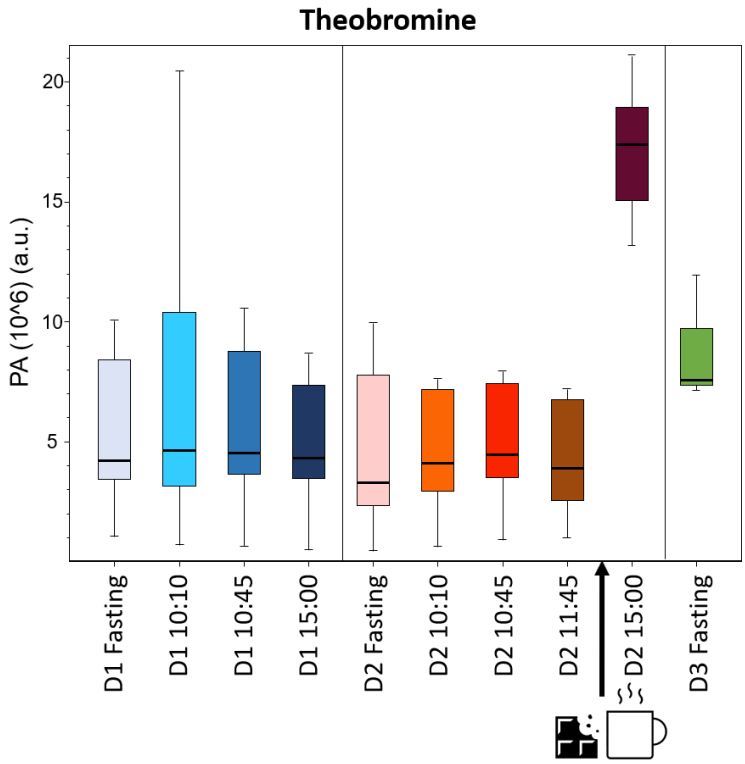

Figure 50: Theobromine. Measured peak area of theobromine in samples from seven healthy volunteers. Day one (D1) the participants had a normal workday with a free diet. Day two (D2) the participants had a controlled diet and participated in a high intensity workout, and a lunch at noon (indicated by the coffee and chocolate). Day 3 (D3) only a fasting sample was collected. The results shown are from positive ionization.

The participants were served pasta salad with bread, with chocolate and coffee for dessert. The significant increase in theobromine in the sample taken three hours after lunch is likely caused by the ingestion of chocolate and coffee [66].

6.4.5 Pooled quality controls for correction of systematic measurement bias

PQC can be used to model and correct for systematic measurement bias. If the metabolite response plotted against the injection order, some systematic variation in the reported metabolites response can often be observed [58], as illustrated in **Figure 51**.

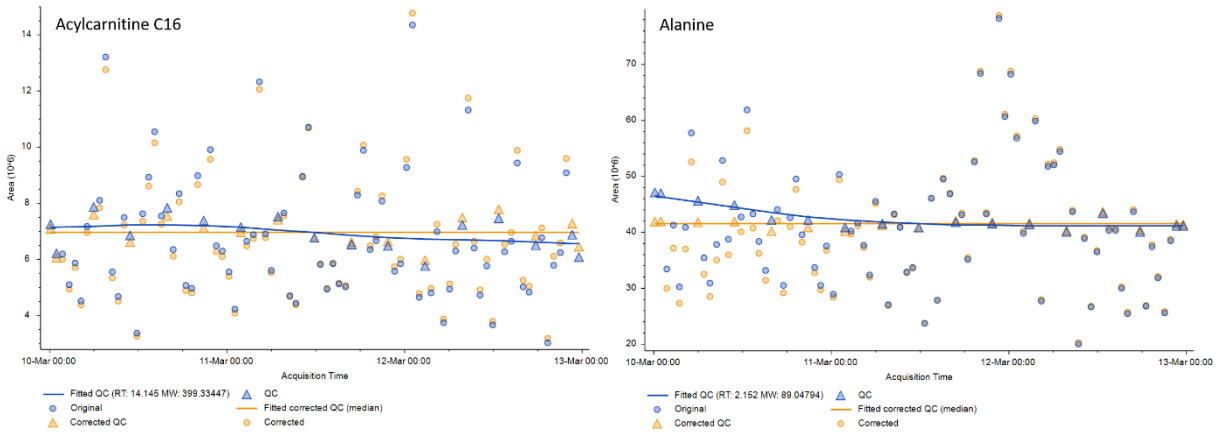

Figure 51: Correction of systematic measurement bias for the metabolite acylcarnitine C16 and alanine. The blue circles represent the measured peak area of the given metabolite in the samples, and the blue triangle represent the measured peak area of the given metabolite in the PQC. The yellow circle represents the corrected peak area of the given metabolite in the samples, and the yellow triangle represents corrected peak area of the given metabolite in the PQC. The blue curve is the regression curve for the measured peak area of the metabolite in the PQC, and the yellow line is the regression curve of the peak area correction for the given metabolite in the PQC.

The blue triangle represents the measured peak area of the given metabolite in the PQC, and the yellow triangle represent the corrected peak area of the given metabolite in the PQC. In the same way, the blue circle represents the measured peak area of the given metabolite in the in the sample, and the yellow circle represents the corrected peak area of the given metabolite in the in the sample. The blue line shows the regression curve for the measured peak area in the PQC, and the yellow line shows the regression curve for the corrected peak area in the PQC.

The PQCs should give the same response for the given metabolite for all injections, but samples come into direct contact with many components of the LC-ESI-MS, which contaminates the surfaces and can causes drift in the measured response and retention time [88]. Systematic errors in metabolite response can also be the result of oxidation or hydrolysis of metabolites as the sample sits in the autosampler, or from instrumental drift. Each metabolite has a different response, and if possible, each metabolite should be corrected for [58]. The software that was used only corrected the signal for metabolites who were detected in 50% of the PQCs, and where the signal % RSD did not exceed 30% in the PQCs.

6.4.6 Pooled quality control samples revealed instrument failure during data acquisition of exercise metabolome samples

The samples taken in relation to the exercise metabolome project had to be prepared and analyzed in a total of three rounds because of instrument failure. **Figure 52** shows the PCA plot for one of these rounds of data acquisition where there was a failure to keep the capillary temperature in the heated electrospray ion source (HESI) constant during data acquisition. The spreading of the PQCs indicated that there had been made serious mistake either in the sample preparation of the DBS, or some instrumental failure during data acquisition. The PQCs were analyzed evenly throughout the data acquisition sequence so any instrumental drift could be detected and corrected for, as shown in the previous section.

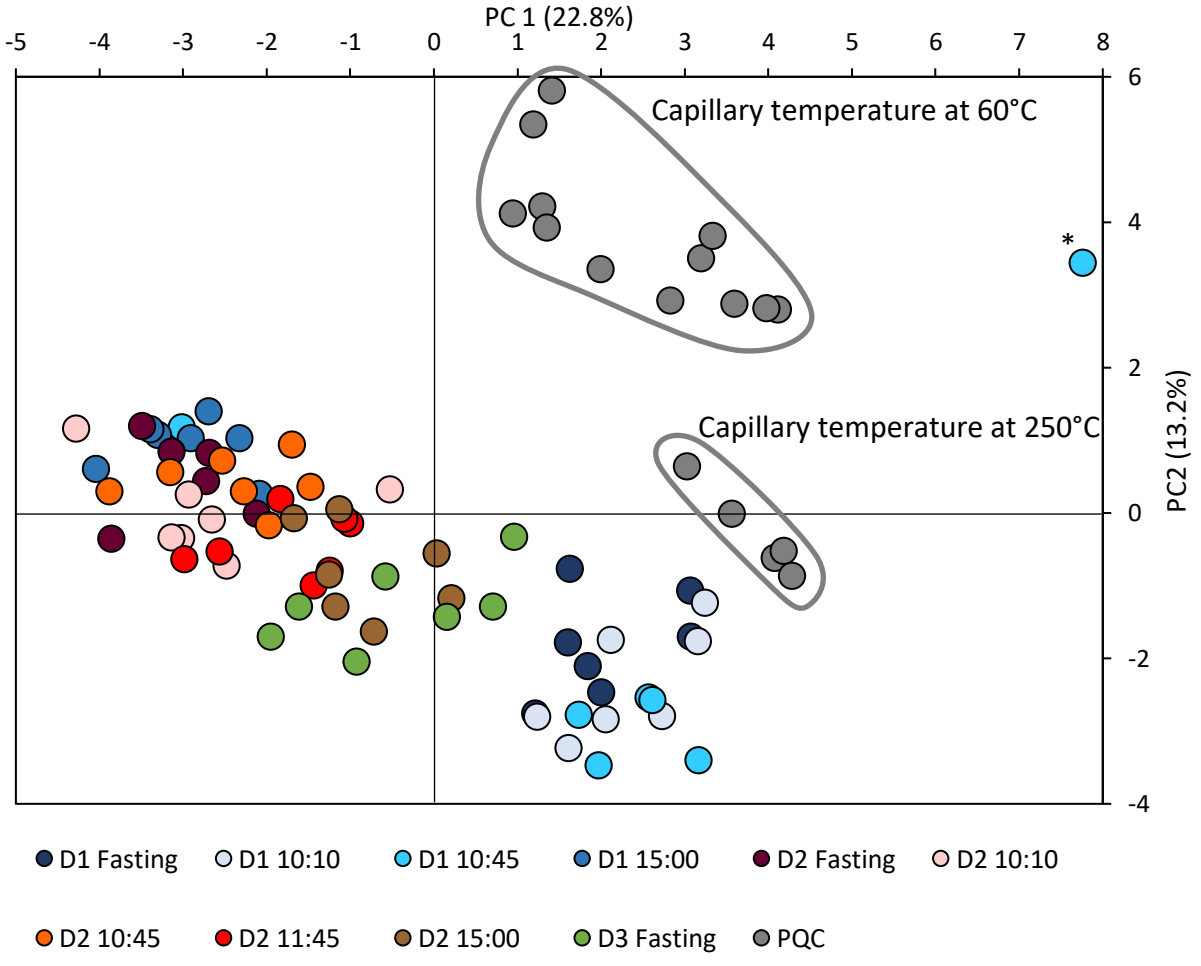

Figure 52: Principal component analysis (PCA) plot of samples acquired show grouping according to instrumental failure. The pooled quality control (PQC) samples are spread out, indicating instrumental failure during data acquisition. PQC samples spread out indicate drift in the analytical instrument, here caused because of a drop in the HESI capillary temperature during data acquistition. *Data for this sample was acquired when capillary temprature was at 89 °C.

It was found that the large variation was caused by a in capillary temperature of the HESI, from 250°C to 60°C during data acquisition.

The capillary temperature was set to 250°C to promote de-solvation and ion transfer into the gas phase, and lowering the temperature will affect signal intensity [32]. To assess the effect the drop in HESI capillary temperature had on signal intensity, the peak area of the metabolites alanine, tryptophan, LPC (16:0), uracil, and acylcarnitine C16, in the PQC was found. **Figure 53** shows the peak area of these metabolites, as well as the recorded HESI capillary temperature, for each injection of the PQC throughout the sequence. **Table 58** in **Appendix** Section 6.2 shows the peak area and temperature of these metabolites.

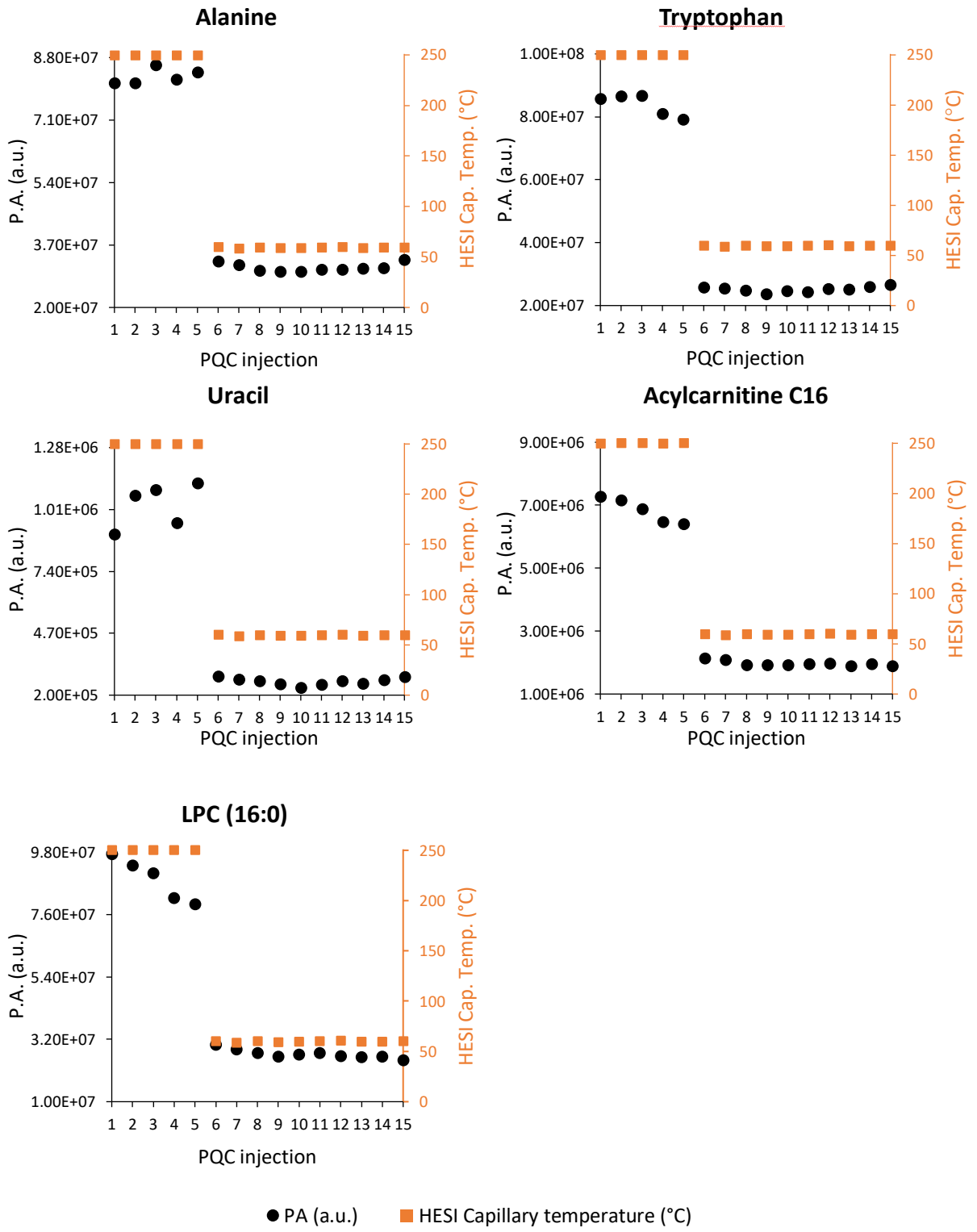

Figure 53: Subsequent drop in peak area (PA) after drop in heated electrospray ion source (HESI) capillary temperature, for a selection of metabolites. The black dots represent the PA of the given metabolite in the different injection of the PQC, at different times throughout data acquisition. The orange squares represent the HESI capillary temperature (°C) recorded for the given injection of the PQC. All metabolites show a significant drop in PA after the sixth injection of the PQC, in correspondence with the drop in the HESI capillary temperature.

The drop in capillary temperature resulted in a subsequent drop in signal intensity for the selected metabolites. This made it clear that these samples had to be re-analyzed.

This approach of checking the signal intensity of a selection of known and relatively abundant metabolites in the PQC can useful during data acquisition of large sample sets and reveal large instrumental drift. In global metabolomics studies large sample sets are often analyzed, resulting in data acquisitions that lasts over several weeks or months. If PQCs are implemented, the peak area of a given set of metabolites can be checked during data acquisition to reveal major instrumental drifts. If the peak area shows a relative standard deviation above a given limit, e.g. >30%, it indicates that there is cause for concern.

Conclusion: These results show the importance of using PQC in metabolomics studies. By comparing the peak area of well-known and relatively abundant metabolites, the PQC can reveal major drifts the analytical instrument causing large changes in signal intensities during data acquisition.

6.4.7 Clustering of pooled quality controls in principal component plot according to time of preparation

Samples from the exercise-project had to be prepared in total three different times, because of instrumental failure during the two first rounds of data acquisition. The PQCs made from the two previous rounds (prepared 04.02.20, and 21.02.20) were stored at 4 ºC before being analyzed again together with the last batch (prepared 09.03.20). This was done to assess the effect of storage on the PQCs. **Figure 54** shows the PCA plot of sample D2 Fasting, D3 Fasting and PQC #1 (from samples prepared 04.02.20), #2 (from samples prepared 21.02.20) and #3 (from samples prepared 09.03.20).

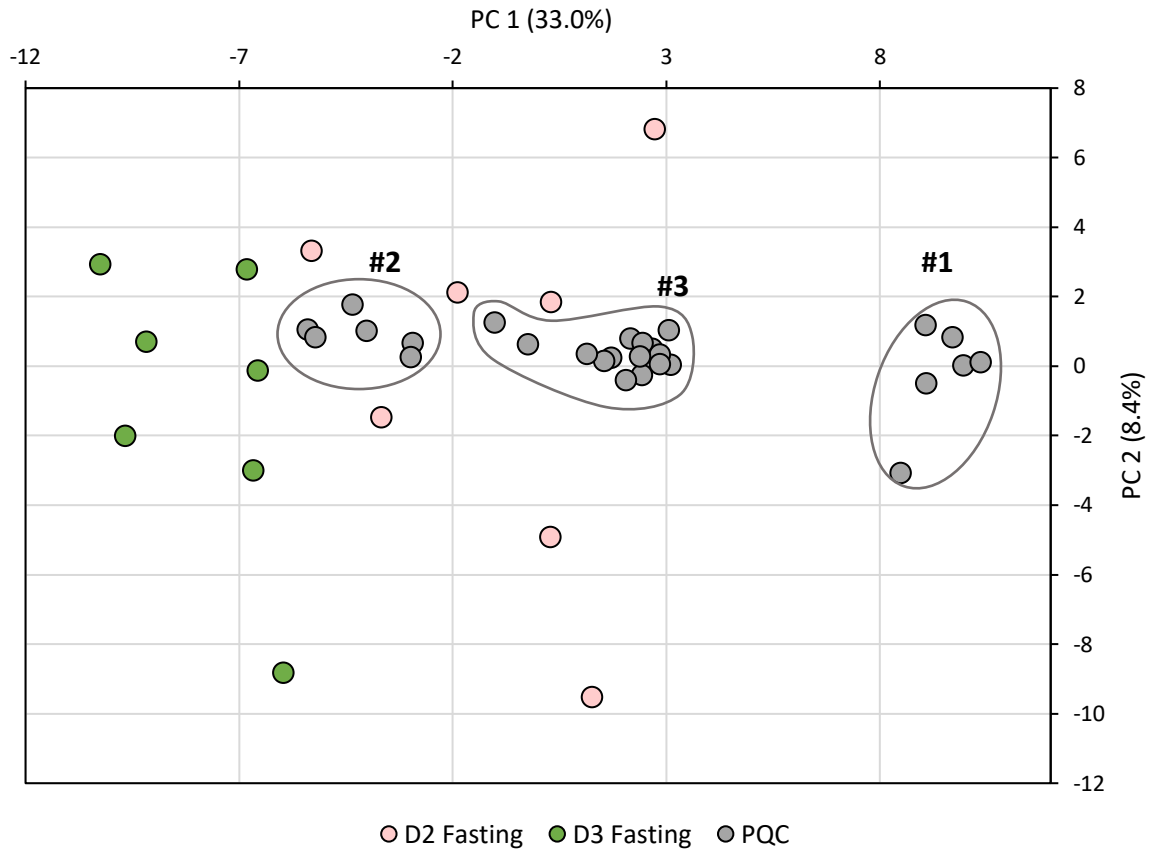

Figure 54: Principal component analysis (PCA) plot of day two (D2) Fasting, day three (D3) Fasting and pooled quality control (PQC) #1 (from samples prepared 04.02.20), #2 (from samples prepared 21.02.20) and #3 (from samples prepared 09.03.20). The PQCs cluster according to date of which they were prepared.

In the PCA plot, there is a clear separation of the PQCs based on time of preparation. Ideally the PQCs should cluster at the origin in a PCA plot, as the input data is mean centered prior to PCA implementation [58]. Deviation from the center is seen, and it is likely because of aging of the samples, or because PQC #1 and #2 are not generated from the same aliquots of sample as #3. With DBS, each spot on the card is potentially a little different, even if they are spotted at the same time with equal amounts of blood. Also, with the older PQC #1 and #2, some of the solvent had evaporated, making them more concentrated. This shows that when using PQC, they should be made from the same aliquots as the samples they are analyzed with.

Conclusion: *The PQC from different batches of the same samples were different after aging. The PQC should be made fresh, and from aliquots of the samples they are to be analyzed with.*

6.5 Poster Presented at "Det 24. Norske Symposium i Kromatografi", Sandefjord 2020

Oslo University Hospital · UiO : University of Oslo · OsloMet Oslo Metropolitan University

Metabolomics of Dried Blood Spots by LC – MS for Clinical Chemistry: Optimizing Sample Preparation of Dried Blood Spots for Improved Coverage of the Lipophilic Metabolome

H.S. Haugan[1,2], E. Sandås[1], A. Østeby[1], H.B. Skogvold[1,3], H. Rootwelt[1], S.R.H. Wilson[2], K.B.P. Elgstøen[1]

[1]Department of Medical Biochemistry, Oslo University Hospital Rikshospitalet, P.O. Box 4950 Nydalen, 0424 Oslo

[2]Department of Chemistry, University of Oslo, P.O. Box 1033 Blindern, 0351 Oslo

[3]Department of Mechanical, Electronic and Chemical Engineering, Oslo Metropolitan University, Norway, Pilestredet 35, 0166 Oslo

Background

The goal of metabolomics is to describe the metabolome of a given biological sample. The metabolome consists of all metabolites in the sample, and is thought to be the closest link to the phenotype. Dried blood spots represent an easy and simple way of sampling the metabolome, and is used in newborn screening for e.g. inborn errors of metabolism. The extraction solution used in newborn screening consists of 80% methanol (MeOH) with 0.1% formic acid (FA). When using dried blood spots for metabolomics studies, the extraction procedure governs which metabolites that can be detected. The aim of this work was to assess extraction solvents with different properties, for extraction of metabolites from dried blood spots to gain better coverage of the lipophilic metabolome using our in-house LC-ESI-MS method which has been implemented in research and diagnostics.

Materials and Methods

The LC-MS instrumentation used was Dionex Ultimate 3000 UHPLC system coupled to a Q Exactive Orbitrap, both from Thermo Scientific. The parameters used in all experiments are shown in **Table 1**.

Table 1: Settings for all experiments.

Parameter	Setting
Analytical column	C18-diphenyl, 2.0 x 250 mm, 3.0 µm
Mobile phase A	Water + 0.1% FA
Mobile phase B	MeOH + 0.1% FA
Flow gradient	**Figure 1**
Injection volume	2 µL
Flow rate	300 µL/min
Analysis time	32.5 min
Re-equilibrium time	10 min
m/z range	80-1200
Scan type	Full MS, MS/MS: Data dependent acquisition, Top 5
Polarity	Positive and negative
Electrospray voltage	3.5 kV
Resolution	Full MS: 70000 MS/MS: 17500

Selection of extraction solutions

Different organic solvents were selected according to Snyder's Solvent Selectivity triangle (**Figure 2**). Water with different proportions of MeOH, iso-propanol, 1-propanol, 1-butanol, acetonitrile (CAN), and methyl-tert butyl ether (MTBE) with 0.1% FA, were used, as shown in **Table 2**.

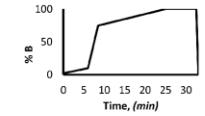

Figure 1: Mobile phase gradient profile. Mobile phase A: Water + 0.1% FA, B: Methanol + 0.1% FA.

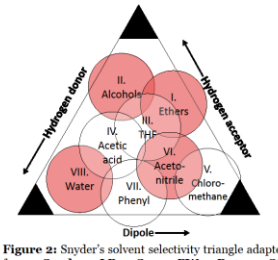

Figure 2: Snyder's solvent selectivity triangle adapted from **Snyder LR, Carr PW, Rutan SC. *Solvatochromically based solvent-selectivity triangle*, Journal of Chromatography A. 1993;656(1):537-47.**

Preparation of samples

One drop of whole blood (healthy volunteers) or standard was applied onto Whatman 903 Protein Saver cards, and after 4 hours of drying at ambient temperature, a 3.2 mm disk was punched out. Extraction solution (100 µL) was added, and the sample mixed at 700 rpm for 45 minutes at 45 °C. The supernatant was transferred to an HPLC-vial, and 2 µL injected.

Lipid standards

Lipid standards (EquiSPLASH) containing phosphatidylcholine (PC) (15:0/18:1(d7)), phosphatidylcholine (LPC) (18:0(d7)), phosphatidylethanolamine (PE) (15:0/18:1(d7)), phosphatidylethanolamine (LPE) (18:1(d7)), phosphatidylglycerol (PG) (15:0/18:1(d7)), phosphatidylinositol (PI) (15:0/18:1(d7)), phosphatidylserine (PS) (15:0/18:1(d7)), triacylglycerol (TG) (15:0/18:1(d7)/15:0), diacylglycerol (DG) (15:0/18:1(d7), monoacylglyserol (MG) (18:1(d7)), cholesterol ester (CE) (18:1(d7)), sphingomyelin (SM) (d18:1/18:1), ceramide(d18:1/15:0) were used, obtained from Avanti Polar Lipids.

Table 2: Extraction solutions

Content, *(v/v %)*
80% MeOH + 0.1% FA
50% MeOH + 0.1% FA
20% MeOH + 0.1% FA
80% ACN + 0.1% FA
50% ACN + 0.1% FA
20% ACN + 0.1% FA
80% iso-propanol + 0.1% FA
50% iso-propanol + 0.1% FA
20% iso-propanol + 0.1% FA
80% 1-propanol + 0.1% FA
50% 1-propanol + 0.1% FA
20% 1-propanol + 0.1% FA
40% 1-butanol + 40% MeOH + 0.1% FA

Results and Discussion

Extraction of lipids using different extraction solutions

Figure 2 shows the extraction efficiency of the different extraction solutions. The same compounds were extracted by all solutions containing 80% organic solvent, although with different efficiency. The extraction efficiency for the selected lipids increased when using acetonitrile. Cholesterol ester (18:1(d7)), phosphatidylglycerol (15:0/18:1(d7)), phosphatidylinositol (15:0/18:1(d7)), phosphatidylserine (15:0/18:1(d7)) were not detected using any of the selected extraction solutions. None of the lipids were extracted using only 20% organic solvent (not included in figures 2 and 3).

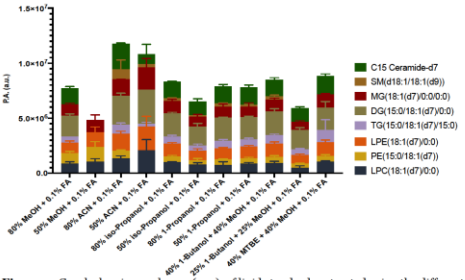

Figure 2: Graph showing peak area (a.u.) of lipid standards extracted using the different extraction solutions.

Metabolites extracted using different extraction solutions

Figure 3a and **3b** show Principal Component Analysis (PCA) plots of dried blood spots from one individual, extracted with the different extraction solutions.

In positive ionization (**Figure 3a**) the biggest variation in the metabolites detected was caused by the proportion of organic solvent. In negative ionization (**Figure 3b**) the type of organic solvent seemed to be of greater importance.

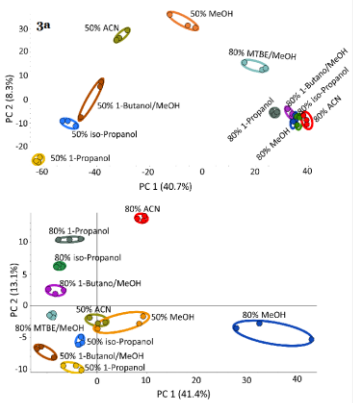

Figure 3a: PCA plot for dried blood sport extracted by different extraction solutions (positive ionization).

Figure 3b: PCA plot for dried blood sport extracted by different extraction solutions (negative ionization).

Concluding remarks

Both the type and proportion of organic solvent affect metabolome coverage. As expected, extraction efficiency of lipids increased with increasing organic proportion. Interestingly, the metabolomes detected in positive and negative ionization mode were differently affected. Although beyond the scope of this work, by replacing formic acid with ammonium acetate in the mobile phase, the compounds not detected using the standardized LC parameters were readily found in negative ionization mode. Our findings emphasize the importance of using both ionization modes.

Contact information: hegsh@uio.no